Engineering Journal

American Institute of Steel Construction

Fourth Quarter 2010 Volume 47, No. 4

www.aisc.org

ENGINEERING JOURNAL

AMERICAN INSTITUTE OF STEEL CONSTRUCTION

Dedicated to the development and improvement of steel construction, through the interchange of ideas, experiences and data.

ENGINEERING JOURNAL (ISSN 0013-8029) is published quarterly. Subscriptions: Members: one subscription, $40 per year, included in dues; Additional Member Subscriptions: $40 per year. Non-Members U.S.: $160 per year. International Members (including Canada and Mexico): $160 per year. International Non-Members (including Canada and Mexico): $320. Published by the American Institute of Steel Construction at One East Wacker Drive, Suite 700, Chicago, IL 60601.

Periodicals postage paid at Chicago, IL and additional mailing offices. **Postmaster:** Send address changes to ENGINEERING JOURNAL in care of the American Institute of Steel Construction, One East Wacker Drive, Suite 700, Chicago, IL 60601.

Message from the Editor

A lot of hard work goes into every issue of *Engineering Journal*. As always, we are grateful for having such a talented pool of authors working on such a wide variety of topics. But behind the scenes, there's another pool of talent: our reviewers. Practitioners and academics just like you have volunteered their time and their brainpower to help us make the journal the best that it can be. Our 2010 reviewers are recognized on the following pages.

One of the journal's biggest changes in 2010 was the introduction of the digital edition. In spite of a few technology kinks, reader response to the digital edition has been overwhelmingly positive.

There is one more change for 2011, but only for those AISC members reading this in a paper copy of *Engineering Journal*—a move toward electronic publication for those who choose to receive EJ that way.

Starting with First Quarter 2011, if you would like to continue to receive a paper copy of *Engineering Journal* with your AISC membership, you can opt in by sending an e-mail with the information from your mailing label to paperplease@aisc.org.

If we do not hear from you by March 31, 2011, we will automatically switch your subscription to electronic access starting with the Second Quarter 2011 issue. You will continue to have access to the *Engineering Journal* digital edition and the PDF *Engineering Journal* archives through your AISC membership.

We are not eliminating the paper version of *Engineering Journal*, and you can opt in to continue to receive EJ in paper form. Simply, we want to make sure that we are sending paper copies of *Engineering Journal* to those who really want them, and ensure we are not wasting paper if you wish to receive it electronically. If you have any questions, please feel free to contact me at grubb@aisc.org.

Keith A. Grubb, P.E., S.E.
Editor

P.S. It's time to start thinking about attending the 2011 NASCC: The Steel Conference in Pittsburgh, Pennsylvania, May 11–14, 2011. Visit *www.aisc.org/nascc* for more information.

Acknowledgment

All AISC *Engineering Journal* articles are peer reviewed prior to publication for accuracy, content, and style. AISC thanks the following engineers for their voluntary review assistance to the *Engineering Journal* Review Board throughout 2010.

Farid Alfawakhiri
American Iron and Steel Institute

Robert Bachman
Consultant

Bruce Butler
Walt Disney World Company

Peter Carrato
Bechtel Corporation

Brad Davis
University of Kentucky

Bo Dowswell
SDS Resources

Rick Drake
Fluor Enterprises, Inc.

Carol Drucker
Drucker Zajdel Structural Engineers, Inc.

Bruce Ellingwood
Georgia Institute of Technology

Larry Fahnestock
University of Illinois at Urbana-Champaign

Shujin Fang
Sargent & Lundy, LLC

Marshall Ferrell
Ferrell Engineering, Inc.

James Fisher
Computerized Structural Design, SC

John Fisher
Lehigh University

Christopher Foley
Marquette University

Theodore Galambos
University of Minnesota

Maria Garlock
Princeton University

Louis Geschwindner
Penn State University

Jerome Hajjar
Northeastern University

Ronald Hamburger
Simpson Gumpertz & Heger Inc. Consulting Engineers

Patrick Hassett
Hassett Engineering, Inc.

Christopher Hewitt
Sargent & Lundy, LLC

John Hooper
Magnusson Klemencic Associates

Nestor Iwankiw
Hughes Associates

Richard Kaehler
Computerized Structural Design, SC

Lawrence Kloiber
LeJeune Steel

Greg Kochalski
HKS Inc.

Venkatesh Kodur
Michigan State University

Lawrence Kruth
Douglas Steel Fabricating Corporation

Geoffrey Kulak
University of Alberta

Susan Lamont
ARUP

Keith Landwehr
Schuff Steel Company

Judy Liu
Purdue University

Robert MacCrimmon
Hatch Canada

James Malley
Degenkolb Engineers

Bonnie Manley
American Iron and Steel Institute

Peter Marshall
Consultant

Ron Meng
Lynchburg Steel Company, LLC

Larry Muir
Consultant

Thomas Murray
Consultant

Jeffrey Packer
University of Toronto

Bing Qu
California Polytechnic State University

Christopher Raebel
Milwaukee School of Engineering

Clinton Rex
Stanley D. Lindsey & Associates

Charles Roeder
University of Washington

John Rolfes
Computerized Structural Design, SC

Paul Rouis
Ryan-Biggs Associates, P.C.

Rafael Sabelli
Walter P Moore

Thomas Sabol
Englekirk & Sabol, Inc.

C. Mark Saunders
Rutherford & Chekene Consulting Engineers

Mehdi Setareh
Virginia Polytechnic Institute & State University

Robert Shaw
Steel Structures Technology Center, Inc.

Raymond Tide
Wiss Janney Elstner Associates, Inc.

Chia-Ming Uang
University of California–San Diego

Timothy Utter
Foster Wheeler North America Corp.

Michael West
Computerized Structural Design, SC

Ronald Yeager
Steel-Art, Inc.

Qiuhong Zhao
University of Tennessee

Prediction of Bolted Connection Capacity for Block Shear Failures along Atypical Paths

QING CAI and ROBERT G. DRIVER

ABSTRACT

Failure modes such as bolt tear-out and the so-called alternate block shear path observed in tees are closely related to the classical block shear limit state, but they have not been addressed as such in current design specifications in North America. In previous work conducted at the University of Alberta, a unified block shear equation was proposed that provides accurate test-to-predicted block shear capacity ratios and results in consistent reliability indices over a variety of connection types. A total of 104 specimens that failed in bolt tear-out and 14 tees that failed on the alternate block shear path are considered from the literature, along with 12 new bolt tear-out tests conducted as part of this research program. It is shown that the unified block shear equation provides accurate and consistent results for these failure modes as well.

Keywords: block shear, bolt tear-out.

INTRODUCTION

Block shear is a well-documented failure mode that can occur in connections when a block of material in the connected region is displaced due to tension fracture on one plane of the block perimeter in combination with shear on one or more others. Bolt tear-out and failure in tees along the "alternate block shear" path can be considered block shear failures with atypical failure paths, and this paper investigates the suitability of different methods of predicting block shear capacity specifically for these modes.

Bolt tear-out failure generally occurs by shear tearing along the two planes adjacent to the bolt hole, and there is no tension fracture in the block of material due to the presence of the hole itself. This path is illustrated in Figure 1a. Bearing is a closely related failure mode and is considered to constitute failure by the excessive deformation of material behind the bolt. If connection deformation is not a design consideration, the ultimate strength of a bolted connection with a relatively small end distance and pitch that fails locally around the bolts would generally be governed by bolt tear-out rather than bearing. Nevertheless, capacities determined using the AISC bearing provisions for when hole deformation at the service load is not a design consideration (Equation J3-6b; AISC, 2005) are also examined for comparison to the block shear approach.

A failure mode observed by Epstein and Stamberg (2002) in tees connected by bolts through the flange only, which was termed "alternate block shear" failure by the researchers, is depicted in Figure 1b. This failure mode is similar to traditional block shear except that it has only one shear plane in the tee stem and tension fracture involves the entire flange.

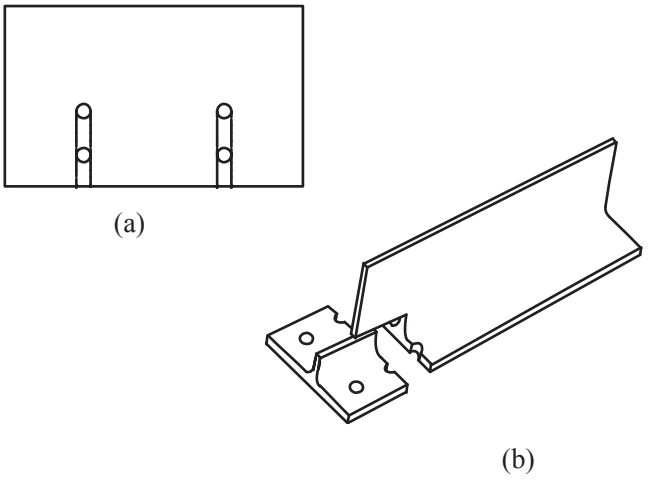

Fig. 1. Failure paths considered: (a) bolt tear-out; (b) alternate block shear path in tees.

Qing Cai, P.Eng., Bridge Engineer, AECOM, Edmonton, AB, Canada (corresponding author). E-mail: catherine.cai@aecom.com

Robert Driver, Professor, Department of Civil and Environmental Engineering, University of Alberta, Edmonton, AB, Canada. E-mail: rdriver@ualberta.ca

DESIGN EQUATIONS

CSA-S16-01 and AISC 360-05

The provisions in the current North American design standards, CSA-S16-01 (CSA, 2001) and the AISC *Specification* (AISC, 2005), for predicting the block shear capacity of tension members with concentrically loaded symmetrical blocks are essentially identical. The block shear capacity is taken as the lesser of:

$$P_r = \phi A_{nt} F_u + 0.60\phi A_{gv} F_y \quad (1)$$

$$P_r = \phi A_{nt} F_u + 0.60\phi A_{nv} F_u \quad (2)$$

Both design specifications provide an effective stress factor on the first (tension) term that is applied in certain circumstances when the stress distribution on the tension plane is nonuniform due to starkly asymmetrical loading on the block. Equation 1 applies when the net tension area, A_{nt}, reaches the ultimate tensile strength, F_u, and the gross shear area, A_{gv}, reaches the shear yield strength, $0.6F_y$. This phenomenon has been observed by many researchers (e.g., Franchuk et al., 2003). However, Equation 2, representing the development of the ultimate capacities of both the net tension area and net shear area, A_{nv}, is not supported by test observations. On the contrary, experimental evidence (e.g., Huns et al., 2002) indicates that tension fracture occurs well before shear fracture and, although the shear yield stress is exceeded, the ductility of the material in tension is inadequate to allow the ultimate shear strength to be reached concurrently with the ultimate tensile strength on the tension area of the block.

There is no equation in the current design specifications in North America given explicitly for bolt tear-out failure as depicted in Figure 1a. However, the AISC *Specification* Commentary (AISC, 2005) states that the bearing provisions can be applied to address the tear-out limit state. Alternatively, design equations for block shear could be used as shown, for instance, in a design example in the CISC *Handbook of Steel Construction* (CISC, 2006). This latter approach is clearly based on the assumption that bolt tear-out is a type of block shear failure. In this case, Equations 1 and 2 become (the lesser of):

$$P_r = 0.60\phi A_{gv} F_y \quad (3)$$

$$P_r = 0.60\phi A_{nv} F_u \quad (4)$$

These block shear equations imply that both gross section yield and net section rupture of the shear planes are possible failure modes, and therefore, both must be checked.

Unified Equation

Based on a large number of experimental results from the literature, Kulak and Grondin (2001) observed that equations existing at that time were inconsistent in predicting the capacities of connections failing in block shear. To address this deficiency, Driver et al. (2006) proposed a single unified block shear equation that has been shown to provide excellent results for a variety of member and connection types failing in block shear. It represents the observation from tests that rupture on the net tension area tends to occur well after yielding has taken place on the gross shear plane, but prior to shear rupture. The effective shear stress in the unified equation is taken as the average of the shear yield and shear ultimate stresses to reflect this fact. The equation also reflects the fact that failure of the shear planes occurs on the gross section adjacent to the holes (Driver et al., 2006). For tension members with symmetrical blocks, it takes the following form:

$$P_r = \phi A_{nt} F_u + \phi A_{gv} \left(\frac{F_y + F_u}{2\sqrt{3}} \right) \quad (5)$$

Effective stress factors were provided on both terms of the unified equation to allow for nonuniform stress distributions on the block perimeter, although the factor on the second (shear) term can generally be taken as 1.0. The unified block shear equation can be applied to the case of bolt tear-out simply by eliminating the tension component:

$$P_r = \phi A_{gv} \left(\frac{F_y + F_u}{2\sqrt{3}} \right) \quad (6)$$

It is postulated that the unified block shear equation can be adopted for a truly unified equation that is also suitable for predicting bolt tear-out failure at the ultimate limit state. It is investigated herein for use with this mode, as well as for the alternate block shear failure path in tees, where both the tension and shear terms are needed.

PREVIOUS RESEARCH

Although many bolt tear-out tests have been conducted on very high strength steels, due to their demonstrably different behavior, this study focuses on common grades of steel with yield strengths no greater than 550 MPa (80 ksi). Considering these grades only, Udagawa and Yamada (1998) conducted 146 tests on plates, and 31 of them failed by bolt tear-out. For these 31 tests, the number of bolt lines running in the direction of the applied load was one or two, while the number of bolt rows running in the direction perpendicular to the applied load varied from two to four. Kim and Yura

Table 1. Tests from Previous Research							
Author (Year)	Section Type	Number of Tests			Mean T/P Ratio Criterion A (COV)		
		Total	Criterion A[a]	Criterion B[b]	S16-01/ AISC 360-05	AISC 360-05 Bearing	Unified Equation
Bolt Tear-out							
Udagawa & Yamada (1998)	Plate	31	0	31	—	—	—
Kim & Yura (1999)	Plate	19	9	19	1.24 (0.14)	0.97 (0.08)	0.95 (0.13)
Aalberg & Larsen (2001, 2002)	Plate	20	10	20	1.17 (0.13)	0.94 (0.08)	0.98 (0.12)
Puthli & Fleischer (2001)	Plate	9	0	9	—	—	—
Rex & Easterling (2003)	Plate	20	11	20	1.21 (0.07)	0.93 (0.11)	0.99 (0.08)
Udagawa & Yamada (2004)	Channel	5	0	5	—	—	—
Alternate Block Shear							
Epstein & Stamberg (2002)	Tee	14	14	14	1.08 (0.09)	—	1.05 (0.09)

a. Tests that meet the minimum end distance and bolt spacing requirements specified in North American design specifications ($F_y \leq 550$ MPa; 80 ksi).
b. Includes tests that do not meet the minimum end distance and bolt spacing requirements specified in North American design specifications ($F_y \leq 550$ MPa; 80 ksi).

(1999) carried out 19 tests on plates with one or two bolts in a single line parallel to the applied load and all of the tests failed by bolt tear-out. Aalberg and Larsen (2001, 2002) used the connection configurations of Kim and Yura (1999) and tested eight one-bolt connections and 12 two-bolt connections, and all specimens failed by bolt tear-out. Puthli and Fleischer (2001) completed 25 tests on plates that had two bolts in a row perpendicular to the applied load, and nine of them failed in the bolt tear-out mode. Rex and Easterling (2003) conducted 46 single bolt bearing tests, and 20 plates ultimately failed by bolt tear-out.

Udagawa and Yamada (2004) carried out 42 tests on web-connected channel sections, and five of them failed by bolt tear-out. All five specimens had a single bolt line in the web in the direction of the applied load, and the number of bolts varied from two to four.

Epstein and Stamberg (2002) conducted 50 tests on a wide variety of flange-connected tees cut from standard wide-flange shapes. Fourteen specimens failed along the alternate block shear path, all but one of which had two bolt rows aligned in the direction perpendicular to the applied load (the other had three).

There are a significant number of tests reported in the literature for which bolt tear-out is the ultimate failure mode. However, to ensure that the bolt tear-out mode governs the failure, most connection configurations tested do not meet the minimum end distance and bolt spacing requirements specified in North American design specifications, and many have only one or two bolts. Table 1 presents the number of test connections that failed by bolt tear-out from seven different research projects and the number of tests that meet each of criteria A and B, as defined in the table. Test-to-predicted values are provided for both the block shear and bearing design equations for criterion A.

The last row of Table 1 represents the tests that failed along the "alternate block shear" path in tees. Due to the relatively small eccentricity in flange-connected tees, an effective stress factor equal to 1.0 has been applied to the stresses on the tension plane in the predicted values.

Table 2. Measured Web Connection Dimensions						
Specimen	Section	Hole Diameter, d_0 (mm)	Web Thickness, w (mm)	End Distance, e_1 (mm)	Pitch, p (mm)	Gage, g (mm)
A1G1	W310×60	20.6	7.48	28.3	54.3	140.6
A2G1	W310×60	20.6	7.52	29.3	54.2	139.9
A3R1	W310×39	20.4	6.30	28.2	53.8	178.8
A4R2	W310×39	20.6	6.22	28.3	54.1	178.6
A5E1	W250×49	20.5	7.55	31.0	54.1	140.1
A6E2	W250×49	20.5	7.51	47.7	54.1	140.0
A7G1	W310×60	20.8	7.43	28.6	53.8	139.7
A8G2	W310×60	20.8	7.44	27.1	54.1	177.8
A9R1	W310×39	20.7	6.54	27.6	53.6	178.2
A10R2	W310×39	20.8	6.55	27.1	54.3	178.2
A11E1	W250×49	20.6	7.30	28.3	53.7	140.2
A12E2	W250×49	20.7	7.34	44.0	54.3	139.9
Note: 1 in. = 25.4 mm						

EXPERIMENTAL PROGRAM

The bolt tear-out experimental program conducted as part of this research included 12 specimens that were connected through the web only, using three different wide-flange sections meeting the requirements of both CSA-G40.21 Grade 350W and ASTM A572 Grade 50 steel. The three main variables were the gage, g (G in the specimen designation), number of bolt rows (R), and end distance, e_1 (E). The connection dimensional parameters are shown in Figure 2 and the associated measured values are listed in Table 2. As depicted in Figure 2, all specimens had four bolts except the two R2 specimens, which had six. Although the gage was varied, in no case did a block tear-out occur that encompassed the entire bolt pattern; rather, the webs tore along each individual bolt line.

The test setup is depicted schematically in Figure 3. All specimens were 1220 mm (48 in.) long. Specimens were

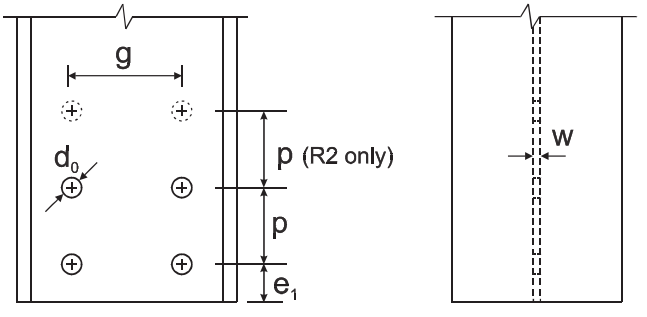

Fig. 2. Connection dimensional parameters.

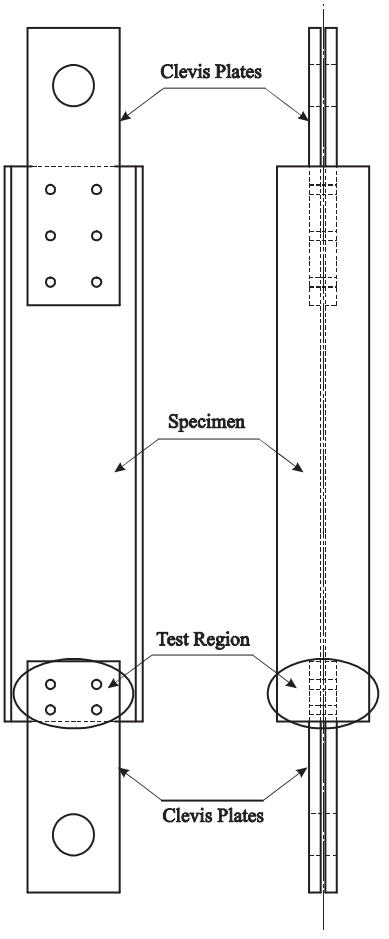

Fig. 3. Test setup.

Table 3. Summary of Test Results				
Specimen	F_y (MPa)	F_u (MPa)	Peak Load (kN)	Unloading Point
A1G1	439	519	690.7	drop of 5% of the peak load
A2G1	439	519	723.8	right after the peak load
A3R1	379	472	634.1	right after the peak load
A4R2	379	472	912.7	right after the peak load
A5E1	343	487	697.7	right after the peak load
A6E2	343	487	775.8	after a sudden load drop
A7G1	411	494	665.1	drop of 5% of the peak load
A8G2	411	494	622.1	right after the peak load
A9R1	369	478	632.8	drop of 5% of the peak load
A10R2	369	478	766.1	drop of 5% of the peak load
A11E1	376	500	691.2	drop of 5% of the peak load
A12E2	376	500	792.6	drop of 5% of the peak load
Note: 1 ksi = 6.895 MPa; 1 kip = 4.448 kN				

connected to clevis plates at both ends, which were in turn connected to the testing machine by pin connections. The clevis plates were designed to remain elastic so they could be reused. This would be a common scenario for cases where bolt tear-out of the internal plate is the governing mode of failure.

Bolts used in the tests were ASTM Grade A490, with a diameter, d_b, of 19.1 mm (¾ in.). The pitch, as a fixed parameter, was nominally 54 mm (2⅛ in.) because both CSA-S16-01 and AISC 360-05 specify that the pitch should not be less than $2.7d_b$. The minimum end distance for the bolts is 25 mm (1 in.) for gas-cut edges. (CSA-S16-01 also specifies that the end distance should not be less than $1.5d_b$ for connections that have either one or two bolts in a line in the direction of the applied force, but this was neglected because it does not apply to both design specifications considered.) All bolt holes were drilled and of standard size, namely, 20.6 mm (13⁄16 in.). Bolts had standard thread lengths that excluded the threads from the shear planes and were tightened to the snug-tight condition as defined in CSA-S16-01 (CSA, 2001).

Ancillary material tensile tests were conducted as per ASTM standard A370 (ASTM, 2007). Three coupons were fabricated from the web of each section in the direction of the applied load. Mean test results for each set of coupons are listed in Table 3.

Specimens were tested in tension in a universal testing machine (MTS 6000). The load was applied quasi-statically under stroke control. One of two typical unloading points was chosen as the terminus of each test: "right after the peak load" and "drop of 5% of the peak load." The former was selected in order to observe the load-carrying mechanism right at the peak load, whereas the latter was chosen to ensure that the ultimate strength of the connection had indeed been captured. Cai and Driver (2008) provide a complete description of the test set-up and experimental procedures.

TEST RESULTS

Test results are summarized in Table 3. All specimens failed by bolt tear-out of the web.

Two kinds of fractures were observed in the bolt tear-out failures: shear tears on one or both shear planes adjacent to the hole, as shown in Figure 4a, or a single tensile splitting crack initiating at the free edge near the hole centerline, as shown in Figure 4b. Tensile splitting cracks were caused by the development of transverse tensile stress as the material behind the bolt shank deformed into an arch shape. Most specimens eventually exhibited either shear tears or splitting cracks, although it is believed that splitting cracks did not occur until well after the peak load had been reached.

From the test results, it is evident that two shear planes adjacent to each bolt participate in resisting the peak load in bolt tear-out failure, despite the subsequent occurrence of tensile splitting in some specimens. In addition, the ductility of the material behind the end bolt hole, as illustrated in Figure 4c, is sufficient to allow the shear stress in the two shear planes to be developed well beyond the yield stress—but not necessarily up to the ultimate stress—before the ultimate load is reached. The specimen shown in Figure 4c was unloaded right after reaching the peak load, although no tearing of any kind had yet initiated. This observation is consistent with the contention that the load-carrying mechanism at the ultimate strength consists of the two shear planes next to the

bolt holes, and that tensile splitting adjacent to the center of the last hole is a post-peak phenomenon.

The predicted capacity for each test specimen, with the assumption that two shear planes at each bolt carry the peak load, was calculated using the CSA-S16-01 and AISC 360-05 block shear equations and the unified equation. The predicted capacities and the resulting test-to-predicted ratios are shown in Table 4. For comparison, values derived from the S16/AISC block shear provisions but considering only the case that assumes gross section failure on the shear planes (Equation 3), as well as those from the AISC bearing provisions, are also provided in Table 4.

The equations in CSA-S16-01/AISC 360-05 give a mean test-to-predicted ratio and coefficient of variation of 1.46 and 0.10, respectively, while the unified equation results in corresponding values of 1.08 and 0.09. A mean test to-predicted ratio much closer to 1.0, combined with a slightly lower coefficient of variation, indicates that the unified equation better represents the behavior of these connections than does the set of two block shear equations from the North American design specifications. By considering only the S16/AISC equation that assumes gross section failure on the shear planes, the test to-predicted ratio is improved from 1.46 to 1.18, but the coefficient of variation is increased slightly. It should be noted that this modified block shear approach gives similar results to the AISC bearing treatment for bolt tear-out failure. The unified equation also provides somewhat improved results over the AISC bearing provisions, which give a mean test-to-predicted ratio of 1.17, with a coefficient of variation of 0.10. The mean test-to-predicted ratio considering these new tests as well as all criterion A specimens from the literature for the unified equation is 1.00, with a coefficient of variation of 0.11, as compared to 1.28 and 0.14, respectively, for the CSA-S16-01/AISC 360-05 equations.

RELIABILITY ANALYSES

In general, an appropriate reliability index, β, which represents the probability of failure of a member or connection, can be achieved by selecting a suitable resistance factor, ϕ, for design. These two parameters are related by the bias coefficient and the coefficient of variation of resistance, which can be determined by the relevant material, geometric, professional and discretization (in this case related to the need for an integer number of bolts) parameters. A summary of the relevant reliability parameters is shown in Table 5. Details of the procedures used in the reliability analysis presented in this paper are outlined by Cai and Driver (2008).

A total of 130 test results have been collected from the literature and this research project, including those from tests on plates, channels, tees, and wide-flange shapes with various connection configurations and conventional yield strengths (not greater than 550 MPa; 80 ksi). The reliability study considers all 130 tests conforming to criterion B, although only the 56 that conform to criterion A meet the minimum end distance and pitch requirements in North American design specifications.

Tables 1 and 4 show the mean test-to-predicted (T/P) ratios and the coefficients of variation (COV) for different research projects using CSA-S16-01/AISC 360-05 and the unified equation. It is evident that the block shear equations in CSA-S16-01/AISC 360-05 generally give high test-to-predicted ratios, while the test-to-predicted ratios for the unified equation are much closer to 1.0. The coefficients of variation for the two methods are similar. The AISC bearing provisions seem to provide low test-to-predicted ratios for the test results taken from the literature, and high values for the tests conducted as part of this research. The reason for this is unclear.

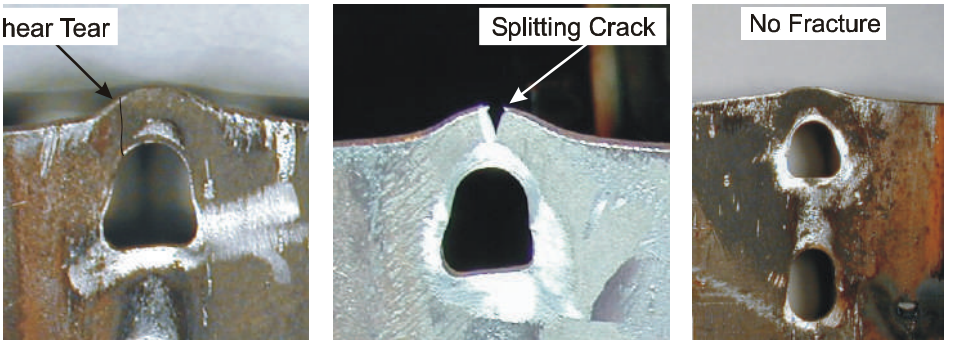

(a) Shear tear *(b) Tensile splitting crack* *(c) Ductility at a hole*

Fig. 4. End material adjacent to bolt hole.

Table 4. Summary of Test-to-Predicted Ratios						
Specimen	Predicted Capacity			Test-to-predicted Ratio		
	S16-01/ AISC 360-05 Block Shear (kN)	AISC 360-05 Bearing (kN)	Unified Equation (kN)	S16-01/ AISC 360-05 Block Shear*	AISC 360-05 Bearing	Unified Equation
A1G1	481.2/650.6	601.5	683.1	1.44/1.06	1.15	1.01
A2G1	492.9/661.4	616.1	694.4	1.47/1.09	1.17	1.04
A7G1	451.1/603.4	563.9	639.2	1.47/1.10	1.18	1.04
A8G2	441.2/595.5	551.5	630.9	1.41/1.04	1.13	0.99
A3R1	366.5/469.6	458.1	507.4	1.731.35	1.38	1.25
A4R2	599.3/772.0	749.1	834.0	1.52/1.18	1.22	1.09
A9R1	376.2/470.0	470.3	519.1	1.68/1.35	1.35	1.22
A10R2	628.9/787.2	786.1	869.3	1.22/0.97	0.97	0.88
A5E1	479.7/528.9	599.6	615.7	1.45/1.32	1.16	1.13
A6E2	623.9/629.8	779.9	733.2	1.24/1.23	0.99	1.06
A11E1	448.1/540.5	560.2	605.8	1.54/1.28	1.23	1.14
A12E2	592.2/651.1	740.2	729.8	1.34/1.22	1.07	1.09
Mean (COV)	—	—	—	1.46/1.18 (0.10/0.11)	1.17 (0.10)	1.08 (0.09)
*The second number considers Equation 3 only.						

Table 5. Parameters for Reliability Analyses			
Reliability Parameter	Plates	Shapes	
		Web Failure	Web and Flange Failure
ρ_M (block shear)	1.07	1.05	1.03
V_M (block shear)	0.054	0.063	0.063
ρ_M (bearing)	1.19	1.13	—
V_M (bearing)	0.034	0.044	—
ρ_G	1.04	1.02	0.98
V_G	0.025	0.038	0.042
ρ_d	1.04	1.04	1.04
V_d	0.033	0.033	0.033

Table 6 presents the reliability indices for the design equations considered, with the values associated with connections that would be permitted by the design specifications shown in blue. Widely accepted target values for the reliability index range from 4.0 to 4.5 for connections. The resistance factor specified in CSA-S16-01 for block shear failure is 0.9, resulting in reliability indices that vary from 3.2 to 5.3. In AISC 360-05, the resistance factor is 0.75 for block shear, resulting in reliability indices that vary from 4.3 to 6.6. For comparison, the AISC bearing provisions result in reliability indices that vary from 5.1 to 5.8 for the bolt tear-out case. The unified equation, with a resistance factor of 0.75, provides an appropriate level of safety, with reliability indices ranging from 4.2 to 4.7. The greatly improved consistency over the various connection types indicates that the unified equation provides a better representation of the bolt tear-out failure behavior than the current block shear equations and is less conservative than the bearing provi-

Table 6. Reliability Indices Provided by Design Equations					
Section	Number of Tests	Reliability Index β[c]			
		S16 01 Block Shear $\phi = 0.90$	AISC 360-05 Block Shear $\phi = 0.75$	AISC 360-05 Bearing $\phi = 0.75$	Unified Equation $\phi = 0.75$
Bolt Tear-out					
Plates	30[a]	4.4	5.5	5.1	4.3
Plates	99[b]	4.3	5.3	5.0	4.0
Channels (Web Failure)	5[b]	4.9	6.3	6.0	4.3
W-Shapes (Web Failure)	12[a,b]	5.3	6.6	5.8	4.7
Alternate Block Shear					
Tees (Web and Flange)	14[a,b]	3.2	4.3	—	4.2

a. Criterion A
b. Criterion B
c. Blue indicates a reliability index associated with connections that would be permitted by the design specification.

sions. Moreover, even if the specimens that violate the North American minimum end distance and pitch requirements are included, the unified equation still gives acceptable levels of safety, as shown in Table 6.

In the specific case of tees failing along the alternate block shear path, the reliability index obtained for CSA-S16-01 is unacceptably low. Conversely, those for the 2005 AISC *Specification* and the unified equation are both considered adequate with no effective stress factor applied.

SUMMARY AND CONCLUSIONS

Twelve full-scale tests designed specifically to investigate bolt tear-out failure have been completed on wide-flange tension members. Along with tests conducted by other researchers, a total of 116 bolt tear-out test results were analyzed. In addition, 14 tees that failed along the so-called alternate block shear path were investigated. It was found that the block shear equations in CSA-S16-01/AISC 360-05 generally provide highly conservative capacity predictions for bolt tear-out. Improved results, similar to those arising from the use of the AISC bearing equation, are achieved using the S16/AISC block shear provisions if only the equation that considers gross section failure on the shear planes is used. With the resistance factor of 0.9, CSA-S16-01 provides inconsistent reliability indices, and an unacceptably low reliability index was revealed in the case of failure of tees along the alternate block shear path. With the resistance factor of 0.75, AISC 360-05 generally provides high and inconsistent reliability indices. On the other hand, with a resistance factor of 0.75, the unified equation achieves appropriate and consistent levels of safety for the atypical block shear paths considered.

The following conclusions can be drawn from the test results of this research project, along with those from the literature:

1. The unified equation gives more accurate connection strength predictions and consistent reliability indices compared to the design equations in North American specifications for block shear failure with atypical failure paths, and the unified equation is therefore recommended for all block shear failures, regardless of whether the failure paths are classical or atypical.
2. In spite of the occurrence of tensile splitting cracks at the end bolts of some specimens that failed by bolt tear-out, the laboratory tests and strength calculations indicate that two shear planes adjacent to each bolt line carry the load approximately until the peak shear stress implied by the unified equation is reached.
3. For the bolt tear-out failure mode, based on the accurate results obtained using the unified equation model, the average stress on the shear planes at failure appears to exceed the shear yield stress but does not reach the ultimate shear stress, as has been observed in several previous research projects for cases of classical block shear failure.

ACKNOWLEDGMENTS

This research program was funded by the Steel Structures Education Foundation and the Natural Sciences and Engineering Research Council of Canada.

REFERENCES

Aalberg, A. and Larsen, P.K. (2001), "Bearing Strength of Bolted Connections in High Strength Steel," *Proceedings*, 9th Nordic Steel Construction Conference, Helsinki, Finland, pp. 859–866.

Aalberg, A. and Larsen, P.K. (2002), "The Effect of Steel Strength and Ductility on Bearing Failure of Bolted Connections," *Proceedings*, 3rd European Conference Steel Structures, Coimbra, Portugal, pp. 869–878.

AISC (2005), *Specification for Structural Steel Buildings*, AISC 360-05, American Institute of Steel Construction, Chicago, IL.

ASTM (2007), *Standard Test Methods and Definitions for Mechanical Testing of Steel Products*, A370-07, ASTM International, West Conshohocken, PA.

Cai, Q. and Driver, R.G. (2008), "End Tear-out Failures of Bolted Tension Members," *Structural Engineering Report No. 278*, Department of Civil and Environmental Engineering, University of Alberta, Edmonton, AB, Canada.

CISC (2006), *Handbook of Steel Construction*, Canadian Institute of Steel Construction, Willowdale, ON, Canada.

CSA (2001), *Limit States Design of Steel Structures*, CSA-S16-01, Canadian Standards Association, Toronto, ON, Canada.

Driver, R.G., Grondin, G.Y. and Kulak, G.L. (2006), "Unified Block Shear Equation for Achieving Consistent Reliability," *Journal of Constructional Steel Research*, Vol. 62, pp. 210–222.

Epstein, H.I. and Stamberg, H. (2002), "Block Shear and Net Section Capacities of Structural Tees in Tension: Test Results and Code Implications," *Engineering Journal*, American Institute of Steel Construction, Vol. 39, No. 4, pp. 228–239.

Franchuk, C.R., Driver, R.G. and Grondin, G.Y. (2003), "Experimental Investigation of Block Shear Failure in Coped Steel Beams," *Canadian Journal of Civil Engineering*, Vol. 30, pp. 871–881.

Huns, B.B.S., Grondin, G.Y. and Driver, R.G. (2002), "Block Shear Behaviour of Bolted Gusset Plates," *Structural Engineering Report No. 248*, Department of Civil and Environmental Engineering, University of Alberta, Edmonton, AB, Canada.

Kim, H.J. and Yura, J.A. (1999), "The Effect of Ultimate-to-Yield Ratio on the Bearing Strength of Bolted Connections," *Journal of Constructional Steel Research*, Vol. 49, No. 3, pp. 255–269.

Kulak, G.L. and Grondin, G.Y. (2001), "Block Shear Failure in Steel Members—A Review of Design Practice," *Engineering Journal*, American Institute of Steel Construction, Vol. 38, No. 4, pp. 199–203.

Puthli, R. and Fleischer, O. (2001), "Investigations on Bolted Connections for High Strength Steel Members," *Journal of Constructional Steel Research*, Vol. 57, No. 3, pp. 313–326.

Rex, C.O. and Easterling, W.S. (2003), "Behavior and Modeling of a Bolt Bearing on a Single Plate," *Journal of Structural Engineering*, American Society of Civil Engineers, Vol. 129, No. 6, pp. 792–800.

Udagawa, K. and Yamada, T. (1998), "Failure Modes and Ultimate Tensile Strength of Steel Plates Jointed with High Strength Bolts," *Journal of Structural and Construction Engineering*, Architectural Institute of Japan, Vol. 505, pp. 115–122, in Japanese.

Udagawa, K. and Yamada, T. (2004), "Ultimate Strength and Failure Modes of Tension Channels Jointed with High Strength Bolts," *Proceedings*, 13th World Conference on Earthquake Engineering Conference, Vancouver, BC, Canada.

Seismic Demand on Column Splices in Steel Moment Frames

JAY SHEN, THOMAS A. SABOL, BULENT AKBAS and NARATHIP SUTCHIEWCHARN

ABSTRACT

This study addresses seismic demands on column splices in steel moment-resisting frames. A comprehensive nonlinear analytic investigation was undertaken to evaluate the seismic response analysis of 4-, 9- and 20-story moment-resisting frames subjected to an ensemble of 20 strong ground motions. The outcomes of the study include an analysis of the comprehensive seismic demand on the column splice and recommended guidelines for design requirements for reliable moment frame column splices. The study concludes that the demand on the column splice can approach the nominal design strength of the smaller column when the critical beam-to-column connection reaches its expected maximum deformation capacity. It is reasonable that seismic design provisions for the column splices in special and intermediate moment frames require the column splice to develop the flexural strength of the smaller column.

Keywords: column splices, steel moment frames, seismic design

Steel moment frames have been one of the most frequently used seismic force resisting systems in regions of high seismicity. During the 1994 Northridge earthquake, some steel moment frames with welded moment connections suffered damage at or near their beam-to-column joints (FEMA, 2000a). Since then, the structural engineering and steel construction communities have undertaken an extensive research effort, centering on the beam-to-column connection, to investigate the cause of the damage and to improve seismic design, construction, inspection, evaluation and retrofit of steel moment frames. This research resulted in much improved understanding of seismic demand and capacity, as well as improved design requirements for beam-to-column connections in steel moment frames. The research also resulted in enhanced requirements for column splices. For example, current seismic design specification provisions (e.g., AISC 341-10) generally require that column splices in intermediate and special moment frames, when not made using complete-joint-penetration (CJP) welds, be designed to develop the expected flexural strength of the smaller connected column and the shear demand associated with flexural hinging at the top and bottom of a spliced column at a given story assuming a point of inflection at mid-height. Partial-joint-penetration (PJP) welds are currently prohibited in intermediate and special moment frame column splices.

The following issues appear to play a role in the seismic design practice of column splices:

1. Unless special precautions are taken, welded connections of steel sections subjected to seismic loads are recognized to be more susceptible to brittle fracture than was commonly acknowledged before the 1994 Northridge earthquake. Thus, higher level of filler metal Charpy V-Notch toughness are required for welded column splices in all types of moment frames covered by AISC 341-10.
2. It has been observed that partial-joint-penetration (PJP) welds, when subjected to tensile loads at right angles to the unfused portion of the welded joint, are more susceptible to brittle fracture due to high levels of stress concentration than CJP welds. Thus, AISC 341-10 requires CJP welds in lieu of PJP welds at column splices because of the potential high for flexural or tensile demands consistent with the increased ductility in the improved beam-to-column connection.
3. As suggested by columns bending in double curvature observed in elastic analyses, the demand on column splices, often located in the middle third of the story height, is assumed to be less than that found in the portion of the column directly adjacent to the beam-column joint. It was assumed that the beam-to-column connection would reach its critical limit state before the column splice did.

Jay Shen, Ph.D., P.E., S.E., Assistant Professor, Department of Civil, Architectural and Environmental Engineering, Illinois Institute of Technology, Chicago, IL (corresponding author). E-mail: shen@iit.edu

Tom Sabol, Adjunct Professor, Department of Civil and Environmental Engineering, University of California, Los Angeles, CA. E-mail: tsabol@ucla.edu

Bulent Akbas, Ph.D., Associate Professor, Department of Earthquake and Structural Engineering, Gebze Institute of Technology, Gebze Kocaeli, Turkey.

Narathip Sutchiewcharn, Graduate Student, Department of Civil, Architectural and Environmental Engineering, Illinois Institute of Technology, Chicago, IL.

Nevertheless, the question arises whether the seemingly more conservative column splice seismic design provisions in the current version of AISC 341 can be justified, compared to the column splice requirements in older seismic design provisions. While bolted column splices are permitted, the high strength required by AISC 341-10 often makes them impractical, and the revised column splice provisions often require erection aids necessary to stabilize the column prior to welding and heavy welds to satisfy the specified strength, both of which increase costs. Given the limited detailed research on this topic, a systematic seismic investigation of column splices was conducted to address the question of whether the seismic design provisions requiring development of the expected plastic flexural strength and groove welds at column splices are justified or unnecessarily conservative. A comprehensive study on column splices in steel moment frames was conducted by Shen and Sabol (2008). This paper summarizes the major results related to the seismic demand on the column splices. This demand was evaluated with respect to the demand on the frame system as whole and the demand on the beam-to-column connection in particular so that the influences of uncertainty, such as the type of ground motion and properties of the structural systems, might be properly considered.

STRUCTURES AND GROUND MOTIONS

Design of 4-, 9- and 20-Story Special Moment Frames

Three typical steel moment frames with heights equal to 4, 9 and 20 stories, representing typical low-, medium-, and high-rise steel buildings (shown in Figures 1, 2 and 3) were designed based on the seismic design requirements in ASCE 7 (2005) and AISC 341 (2005, 2010). These buildings are similar to those developed as part of the FEMA-sponsored steel frame research program conducted following the 1994 Northridge earthquake (FEMA, 2000b). The footprint of each building is symmetrical. As shown in Figure 1, the four-story building has plan dimensions of 120 ft by 180 ft with four 30-ft bays and six 30-ft bays in the two orthogonal directions, respectively, and a typical story height of 13 ft. The columns are assumed to be fixed at the ground level.

The nine-story building has plan dimensions of 150 ft by 150 ft and consists of five bays of framing in both orthogonal directions spaced at 30 ft on center. The building has a basement level (level B1 in Figure 2b). The typical story height is 13 ft except at the ground and B1 levels, where it is 18 ft and 12 ft, respectively (Figure 2b).

The 20-story building has plan dimensions of 100 ft by 120 ft and consists of five 20-ft bays and six 20-ft bays of framing in the two orthogonal directions, respectively. The building has two basements levels (levels B1 and B2). The typical story height is 13 ft except at the ground B1 and B2 levels, where it is 18 ft and 12 ft, respectively (see Figure 3b).

The columns are assumed to be pinned at the lowest basement level for the 9- and 20-story buildings respectively, although they run continuously through the ground level framing. For the 9- and 20-story buildings, concrete foundation walls and surrounding soil are assumed to prevent any significant horizontal displacement of the structure at the ground level, so the seismic base is taken at the ground level.

The buildings were designed for a site in downtown Los Angeles, where S_S is 2.0 g and S_1 is 1.0 g. The perimeter frames of the buildings in the direction of the design earthquake were designed as special moment frames using response modification factor of R = 8. The ASCE 7 (2005) base shears corresponding to the 4-, 9- and 20-story buildings were 1,440 kips, 1,950 kips and 1,530 kips, respectively. The structural system for each building consists of steel perimeter moment resisting frames and interior simply connected framing for gravity; that is, lateral loads are

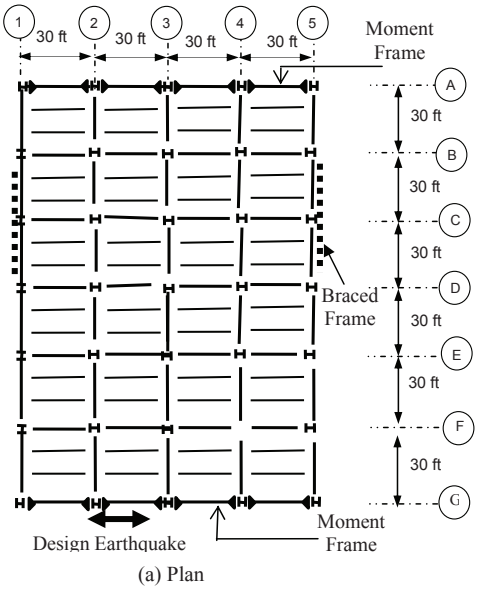

(a) Plan

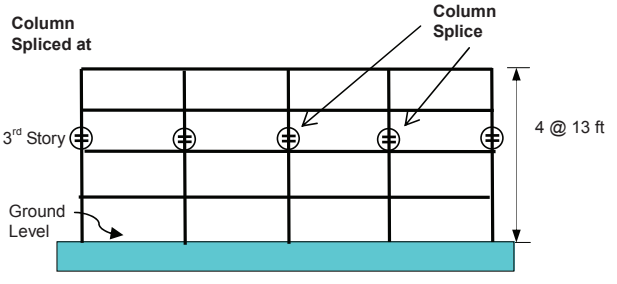

(b) Column location in the 4-story moment frame on Lines A and G

Fig. 1. Plan and elevation of the four-story frame.

carried by perimeter frames and interior frames are not explicitly designed to resist seismic loads in the direction of the earthquake and are not included in the analysis. The approximate period equation prescribed in ASCE 7 (2005) was first used to check for strength before the drift requirements were evaluated. As expected, drift requirements governed the design for all three buildings. The member sizes are summarized in Tables 1, 2 and 3, respectively. Braced frames, shown in Figures 1, 2 and 3, are used as the seismic force resisting system in the direction perpendicular to the moment frames.

The location of a column splice is considered to be a factor affecting flexural demand at the splice. With some exceptions, AISC 341 (2005, 2010) requires that column splices be located 4 ft or more away from the beam-column connection. The 4-ft offset is considered to be convenient for field welding and erection and moves the splice closer to the middle of the story height, where the flexure demand is generally thought to be lower than that at the beam-to-column connection. The 4-ft offset is typically interpreted as the distance between the column splice and top of steel girders, but actual locations of column splices may vary to some degree in any given steel building. For example, the User Note in Section D.5a of AISC 341-10 recommends that where possible, splices should be located at least 4 ft above the finished floor elevation to permit installation of perimeter safety cables prior to erection of the next tier and to improve accessibility. On the other hand, Section D.5a(2) of AISC 341-10 also permits a column splice to be located as close to the beam-to-column flange connection as the depth

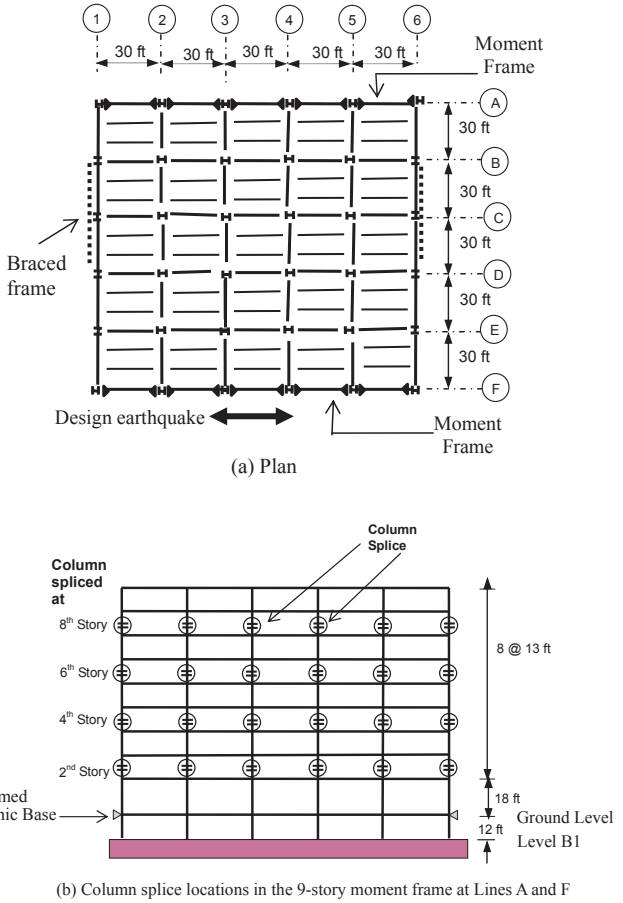

(a) Plan

(b) Column splice locations in the 9-story moment frame at Lines A and F

Fig. 2. Plan and elevation of the nine-story frame.

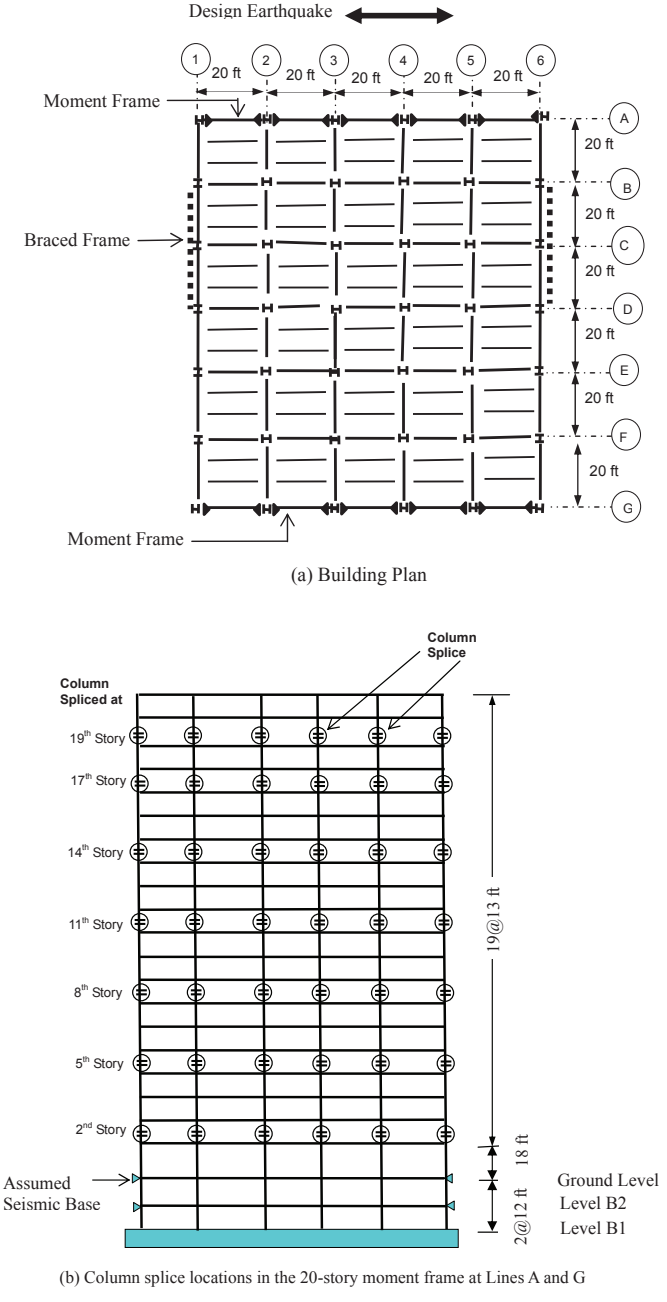

(a) Building Plan

(b) Column splice locations in the 20-story moment frame at Lines A and G

Fig. 3 Plan and elevation of the 20-story frame.

Table 1. Member Sizes of the Four-Story Frame			
Level	Exterior Column	Interior Column	Beam
4	W14×257	W14×342	W27×94
3	W14×257	W14×342	W30×148
2	W14×342	W14×426	W30×148
1	W14×342	W14×426	W30×148

Table 2. Member Sizes of the Nine-Story Frame			
Level	Exterior Column	Interior Column	Beam
9	W14×257	W14×311	W24×55
8	W14×257	W14×311	W27×94
7	W14×311	W14×426	W30×132
6	W14×311	W14×426	W30×132
5	W14×398	W14×500	W33×141
4	W14×398	W14×500	W33×141
3	W14×455	W14×550	W33×141
2	W14×455	W14×550	W33×141
1	W14×550	W14×730	W36×194
Basement	W14×550	W14×730	W36×194

of the column when the webs and flanges of the splice are connected by complete-joint-penetration groove welds. Two bounding cases, primary (PC) and secondary (SC), were included in this study, as shown in Figure 4. The PC column splice location is 4 ft above the finished floor elevation. The SC column splice location is 4 ft from the beam centerline. These two cases were studied to investigate the impact of shifts in the location of column splices. Nearly all column splices are expected to fall within the locations described by the PC and SC locations. With the 4-ft dimension taken from the top of finished floor, the PC location is considered representative of typical slabs constructed of metal deck and concrete fill and represents the expected upper bound column splice offset. The SC location moves the column splice closer to the beam-column connection (actual distances between column splices and top of steel girders are between $1.20d_c$ and $1.80d_c$ in the three frames studied) and is considered representative of the column splice location permitted by the exception listed in Section D.5a(2) of AISC 341-10. The column splices were located at every second floor of the 9-story frame and at every two to three floors in the 20-story frame. This slight deviation from common practice is not expected to affect the significance of the results, but it did ease the computational burden by reducing the number of column splices that has to be monitored. The columns in the four-story frame were spliced only at its third floor.

Table 3. Member Sizes of the 20-Story Frame			
Level	Exterior Column	Interior Column	Beam
20	W24×207	W24×103	W24×55
19	W24×207	W24×103	W27×94
18	W24×207	W24×146	W27×94
17	W24×207	W24×146	W27×94
16	W24×207	W24×192	W27×114
15	W24×207	W24×192	W27×114
14	W24×207	W24×192	W27×114
13	W24×207	W24×279	W30×148
12	W24×207	W24×279	W30×148
11	W24×207	W24×279	W30×148
10	W24×250	W24×306	W30×148
9	W24×250	W24×306	W30×148
8	W24×250	W24×306	W30×148
7	W24×250	W24×335	W30×173
6	W24×250	W24×335	W30×173
5	W24×250	W24×335	W30×173
4	W24×306	W24×370	W30×191
3	W24×306	W24×370	W30×191
2	W24×306	W24×370	W30×191
1	W24×306	W24×370	W30×191
B1	W24×306	W24×370	W30×191
B2	W24×306	W24×370	W30×191

Earthquake Ground Motions and Evaluation Method

The seismic demand on the column splice is significantly affected by selected ground motions included in the analysis, and we have strived to minimize the effects of the uncertainties involved in the ground motion. One approach to minimizing such effects is to take advantage of well established seismic design principles for steel moment frames. The fundamental philosophy in the seismic design of an intermediate or special steel moment frame is to have ductile beam-to-column connections dissipate significant amounts of seismic energy through extensive inelastic deformation so that other structural parts of the frame, including column splices, are not overloaded and remain functional. This helps reduce the potential for collapse during the design earthquake event. In other words, the peak seismic demand on the column splice can be controlled by limiting the maximum rotational capacity of the beam-to-column connection. Therefore, the seismic demand on the column splice ought to be evaluated in comparison with the demand on the entire

frame system in general, and on the beam-to-column connection in particular, for any given earthquake ground motion intensity. Thus, we developed a seismic demand evaluation methodology based on a performance-chain concept (Shen et al., 2010) in evaluating the seismic demand on the column splice under meaningful intensities in ground motions. The concept introduced in this study states that the seismic demand on the column splice should be compatible with its intended performance in comparison with that of the frame and beam-to-column connections. Based on this concept, the maximum seismic demand on the column splice is directly related to the seismic demand on the frame as a whole, regardless of the types and intensities of the ground motions selected for the study.

In this study, an ensemble of ground motions was selected so that the seismic response of each of the three frames would range from moderate to severe and the seismic demand on the column splice would be evaluated based on the response of the frames. A total of 20 ground motion records, identified as LA21 to LA40, were used. This set of ground motions were used in a Federal Emergency Management Agency (FEMA)–sponsored research project on steel moment frames damaged in the 1994 Northridge earthquake. This set of ground motions was identified as having a 2% probability of exceedance in 50 years by SAC, a consortium conducting the FEMA-sponsored project. Table 4 provides detailed information on the records. These acceleration time histories were derived from historical recordings or from physical simulations and altered so that their mean response spectrum matches the 1997 National Earthquake Hazards Reduction Program (NEHRP) design spectrum, modified from soil type of S_B–S_C to soil type S_D and having a hazard specified by the 1997 USGS maps (Somerville et al., 1997). Figure 5 summarizes the response spectra of these ground motions.

The seismic response evaluation of the column splice is based on two groups of response parameters reflecting deformation and load: (1) peak story drift ratios and inelastic deformation of the structure, represented by the maximum plastic hinge rotations at beam ends; and (2) peak load demands at the column splice, represented by (a) the maximum bending moment at the splice, M_s, normalized by the plastic moment of the smaller column (on the top of the splice), M_{pt}, and (b) the maximum combination of the normalized bending moment and tensile axial force in the column splice, P_s, normalized by the nominal tensile strength of the smaller column, P_{yt}. The first group of the response parameters provides information about the seismic performance of the frame as a whole for a given ground motion. With the seismic performance of the frame as a reference, the information in the second group is used to evaluate the severity of the demand on the column splice relative to the ground motion with respect to that of the whole frame system. This approach leads to a rational design strength requirement for the column splice within the system, where all components are interrelated, and a desirable hierarchy in the chain of the possible limit states is well defined.

In a special steel moment frame, the beam-to-column connection may well be the most critical component when subjected to strong ground motions, and its seismic behavior has been well documented in other research studies. The demand on the connection, therefore, is considered to be a reliable reference for gauging seismic design strength requirements for other components that are intended to remain elastic. In particular, the seismic demand on the column splice should be limited to a reasonable percentage of its nominal capacity compared to the deformation demand on the beam-to-column connection for any given ground motion intensity. This comparative approach provides a solid basis for developing a "capacity design" method for column splices in a

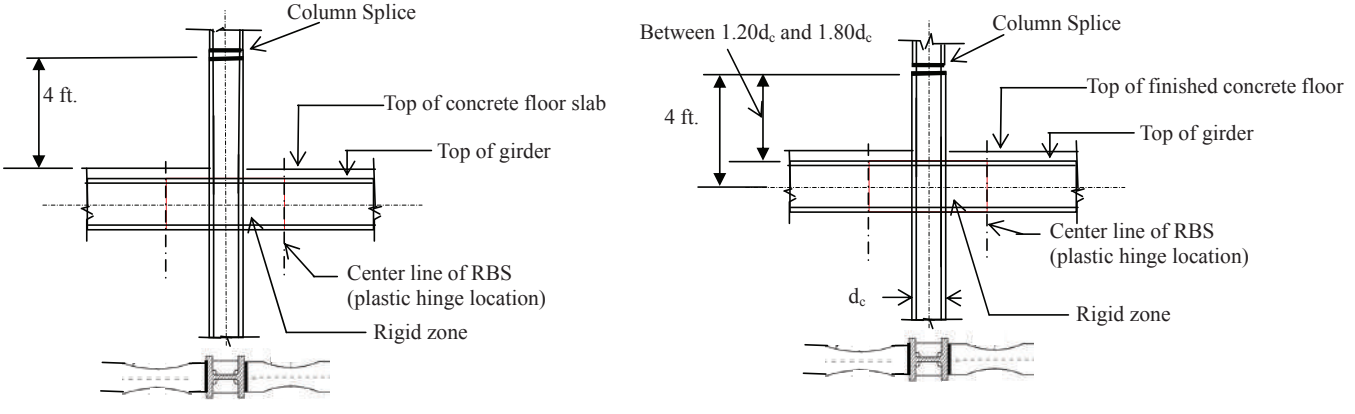

(a) Location of the column splice in Primary Case (PC)

(b) Location of the column splice in Secondary Case (SC)

Fig. 4. Locations of column splices evaluated.

Table 4. Ground Motions Used in the Study					
SAC Name	**Record**	**Earthquake Magnitude**	**Distance (km)**	**Scale Factor**	**PGA (g)**
LA21	1995 Kobe	6.9	3.4	1.15	1.28
LA22	1995 Kobe	6.9	3.4	1.15	0.92
LA23	1989 Loma Prieta	7	3.5	0.82	0.42
LA24	1989 Loma Prieta	7	3.5	0.82	0.49
LA25	1994 Northridge	6.7	7.5	1.29	0.87
LA26	1994 Northridge	6.7	7.5	1.29	0.94
LA27	1994 Northridge	6.7	6.4	1.61	0.93
LA28	1994 Northridge	6.7	6.4	1.61	1.33
LA29	1974 Tabas	7.4	1.2	1.08	0.81
LA30	1974 Tabas	7.4	1.2	1.08	0.99
LA31	Elysian Park (simulated)	7.1	17.5	1.43	1.30
LA32	Elysian Park (simulated)	7.1	17.5	1.43	1.19
LA33	Elysian Park (simulated)	7.1	10.7	0.97	0.78
LA34	Elysian Park (simulated)	7.1	10.7	0.97	0.68
LA35	Elysian Park (simulated)	7.1	11.2	1.1	0.99
LA36	Elysian Park (simulated)	7.1	11.2	1.1	1.10
LA37	Palos Verdes (simulated)	7.1	1.5	0.9	0.71
LA38	Palos Verdes (simulated)	7.1	1.5	0.9	0.78
LA39	Palos Verdes (simulated)	7.1	1.5	0.88	0.50
LA40	Palos Verdes (simulated)	7.1	1.5	0.88	0.63

special steel moment frame, in which the only designated energy dissipation portion is at the end of the beam, and all other portions (including the column splice, in the frame) are designed to remain essentially elastic with a reasonable margin of safety. This concept would still be expected to apply if inelastic deformation of the column panel zone were anticipated by the designer.

SEISMIC RESPONSE OF FRAME SYSTEMS AND PERFORMANCE CRITERIA

Inelastic dynamic analyses were conducted to study seismic column splice demands of three frames. The frames were subjected to 20 ground motion accelerations with spectral ordinates defined as having 2% probability of exceedance in 50 years. The frames were modeled as beam and column elements with potential plastic hinges at their ends. The interaction between the axial force and bending moment was considered in columns. A 5% strain-hardening ratio was assumed in the plastic hinges. P-Δ effects were always included in the time-history analyses. Modal analyses were conducted prior to time-history evaluations and indicated that the fundamental period of vibration of the 4-, 9- and 20-story frames is 0.80 s, 1.60 s and 2.40 s, respectively.

The dynamic response of the frames to the selected 20 ground motions showed dramatic variations throughout

the suite of time histories, ranging from elastic behavior to near collapse. Thus, the suite of ground motions provided a wide range of demand on the seismic column splices. Two response indices—interstory drift ratio and plastic hinge rotation at the beam end—were chosen to represent the system performance. Based on these system response indices, the seismic performance of the three frames was divided into general categories based on the severity of observed interstory drift ratio and plastic hinge rotation at the beam end. Severity was judged qualitatively based on the amount of interstory drift ratio and plastic hinge rotation demands.

Seismic Response Category and Ground Motion Group

Seismic response of frame systems, in terms of peak story drift and plastic hinge rotation at beam ends, was used to categorize the intensities of ground motions for each individual frames. The response of each frame demonstrated dramatic differences among the 20 ground motions and was divided into groups based on peak story drift ratio and plastic hinge rotation.

Table 5 presents 20 time histories divided into three ground motion groups for each of the frames, named GMG1, GMG2 and GMG3, respectively, in order of increasing peak story drifts and plastic hinge rotation at beams (i.e., from mild to very severe response). This is a shifting of the time histories that make up each group, depending on which frame is being considered. Figures 6, 7 and 8 present the system responses in terms of (1) peak story drift ratio and (2) peak plastic hinge rotation at beam ends in 4-, 9- and 20-story frames, respectively. The data show that the peak drift and plastic hinge rotation response of 4-, 9- and 20-story frames vary dramatically over the 20 ground motions, and have been divided into three qualitative groupings corresponding to GMG1, GMG2 and GMG3, as just described. It appears that the set of 20 ground motions used in this study serves the purpose of evaluating a range of seismic demands on column splices in a reasonable manner.

In order to evaluate seismic demand of column splices, the system responses of the 4-, 9- and 20-story frames to the 20 ground motions, represented by story drifts and plastic hinge rotations, are divided approximately into three seismic response categories (SRC) as described in Table 6. The SRC is defined as follows:

1. SRC I, Functional to Moderate Structural Damage: the structure is likely to be functional with limited inelastic deformation in a small number of beams having less than 0.02 rad plastic hinge rotation in any beam.
2. SRC II, Near Life-Safety: the structure is expected to sustain moderate to heavy structural damage to

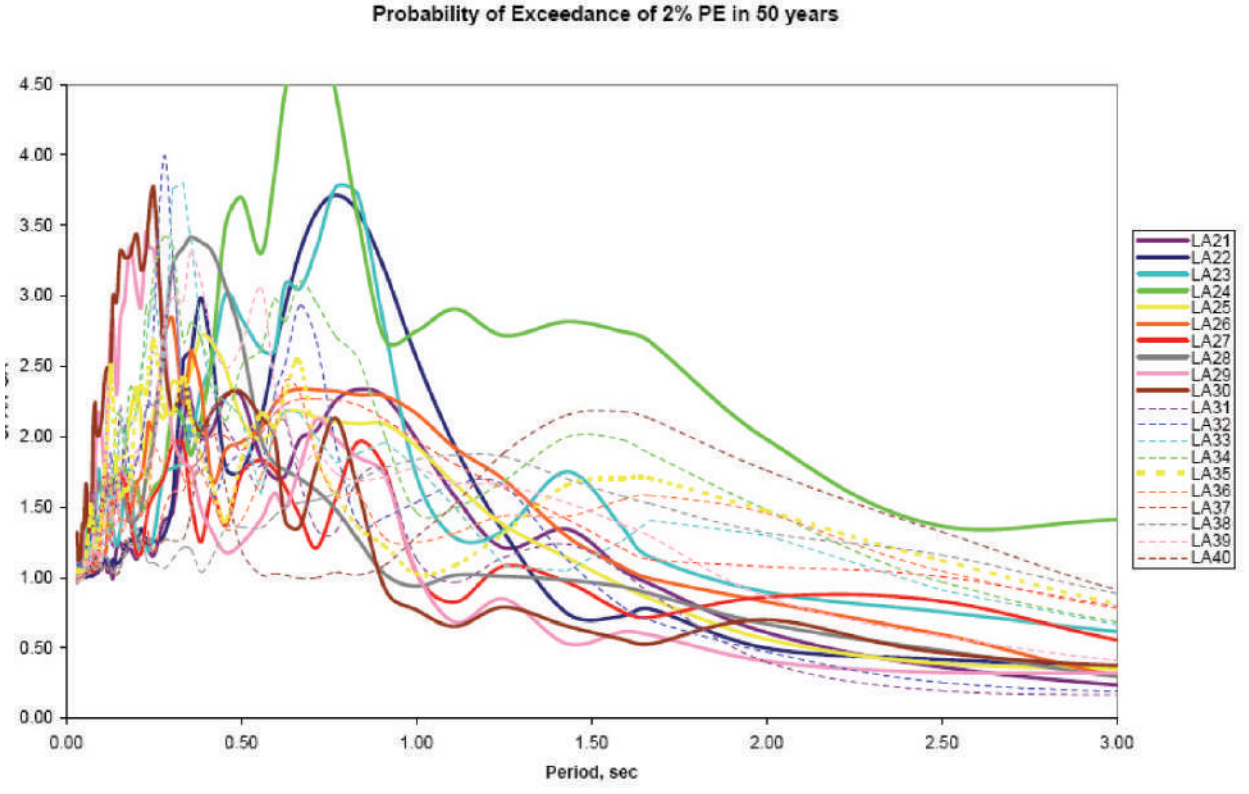

Fig. 5. Response spectra of the ground motions used in the seismic analyses.

Table 5. Ground Motion Group (GMG)			
Frame	**GMG 1**	**GMG 2**	**GMG 3**
4-story	LA23, LA24, LA27, LA28, LA29, LA30, LA31, LA33, LA34, LA35, LA39, LA40	LA21, LA22, LA25, LA26, LA32, LA36, LA37, LA38	Not Applicable
9-story	LA23, LA29, LA30, LA39	LA21, LA24, LA25, LA26, LA28, LA32, LA34, LA37	LA22, LA27, LA31, LA33, LA35, LA36, LA38, LA40
20-story	LA23, LA29, LA31, LA39	LA21, LA22, LA25, LA27, LA28, LA30, LA32, LA33, LA34, LA37, LA40	LA24, LA26, LA35, LA36, LA38

Table 6. System Response Category (SRC) of the Steel Moment Frames			
SRC	**GMG**	**Story Drift Ratio (SDR)**	**Plastic Hinge Rotation (PHR)**
I	1	0.01 to 0.02	0.01 to 0.02
II	2	0.02 to 0.04	0.02 to 0.04
III	3	0.04 to 0.05	0.04 to 0.05

its connections with many beam ends having plastic hinge rotations on the order of 0.02 to 0.04 rad.

3. SRC III, Life-Safety to Near Collapse: the structure has extensive and widely spread plastic hinge rotations on the order of 0.04 to 0.05 rad in many beams.

It is noted that the four-story frame suffers consistently lower system response than that in other two taller frames, and does not experience SRC III response.

Correlations between Column Splice Demand and System Response

The response indices, story drift ratio (SDR) and plastic hinge rotation (PHR), together with more detailed information about structural response of the three frames subject to the 20 ground motions (Shen and Sabol, 2008), have demonstrated that it is possible for the seismic demand on the column splice to be directly related to the response of the system, instead of ground motions themselves, because of strong correlation between the column splice demand and system response. This suggests the following observations:

1. The ground motions that produce the maximum bending moments at column splices also result in maximum plastic hinge rotations at beam ends, indicating a close correlation between the bending moment in the column splice and the level of inelastic deformation in the structural system as a whole.
2. Extensive beam plastic hinge rotations in the frames subject to GMG 3 ground motions cause some columns in the 9- and 20-story frames to bend in single curvature and, in some extreme events, force some exterior columns to form plastic hinges at their ends under combined tensile axial force and bending moment. This behavior leads to significant bending moments at column splices and high tensile forces in interior columns. The frames in these events would be near their collapse thresholds with beam plastic hinge ration approaching or exceeding 0.06 rad.
3. The formation of plastic hinges in exterior columns due to high beam-end plastic hinge rotations under GMG 3 is responsible for unusually large P_s/P_{yt} ratios in some interior columns.

Maximum plastic hinge rotations on the order of 0.06 rad are expected to have resulted in extensive damage, evidenced by the fact that the ultimate plastic hinge rotation capacity of special moment frame beam-to-column connections under seismic loads are expected to be in the range of 0.04 to 0.06 rad. An evaluation of seismic design requirements for column splices must answer the question of whether or not the splice is adequate to survive theses large demands in the beams with an adequate margin of safety.

When the frames are exposed to significant inelastic deformation demands, the analytic results suggest seismic demands on the splice that are different from those conventionally assumed to occur based on an elastic analysis. For

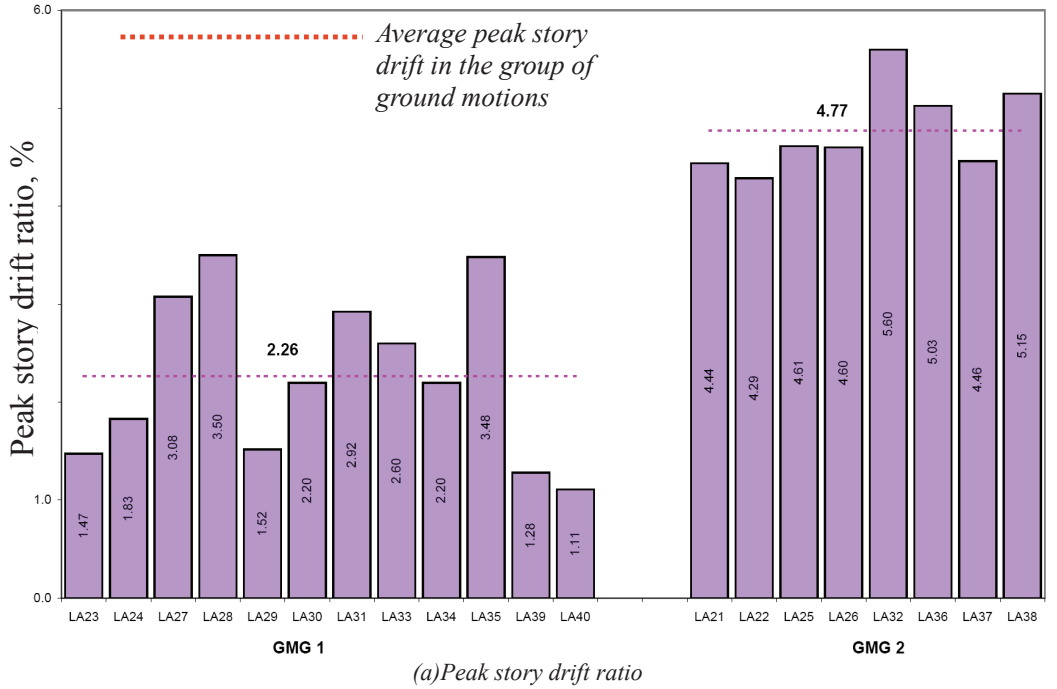

(a)Peak story drift ratio

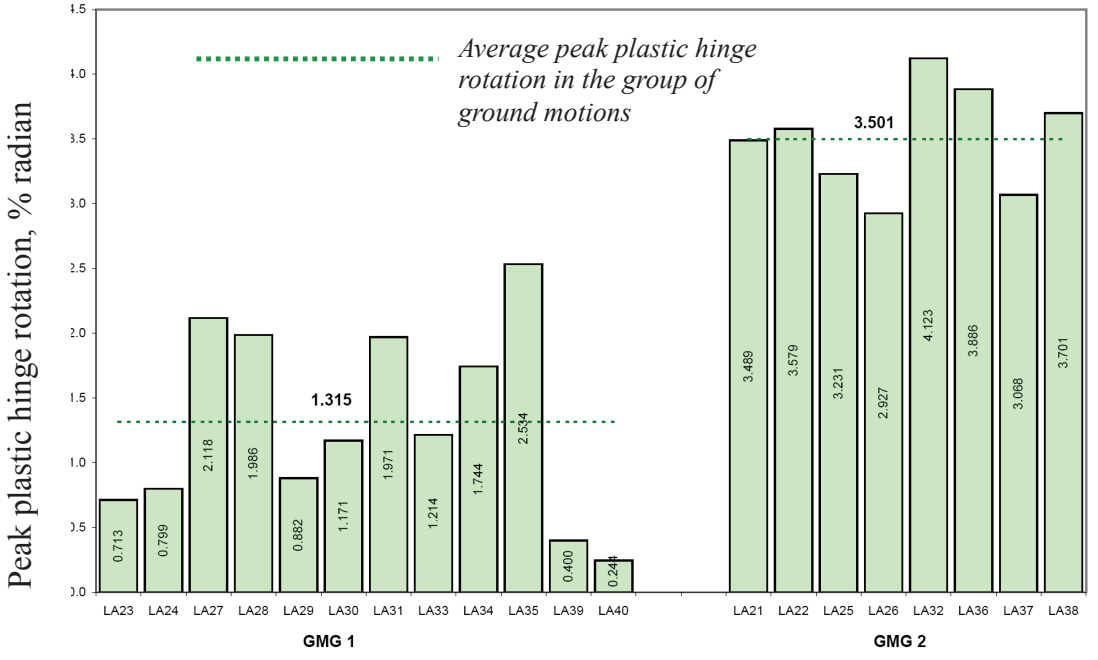

(b)Peak plastic hinge rotation at beam ends

Fig. 6. System response of the four-story frame subjected to the 20 ground motions.

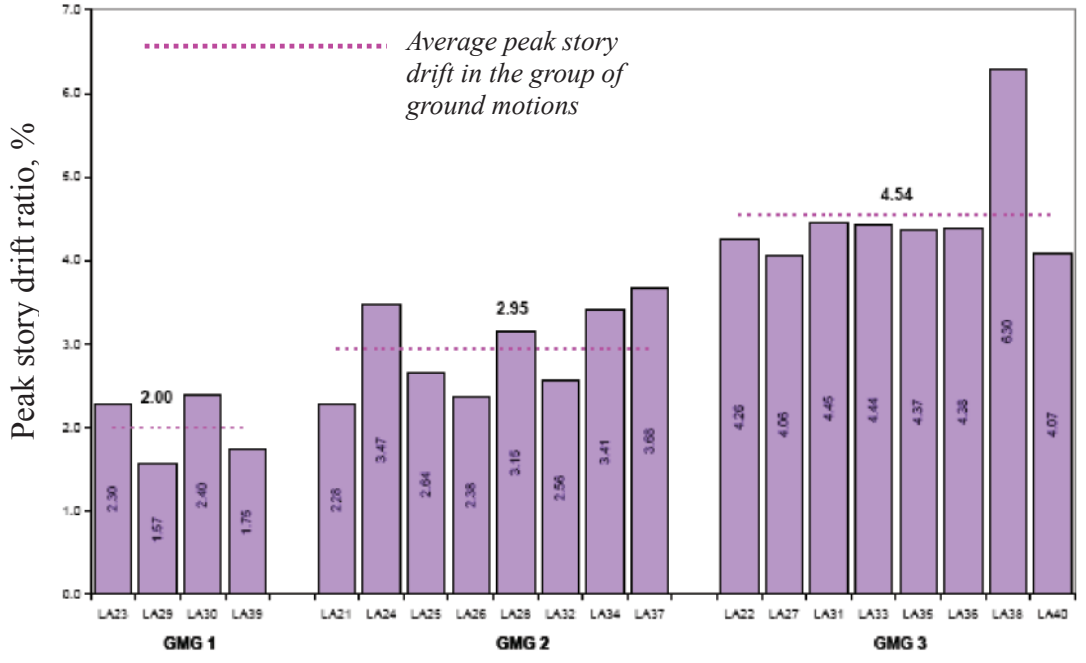

(a)Peak story drift ratio

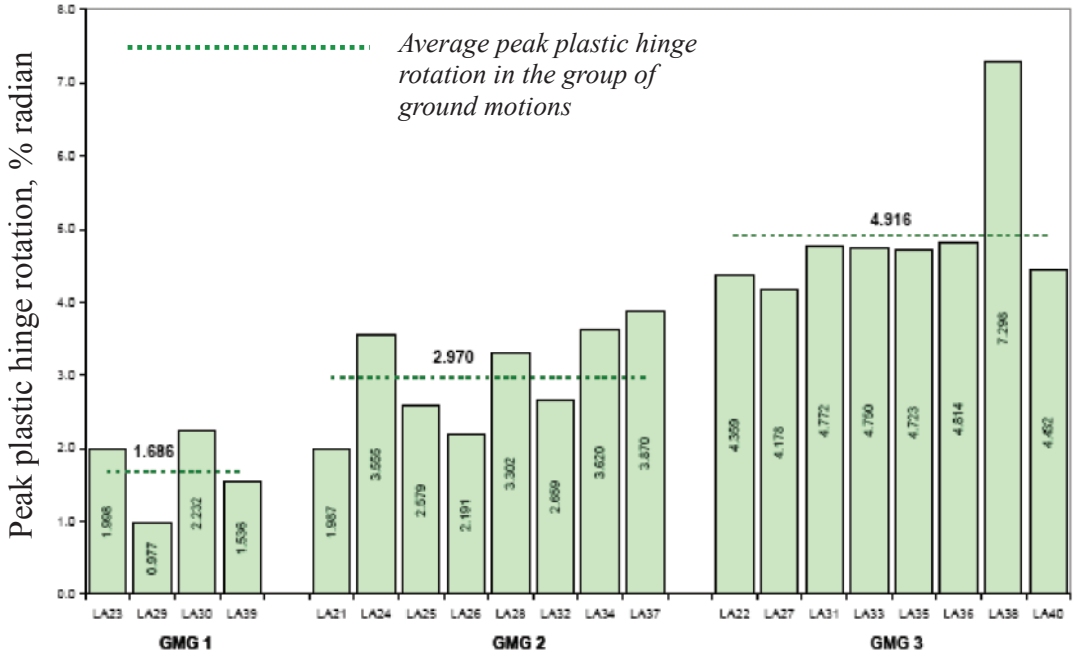

(b)Peak plastic hinge rotation at beam ends

Fig. 7. System response of the nine-story frame subjected to the 20 ground motions.

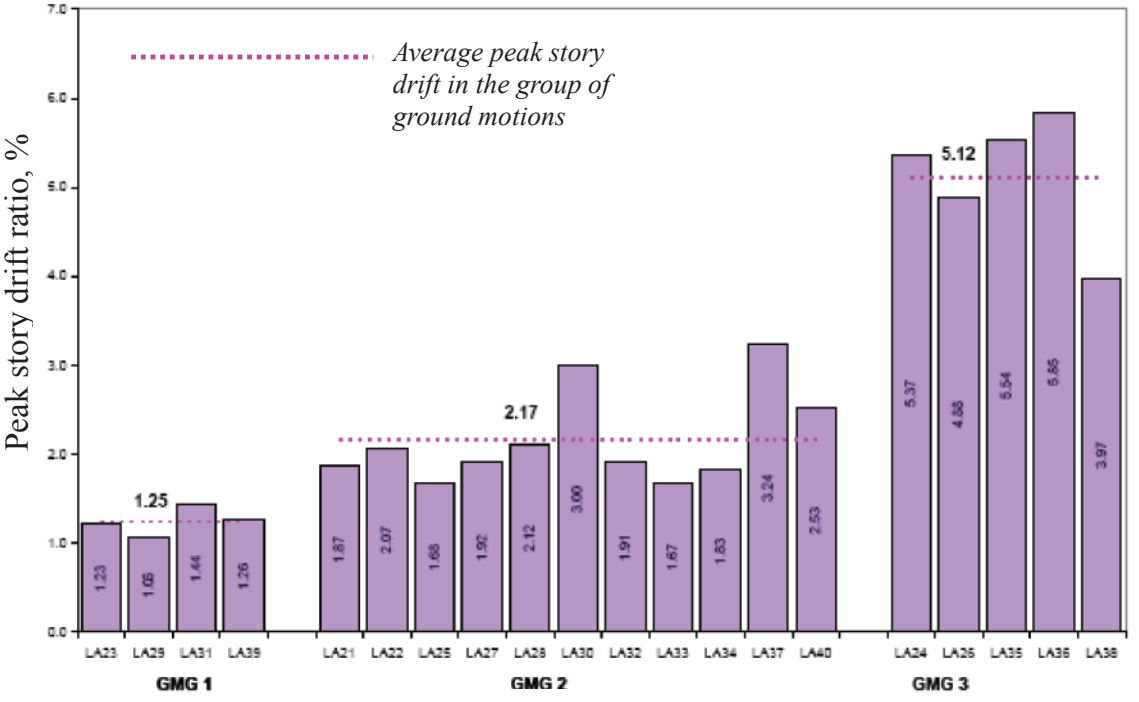

(a)Peak story drift ratio

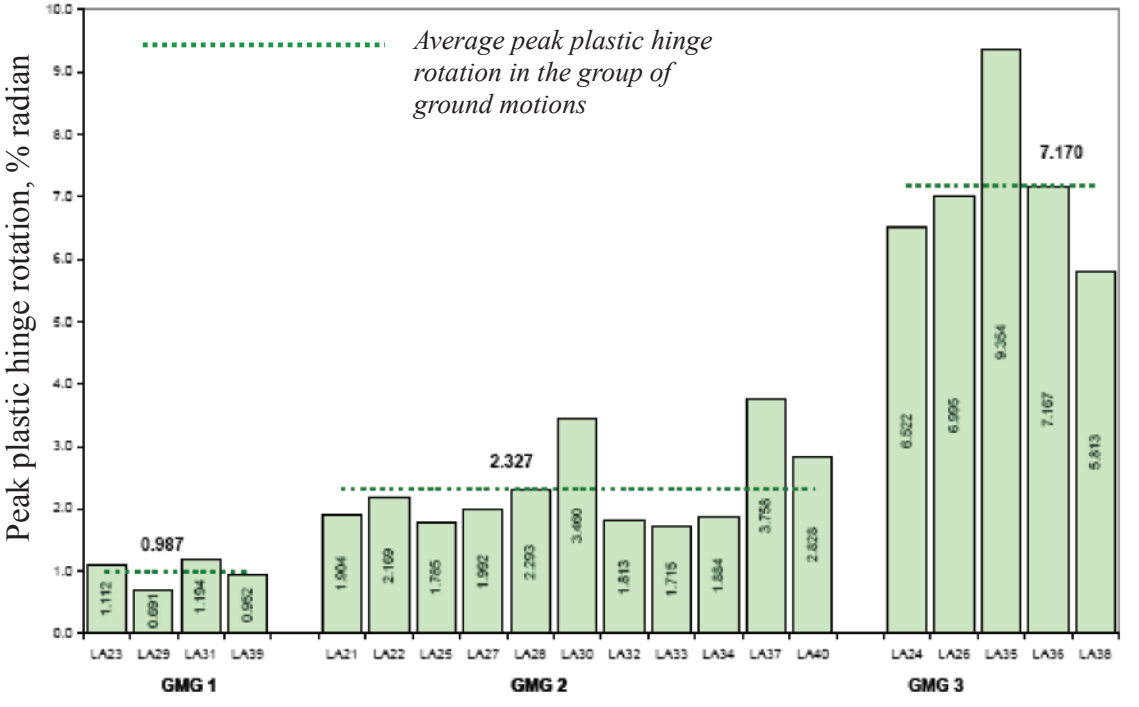

(b)Peak plastic hinge rotation at beam ends

Fig. 8. System response of the 20-story frame subjected to the 20 ground motions.

Table 7. $\frac{M_s^{PC}}{M_s^{SC}}$ Ratio Statistics

Frame	GMG 1/SRC I		GMG 2/SRC II		GMG 3/SRC III	
	Mean μ	Standard Deviation σ	Mean μ	Standard Deviation σ	Mean μ	Standard Deviation σ
4-story	0.57	0.13	0.92	0.07	Not Applicable	
9-story	0.68	0.03	0.76	0.07	0.79	0.05
20-story	0.65	0.02	0.79	0.09	0.90	0.06

example, if we assume a point of inflection at mid-story and a straight line moment diagram with the maximum column moment at the beam centerline, it is expected that the column moment at the typical column splice location will be approximately 20% of that maximum moment. On the other hand, for GMG 2 and GMG 3, the average bending moment in the splice was found to be approximately 60% to more than 80% of the plastic moment capacity of the smaller column, as shown in Figures 9a, 10a and 11a.

SEISMIC DEMAND ON THE COLUMN SPLICES

Peak Bending Moment at the Column Splice, M_s

The peak bending moment in all column splices in a given frame, M_s, normalized by M_{pt}, the plastic moment of the smaller column on the top of splice, is summarized in Figures 9a, 10a and 11a for the 4-, 9- and 20-story frames, respectively, subjected to the suite of 20 ground motion time histories. Two different structural models, primary case (PC) and secondary case (SC), were analyzed. The only difference between the two models was the column splice location. In the PC model, the column splices were placed 4 ft above the floor slab. In the SC model, the column splices were assumed 4 ft above the beam center line, which serves as a reference to compare with the PC model in order to discuss the influence of the column splice location on column splice demand.

The difference in the bending moment at the column splice, M_s, between two models is presented in Table 7 as the mean value and standard deviation of M_s^{PC}/M_s^{SC} ratio for the three frames studied, where M_s^{PC}, M_s^{SC} is the peak bending moment at any column splice in PC and SC models, respectively.

Influence of Column Splice Location on Moment Demand

From Figures 9, 10, and 11 and Tables 7 and 8, one can observe the following:

1. The peak bending moment at column splices is generally lower from the PC model than the SC model. This is consistent with the general expectation that the column splice moment will generally be lower as the splice is moved away from the beam-column joint.
2. The difference in the peak bending moment between the PC and SC models appears to be significant when the frame system response is mild or moderately severe (i.e., response to GMG 1 and GMG 2); however, such differences become less significant when the structure experiences large inelastic deformation (i.e., responses to GMG 3). As shown in Table 7, the difference in moment demand at column splices between the two models was about 30% to 40% when seismic response of the frames was mild (in GMG 1/SRC I case) and about 10% to 20% when seismic response of the frame was moderately severe (in GMG 2/SRC II case) in all three frames. When seismic response of the frames was very severe (in GMG 3/SRC III case), the difference in moment demand at column splices between two models is about 10% in the 20-story frames, and about 20% in the 9-story frame. This suggests that the moment gradient is less steep than it is for the smaller seismic demand. The less steep moment gradient would be consistent with columns bent in single curvature.

Bending Moment Demand on Column Splice with Respect to Seismic Response of the Frame

The following discussions focuses on the general trends of column splice moment demand with respect to the severity of structural response based on the PC model since the results from both PC and SC models have the similar trends. As shown in Table 9, the following points appear relevant:

1. When the frames had a mild (i.e., little or limited inelastic) response (GMG 1/SRC I response), the M_s/M_{pt} ratio at the column splice was consistently less than 0.40 in the four-story frame, and less than 0.35 in the 9- and 20-story frames.

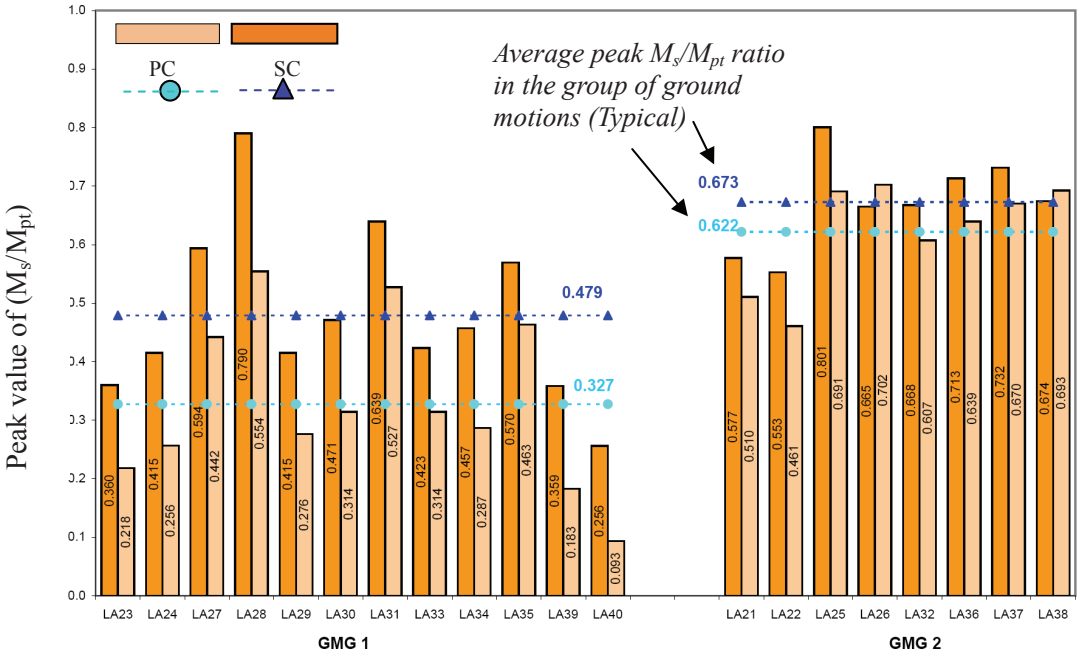

(a)Peak value of M_s/M_{pt}

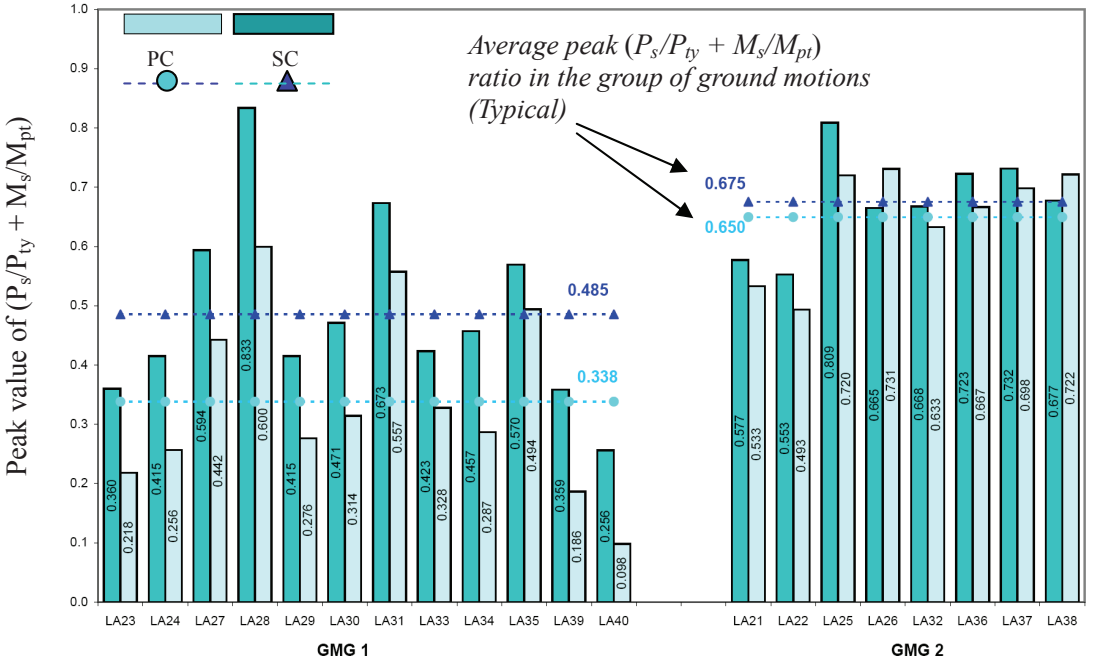

(b)Peak value of (P_s/P_{ty} + M_s/M_{pt})

Fig. 9. Column splice response of the four-story frame subjected to the 20 ground motions.

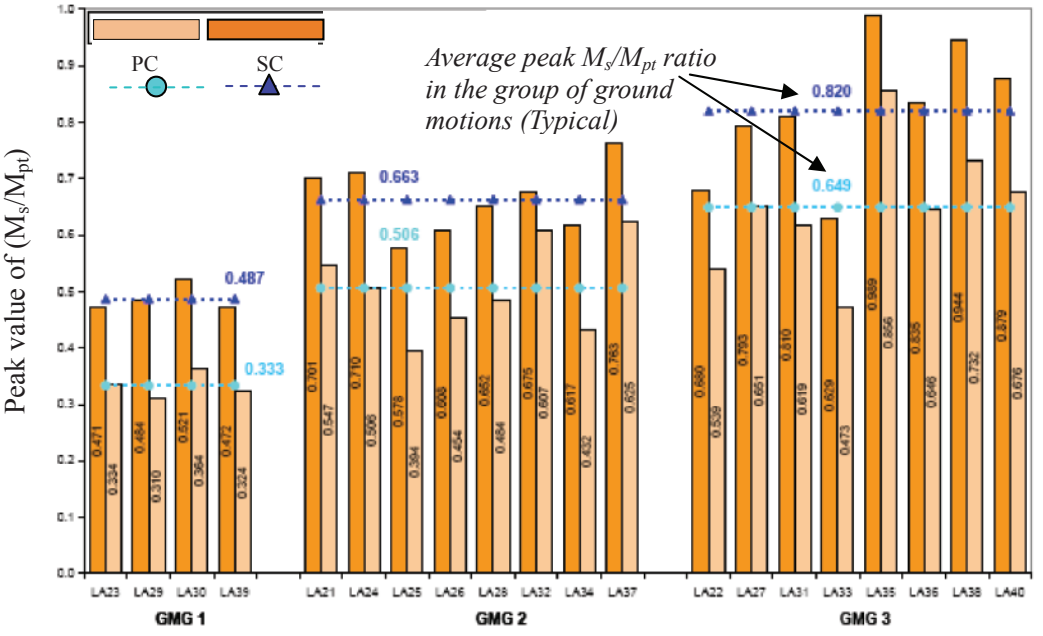

(a)Peak value of M_s/M_{pt}

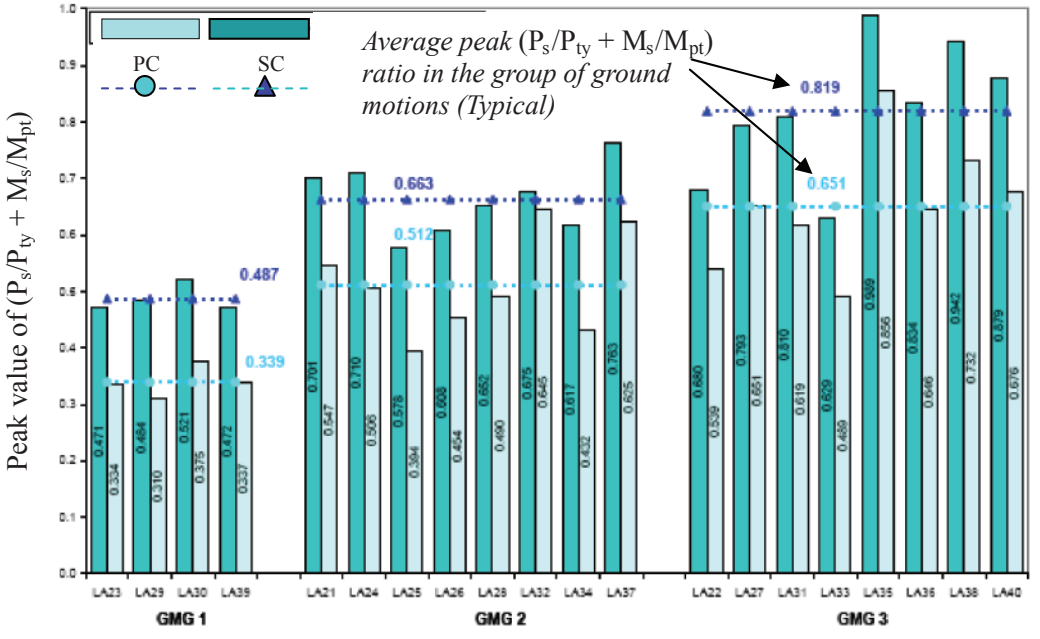

(b)Peak value of ($P_s/P_{ty} + M_s/M_{pt}$)

Fig. 10. Column splice response of the nine-story frame subjected to the 20 ground motions.

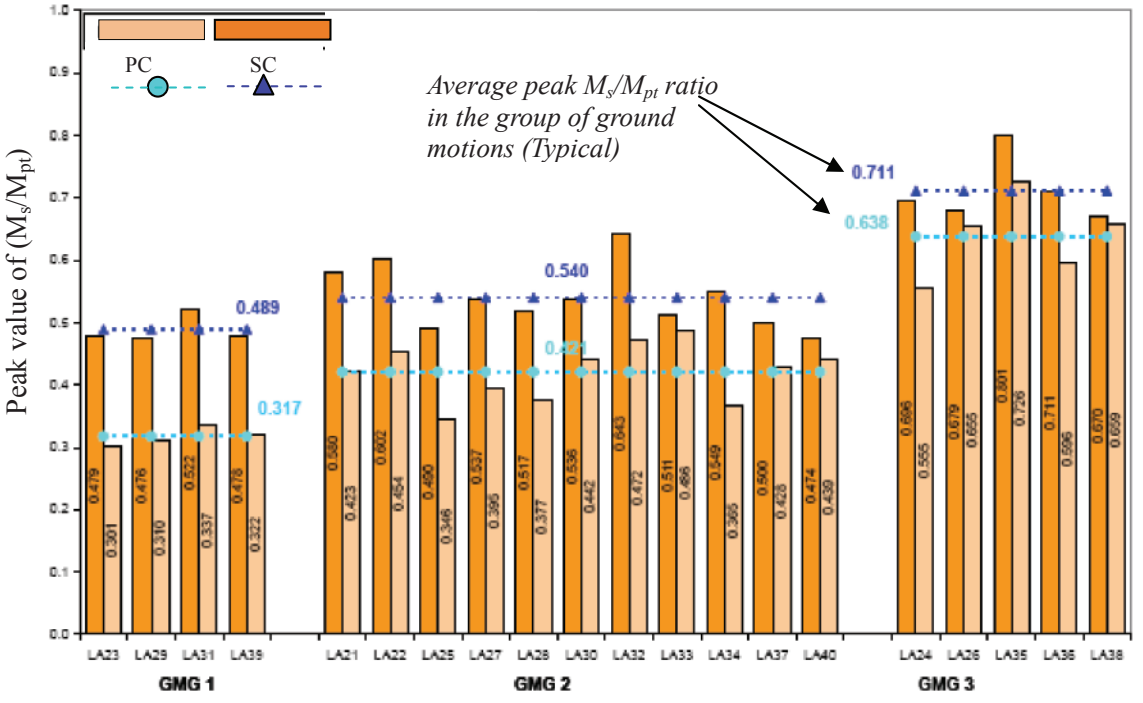

(a)Peak value of M_s/M_{pt}

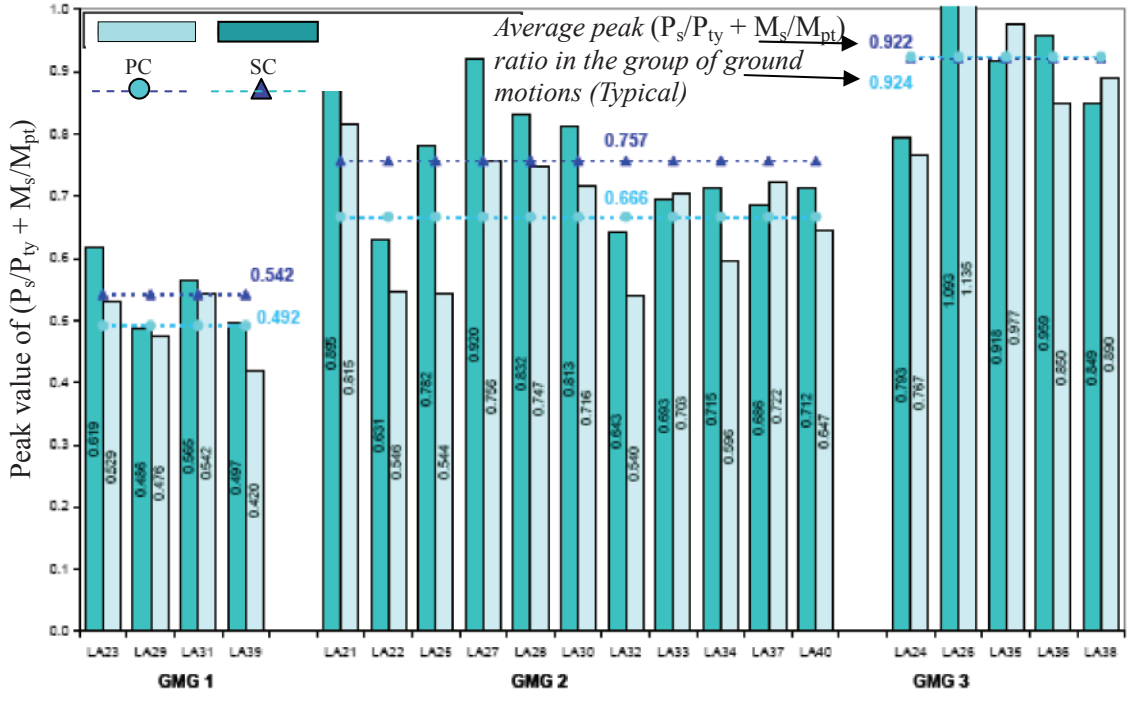

(b)Peak value of (P_s/P_{ty} + M_s/M_{pt})

Fig. 11. Column splice response of the 20-story frame subjected to the 20 ground motions.

Table 8. $\frac{\left(P_s/P_{ty} + M_s/M_{pt}\right)^{PC}}{\left(P_s/P_{ty} + M_s/M_{pt}\right)^{SC}}$ Ratio Statistics

Frame	GMG 1/SRC I		GMG 2/SRC II		GMG 3/SRC III	
	Mean μ	Standard Deviation σ	Mean μ	Standard Deviation σ	Mean μ	Standard Deviation σ
4-story	0.67	0.13	0.96	0.07	Not Applicable	
9-story	0.70	0.03	0.77	0.08	0.80	0.05
20-story	0.91	0.06	0.89	0.09	1.00	0.07

2. When the frames experience moderate to large amounts of inelastic deformation (GMG 2/SRC II response with beam end plastic hinge rotations between 0.02 and 0.04 rad), the M_s/M_{pt} ratio has a mean value of 0.622 with a standard deviation of 0.092 in the 4-story frames, a mean value of 0.506 with a standard deviation of 0.075 in the 9-story frame, and a mean value of 0.421 with a standard deviation of 0.043 in the 20-story frame.
3. When the frames experience extremely large inelastic deformation with the beam end plastic hinge rotations between 0.05 and 0.07 rad (GMG 3/SRC III response), the M_s/M_{pt} ratio has a mean value of 0.649 with a standard deviation of 0.100 in the 9-story frame and a mean value of 0.638 with a standard deviation of 0.059 in the 20-story frame.

Peak Combination of Bending Moment and Axial Tensile Force in the Column Splice

Axial tensile forces can result in significant demands on the column splice, particularly in a taller frame, such as the 20-story frame examined in this study. Figures 9b, 10b and 11b summarize the peak combination of normalized bending moment and axial tensile force in column splices in the 4-, 9- and 20-story frames, ($P_s/P_{ty} + M_s/M_{pt}$), where P_s is the tensile force at the splice, and P_{ty} (= F_yA_g) is the nominal tensile strength of the smaller column. The results from two structural models, PC and SC, are plotted in the same figures for comparison.

Influence of Column Splice Location on the Combined Moment and Axial Force Demand

Because the axial force demand at the column splice is independent of splice location, the total seismic demand on a column splice, in terms of combined moment and axial force, appears less affected by the splice location when axial force demand is significant. From Figures 9b, 10b and 11b and Table 8, one can make the following observations:

1. Peak combined moment and axial force demand at column splices is consistently lower in the PC model than in the SC model for all three frames when the frame system response was mild or moderately severe (in GMG 1/SRC I and GMG 2/SRC II cases). This is consistent with the observation that overall peak demand is highly correlated with peak flexural demand and that splice location does not affect peak tensile demand for less significant ground motions in short- or medium-height frames.
2. When the seismic response of the frames was very severe (in GMG 3/SRC III case), the difference in the combined moment and axial force demand due to different splice locations became less insignificant. In particular, the peak combined moment and axial force demand in the 20-story frame appears to be independent of the column splice location. It was noted, for example, that the demands at the column splice are higher in the PC model than those in the SC models for some ground motions in GMG 3 group, but for other ground motions in the group the opposite was true. This suggests that the maximum combined demand was significantly more sensitive to axial forces in the taller frames.

Combined Moment and Axial Force Demand on Column Splice with Respect to Seismic Response of the Frame

Based on a review of the PC model simulation data, the following general trends were observed for combined moment and axial force demand at a column splice with respect to the severity of structural response:

1. Tensile axial forces in columns in taller frames may be significant for frames that have experienced moderate or extensive inelastic deformation.
2. A more significant impact of the tensile axial force on the column splice is observed in a taller frame even under less severe ground motions. In particular, the peak

Table 9. Summary of Seismic Response (of PC Model)					
Ground Motion Group (GMG)	System Response Category (SRC)	Building Type	Peak System Response (PHR) $\mu \pm \sigma$	Peak Demand on Column Splices	
				M_s/M_{pt} $\mu \pm \sigma$	$P_s/P_{ty} + M_s/M_{pt}$ $\mu \pm \sigma$
1	I	4-story	0.013 ± 0.007	0.327 ± 0.135	0.338 ± 0.141
		9-story	0.017 ± 0.008	0.333 ± 0.020	0.339 ± 0.020
		20-story	0.010 ± 0.002	0.317 ± 0.013	0.492 ± 0.048
2	II	4-story	0.035 ± 0.004	0.622 ± 0.092	0.650 ± 0.085
		9-story	0.030 ± 0.007	0.506 ± 0.075	0.512 ± 0.080
		20-story	0.023 ± 0.007	0.421 ± 0.043	0.666 ± 0.089
3	III	4-story	Not Applicable	Not Applicable	
		9-story	0.050 ± 0.009	0.649 ± 0.100	0.651 ± 0.090
		20-story	0.070 ± 0.012	0.638 ± 0.059	0.924 ± 0.125

combination of normalized bending moment and axial tensile force of the column splice in the 20-story frame has reached a mean ratio of 0.666 with a standard deviation of 0.089 when the frame has 0.02 to 0.03 rad plastic hinge rotation subjected to GMG 2 ground motions. This ratio reaches a mean value of 0.924 with a standard deviation of 0.125 when the frame has around 0.07 rad plastic hinge rotations.

SUMMARY, CONCLUSIONS AND RECOMMENDATIONS

For the 4-, 9- and 20-story frames reviewed in this study, column splice demand based on a structural model assuming the column splice located 4 ft above the floor (i.e., the PC model), the following conclusions can be drawn:

1. The response of all three types of frames to the selected 20 ground motions, all defined as having a 2% probability of exceedance in 50 years, may be qualitatively divided into three different seismic response categories (SRC) consisting of little to moderate structural damage (SRC I system response), moderate to severe structural damage (SRC II system response), and near collapse (SRC III system response), respectively. In other words, the frames, representing low to moderately tall moment frames, show a wide range of seismic response to the 20 ground motions, as can be seen in Table 9.
2. The seismic demand on the column splice appears to be closely related to primary system response indices such as the magnitude of plastic hinge rotations at the beam end. These facts enable us to evaluate the seismic demand on the column splice based on the response of the frame to the selected ground motions, rather than solely on the ground motions themselves.
3. When the seismic response of the frame is low to moderate, a comparison between different column splice locations (e.g., the PC and SC models) suggests that the bending moment demand at a splice closer to the column mid-height (i.e., the PC model) is consistently lower than when the splice is taken at the beam-column joint centerline.
4. When frames experience heavy inelastic deformation (e.g., the SRC III case), the influence of the column splice location on observed splice demand becomes less significant. In particular, when axial force is a significant contributor to overall splice demand, the seismic demand at the column splice appears to be independent of splice location.
5. The peak bending moment at a column splice may reach 60% of the flexural strength of the smaller column when the maximum plastic hinge rotations are less than 0.04 rad (i.e., SRC I and II response) and up to 70% to 80% of flexural strength of the smaller column when the maximum plastic hinge rotations are between 0.05 and 0.07 rad (i.e., SRC III system response).
6. The significant impact of applied tensile axial forces on the column splice is observed in taller frames even under less severe ground motions (e.g., GMG 2). Some column splices appear to experience demand-to-capacity ratios (D-C) considering peak combined bending moment and tensile demand of up to 0.8 when the maximum plastic hinge rotation is as low as 0.02 rad and between 0.9 and 1.0 when the maximum plastic hinge rotation is on the order of 0.07 rad.

7. Given the many uncertainties inherent in these types of analyses, it would be reasonable to anticipate at least SRC II system response when a frame is subjected to the 2% probability of exceedance design earthquake. SRC III system response is certainly possible for some types of ground motions and may be relatively more frequent for taller frames. Demand on the column splice can be on the order of the smaller column's strength when the critical beam-to-column connection reaches its expected maximum deformation capacity.

Based on this analytical study, the following recommendations are suggested:

1. Until additional research considering combined cyclic flexural and tensile actions reduces the uncertainty inherent in reliably estimating the capacity of a welded column splice constructed using partial-joint-penetration groove welds, it is recommended that a significant margin of safety be provided for column splices in seismic load-resisting structures.
2. For special moment frames in moderately tall structures (e.g., those taller than approximately nine stories, where the effects of tensile axial loads on column splices may be significant), current requirements mandating use of complete-joint-penetration groove welds in welded column splices appears reasonable.
3. For special moment frames in shorter structures (e.g., those less than or equal to approximately nine stories), current requirements mandating use of complete-joint-penetration groove welds in welded column splices appear conservative. Welded splices using partial-joint-penetration groove welds (or the equivalent bolted splice) designed to develop at least $0.8M_p$ of the smaller column appear to provide a reasonable margin of safety and could be permitted.
4. Based on the seismic demands on the column splices determined from this study, it is recommended that an experimental and analytical study be undertaken to investigate the performance of column splices using partial-joint-penetration groove welds (or equivalent bolted splices) under combined cyclic flexural and tensile axial force demands. This additional research could also investigate the reliability of the proposed height limitations proposed (e.g., above and below nine stories) using methodologies such as those outlined in ATC-63 (FEMA P695 [FEMA, 2006]).

ACKNOWLEDGMENTS

The paper was made possible in part by the support of the American Institute of Steel Construction, the Illinois Institute of Technology, and the University of California at Los Angeles. The authors wish to thank all reviewers for their invaluable comments. Particularly, special thanks are due to Tom Schlafly of AISC for his encouragement and detailed comments throughout the project, of which this paper is one of the products. The opinions expressed in this paper are solely those of the authors and do not necessarily reflect the views of the Illinois Institute of Technology, the University of California at Los Angeles, or the Gebze Institute of Technology; nor the American Institute of Steel Construction; nor other agencies and individuals whose names appear in this document.

REFERENCES

AISC (2005), *Seismic Provisions for Steel Structural Buildings*, AISC 341-05, American Institute of Steel Construction, Chicago, IL.

AISC (2010), *Seismic Provisions for Steel Structural Buildings*, AISC 341-10, American Institute of Steel Construction, Chicago, IL.

ASCE (2005), *Minimum Design Loads for Buildings and Other Structures*, ASCE 7-05, American Society of Civil Engineers, Reston, VA.

FEMA (2000a), *Recommended Seismic Design Criteria for New Steel Moment-Frame Buildings*, FEMA 350, Federal Emergency Management Agency, Washington, DC.

FEMA (2000b), *State of the Art Report on Systems Performance of Steel Moment Frames Subject to Earthquake Ground Shaking*, FEMA 355C, Emergency Management Agency, Washington DC.

FEMA (2006), *Quantification of Building Seismic Performance Factors*, FEMA P695, Federal Emergency Management Agency, Washington, DC.

Shen, J. and Sabol, T. (2008), "Seismic Demand on the Column Splices in Special Steel Moment Frames," *Technical Report to American Institute of Steel Construction*, American Institute of Steel Construction, Chicago, IL.

Shen, J., Sabol, T. and Akbas, B. (2010), "Performance-Chain Concept for Performance-based Seismic Design," *Journal of Structural Engineering*, ASCE, in press.

Somerville, P., Smith, N., Punyamurthula, S. and Sun, J. (1997), "Development of Ground Motion Time Histories for Phase 2 of the FEMA/SAC Steel Project," SAC Background Document, Report No. SAC/BD-97/04.

Design of Structural Steel Pipe Racks

RICHARD M. DRAKE and ROBERT J. WALTER

ABSTRACT

Pipe racks are structures in petrochemical, chemical and power plants that are designed to support pipes, power cables and instrument cable trays. They may also be used to support mechanical equipment, vessels and valve access platforms. Pipe racks are non-building structures that have similarities to structural steel buildings. The design requirements found in the building codes are not clear on how they are to be applied to pipe racks. Several industry references exist to help the designer apply the intent of the code and follow expected engineering practices. This paper summarizes the building code and industry practice design criteria, design loads and other design consideration for pipe racks.

Keywords: non-building structures, pipe, racks, support, design

Pipe racks are structures in petrochemical, chemical and power plants that support pipes, power cables and instrument cable trays. Occasionally, pipe racks may also support mechanical equipment, vessels and valve access platforms. Pipe racks are also referred to as pipe supports or pipeways. Main pipe racks transfer material between equipment and storage or utility areas. Storage racks found in warehouse stores are not pipe racks, even if they store lengths of piping.

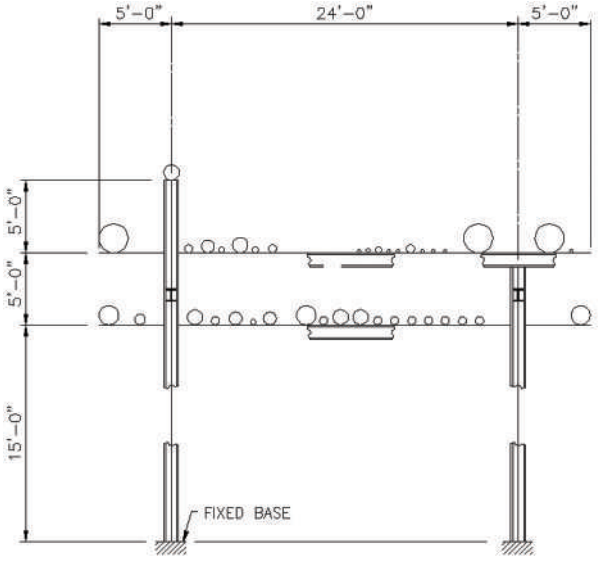

Fig 1. Typical transverse frame (bent).

Richard M. Drake, S.E., SECB, Senior Fellow, Structural Engineering, Fluor Enterprises, Inc., Aliso Viejo, CA (corresponding author). E-mail: rick.drake@fluor.com

Robert J. Walter, S.E., P.E., Principal Civil/Structural Engineer, CB&I Steel Plate Structures, Plainfield, IL. E-mail: rwalter@cbi.com

To allow maintenance access under the pipe rack, transverse frames (bents) are typically moment-resisting frames that support gravity loads and resist lateral loads transverse to the pipe rack. See Figure 1 for a typical pipe bent. Although the bent is shown with fixed base columns, it can also be constructed with pinned base columns if the supported piping can tolerate the lateral displacement.

The transverse frames are typically connected with longitudinal struts. If diagonal bracing is added in the vertical plane, then the struts and bracing act together as concentrically braced frames to resist lateral loads longitudinal to the pipe rack. See Figure 2 for an isometric view of a typical pipe rack.

If the transverse frames are not connected with longitudinal struts, the pipe rack is considered to be "unstrutted." The frame columns act as cantilevers to resist lateral loads longitudinal to the pipe rack.

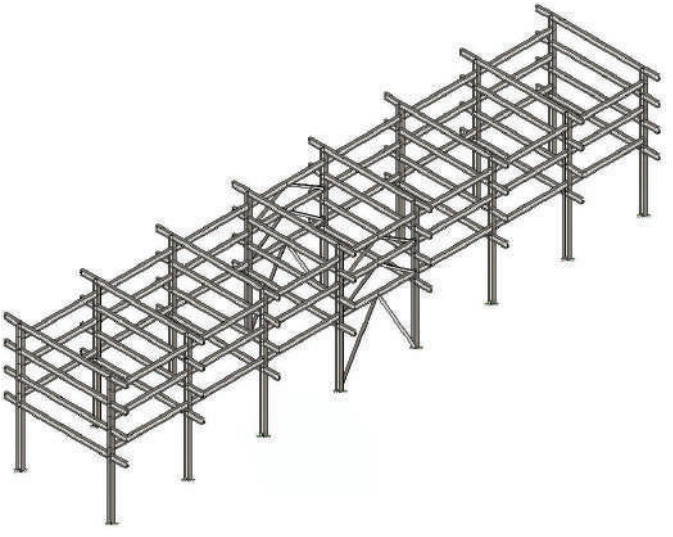

Fig. 2. Typical four-level pipe rack consisting of eight transverse frames connected by longitudinal struts.

DESIGN CRITERIA

In most of the United States, the governing building code is the International Building Code (IBC) (ICC, 2009). The scope of this code applies to buildings and other structures within the governing jurisdiction. The IBC prescribes structural design criteria in Chapters 16 through 23. These design criteria adopt by reference many industry standards and specifications that have been created in accordance with rigorous American National Standards Institute (ANSI) procedures.

By reference, many loads are prescribed in ASCE 7 (ASCE, 2006). Similarly, most structural steel material references are prescribed in AISC 360 (AISC, 2005b). Most structural steel seismic requirements are prescribed in AISC 341 (AISC, 2005a) and AISC 358 (AISC, 2006, 2009).

The IBC and its referenced industry standards and specifications primarily address buildings and other structures to a lesser extent. Design criteria for non-building structures are usually provided by industry guidelines. These guidelines interpret and supplement the building code and its referenced documents. In the case of pipe racks, additional design criteria are provided by Process Industry Practices, PIP STC01015 (PIP, 2007) and ASCE guidelines for petrochemical facilities (ASCE, 1997a, 1997b). In this article, the IBC requirements govern. The aforementioned industry standards and specifications apply because they are referenced by the IBC. The PIP practices and ASCE guidelines may be used for pipe racks because they supplement the IBC and the referenced industry standards and specifications. However, the PIP practices and ASCE guidelines are not code-referenced documents.

DESIGN LOADS

Dead Loads *(D)*

Dead loads are defined in the IBC as "the weight of materials of construction … including, but not limited to … structural items, and the weight of fixed service equipment, such as cranes, plumbing stacks and risers, electrical feeders …" Dead loads are prescribed in the IBC Section 1606, with no reference to ASCE 7 or any industry standard or specification.

The PIP *Structural Design Criteria* prescribes specific dead loads for pipe racks. Pipe racks and their foundations should be designed to support these loads applied on all available rack space, unless other criteria is provided by the client.

- Structure dead load (D_s): The weight of materials forming the structure and all permanently attached appurtenances. This includes the weight of fire protection material, but does not include the weight of piping, cable trays, process equipment and vessels.
- Operating dead load (D_o): The operating dead load is the weight of piping, piping insulation, cable tray, process equipment and vessels plus their contents (fluid load). The piping and cable tray loads may be based on actual loads or approximated by using uniform loads. The PIP *Structural Design Criteria* recommends a uniformly distributed load of 40 psf for pipe, which is equivalent to 8-in.-diameter schedule 40 pipes filled with water at 15-in. spacing. Other uniform loads may be used based on client requirements and engineering judgment. For cable tray levels, a uniform distributed load of 20 psf for a single level of cable trays and 40 psf for a double level of cable trays may be used unless actual loading is greater.
- Empty dead load (D_e): The empty weight of piping, piping insulation, cable tray, process equipment and vessels. When using approximate uniform loads, 60% of the operating dead load for piping levels is typically used. Engineering judgment should be used for cable tray levels.
- Test dead load (D_t): The empty weight of the pipes plus the weight of the test medium.

The use of large approximate uniform loads may be conservative for the sizing of members and connections. However, conservatively large uniform loads can become unconservative for uplift, overturning and period determination.

Live Loads (*L*)

Live loads are defined in the IBC as "Those loads produced by the use and occupancy of the … structure, and do not include construction or environmental loads such as wind load, snow load, rain load, earthquake load, flood load, or dead load." Live loads are prescribed in IBC Section 1607, with no reference to ASCE 7 or any industry standard or specification.

The minimum live loads applied to platforms and stairs that are part of the pipe rack structure shall meet the minimum loads per IBC Table 1607.1:

- Stairs: Per item 35, "stairs and exits—all others" shall be designed for a 100-psf uniform load or a 300-lb point load over an area of 4 in.^{2}, whichever produces the greater load effects.
- Platforms: Per item 39, "Walkways and elevated platforms" shall be designed for 60-psf uniform load.

The PIP *Structural Design Criteria* also prescribes specific live loads which may be applicable to platforms and stairs that are part of the pipe racks. These loads are higher than required by the IBC Building Code:

- Stairs: Design for separate 100-psf uniform load and 1,000-lb concentrated load.

- Platforms: Design for separate 75-psf uniform load and 1,000-lb concentrated load assumed to be uniformly distributed over an area 2½ ft by 2½ ft.

Either of the preceding design criteria is acceptable and may be reduced by the reduction in live loads provisions of IBC. Often, the live load design criteria are specified by the client and may be larger to accommodate additional loads for maintenance.

Thermal Loads (*T*)

Thermal loads are defined in the IBC as "Self-straining forces arising from contraction or expansion resulting from temperature change." Thermal loads may be caused by changes in ambient temperature or may be caused by the design (operating) temperature of the pipe.

The PIP *Structural Design Criteria* prescribes specific thermal loads for pipe racks:

- Thermal forces (T): The self-straining thermal forces caused by the restrained expansion of the pipe rack structural members.
- Pipe anchor and guide forces (A_f): Pipe anchors and guides restrain the pipe from moving in one or more directions and cause expansion movement to occur at desired locations in a piping system. Anchor and guide loads are determined from a stress analysis of an individual pipe. Beams, struts, columns, braced anchor frames and foundations must be designed to resist actual pipe anchor and guide loads.
- Pipe friction forces (F_f): These are friction forces on the pipe rack structural members caused by the sliding of pipes in response to thermal expansion due to the design (operating) temperature of the pipe. For friction loads on individual structural members, use the larger of 10% of the total piping weight or 40% of the weight of the largest pipe undergoing thermal movement: 10% of the total piping weight assumes that the thermal movements on the individual pipes do not occur simultaneously; 40% of the largest pipe weight assumes steel-on-steel friction.

Earthquake Loads (*E*)

Earthquake loads are prescribed in IBC Section 1613. This section references ASCE 7 for the determination of earthquake loads and motions. Seismic detailing of materials prescribed in ASCE 7 Chapter 14 is specifically excluded from this reference. Seismic detailing of structural steel materials are prescribed in IBC Chapter 22.

The PIP *Structural Design Criteria* prescribes that earthquake loads for pipe racks are determined in accordance with ASCE 7 and the following:

- Evaluate drift limits in accordance with ASCE 7, Chapter 12.
- Consider pipe racks to be non-building structures in accordance with ASCE 7, Chapter 15.
- Consider the recommendations of *Guidelines for Seismic Evaluation and Design of Petrochemical Facilities* (ASCE, 1997a).
- Use occupancy category III and an importance factor (I) of 1.25, unless specified otherwise by client criteria.
- Consider an operating earthquake load (E_o). This is the load considering the operating dead load (D_o) as part of the seismic effective weight.
- Consider an empty earthquake load (E_e). This is the load considering the empty dead load (D_e) as part of the seismic effective weight.

The ASCE *Guidelines for Seismic Evaluation and Design of Petrochemical Facilities* is based on the 1994 Uniform Building Code (UBC) (ICBO, 1994), and references to various seismic load parameters are based on obsolete allowable stress design equations not used in the IBC. Nevertheless, this document is a useful resource for consideration of earthquake effects.

Wind Loads (*W*)

Wind loads are prescribed in IBC Section 1609. This section references ASCE 7 as an acceptable alternative to the IBC requirements. Most design practitioners use the ASCE 7 wind load requirements.

The PIP *Structural Design Criteria* prescribes that wind loads for pipe racks are determined in accordance with ASCE 7 and the following:

- Wind drift with the full wind load should not exceed the pipe rack height divided by 100.
- Consider partial wind load (W_p). This is the wind load determined in accordance with ASCE 7 based on a wind speed of 68 mph. This wind load should be used in load combination with structure dead loads (D_s) and test dead loads (D_t).

The ASCE Wind Guideline (ASCE, 1997b) recommends that wind loads for pipe racks are determined in accordance with ASCE 7 and the following:

- Calculate wind on the pipe rack structure, neglecting any shielding. Use a force coefficient of $C_f = 1.8$ on structural members, or alternatively use $C_f = 2.0$ below the first level and $C_f = 1.6$ above the first level.
- Calculate transverse wind on each pipe level. The tributary height for each pipe level should be taken as the

pipe diameter (including insulation) plus 10% of the pipe rack transverse width. The tributary area is the tributary height times the tributary length of the pipes. Use a minimum force coefficient of $C_f = 0.7$ on pipes.

- Calculate transverse wind on each cable tray level. The tributary height for each pipe level should be taken as the largest tray height plus 10% of the pipe rack transverse width. The tributary area is the tributary height times the tributary length of the cable tray. Use a minimum force coefficient of $C_f = 2.0$ on cable trays.

Rain Loads (R)

Rain loads are prescribed in IBC Section 1611. The IBC requirements are intended for roofs that can accumulate rain water. Pipe rack structural members, piping and cable trays do not accumulate rain water. Unless the pipe rack supports equipment that can accumulate rain water, rain loads need not be considered.

Snow Loads (S)

Snow loads are prescribed in IBC Section 1608. This section references ASCE 7 for the determination of snow loads. The IBC provisions are intended for determining snow loads on roofs. Typically, pipe racks are much different than building roofs, and the flat areas of a pipe rack where snow can accumulate vary. Thus, engineering judgment must be used when applying snow loads.

The flat-roof snow load could be used for determining the snow load on a pipe rack. The area to apply the snow load depends on what is in the pipe rack and how close the items are to each other. For example, if the pipe rack contains cable trays with covers, the area could be based on the solidity in the plan view. If the pipe rack only contains pipe with large spacing, the area would be small because only small amounts of snow will accumulate on pipe.

By using this approach, combinations with snow load usually do not govern the design except in areas of heavy snow loading. In areas of heavy snow loading, the client may provide snow load requirements based on their experience.

Ice Loads (D_i)

Atmospheric ice loading is not a requirement of the IBC code. However, atmospheric ice load provisions are provided in ASCE 7, Chapter 10. It is recommended that ice loading be investigated to determine if it may influence the design of the pipe rack.

Load Combinations

Load combinations are defined in IBC Section 1605, with no reference to ASCE 7 or any industry standard or specification. The IBC strength load combinations that are listed below consider only the load types typically applicable to pipe racks (D, L, T, W and E). Loads usually not applicable to pipe racks are roof live (L_r), snow (S), rain (R), ice (D_i) and lateral earth pressure (H).

$$1.4(D + F) \quad \text{[IBC Eq. 16-1]}$$

$$1.2(D + T) + 1.6L \quad \text{[IBC Eq. 16-2]}$$

$$1.2D + (0.5L \text{ or } 0.8W) \quad \text{[IBC Eq. 16-3]}$$

$$1.2D + 1.6W + 0.5L \quad \text{[IBC Eq. 16-4]}$$

$$1.2D + 1.0E + 0.5L \quad \text{[IBC Eq. 16-5]}$$

$$0.9D + 1.6W \quad \text{[IBC Eq. 16-6]}$$

$$0.9D + 1.0E \quad \text{[IBC Eq. 16-7]}$$

The PIP *Structural Design Criteria* prescribes specific strength load combinations for pipe racks. However, the PIP load combinations do not consider platforms as part of a pipe rack structure and do not include live loads. The following combinations have been modified by the authors to include live loads for pipe racks that may have platforms. These load combinations are judged to be consistent with the IBC load combinations and include loads not considered by the IBC.

$$1.4(D_s + D_o + F_f + T + A_f)$$

$$1.4(D_s + D_t)$$

$$1.2(D_s + D_o + F_f + T + A_f) + 1.6L$$

$$1.2(D_s + D_o + A_f) + (1.6W \text{ or } 1.0E_o) + 0.5L$$

$$1.2(D_s + D_t) + 1.6W_{partial}$$

$$0.9(D_s + D_e) + 1.6W$$

$$0.9(D_s + D_o) + 1.2A_f + 1.0E_o$$

$$0.9(D_s + D_e) + 1.0E_e$$

To evaluate effects of these load combinations, they must be further expanded to consider the possible directions that lateral loads may occur. For example, wind loads would be applied in all four horizontal directions. In addition, lateral loads must consider multiple gravity load conditions.

DESIGN CONSIDERATIONS

Layout

An elevated multi-level pipe rack may be required for plant layout, equipment or process reasons. Multiple levels are not mandatory; it is simply a question of space. As long as the required space beneath the pipe rack for accessibility and road crossings has been taken into account, the rack can remain single level. However, in most cases, multiple levels will be required. Within plant units, most process pipes are connected to related unit equipment. Placing these pipes in the lower levels results in shorter pipe runs, savings on piping costs and better process flow conditions.

There are two main purposes of the cantilevers outside the pipe-rack columns: (1) to support sloping nonpressure pipes and (2) to support lines connecting adjacent equipment on the same side of the pipe rack. In both cases, using cantilevers allows long straight runs of level pressure piping and electrical work without interruption.

Ambient thermal loads are typically neglected for pipe racks because they are often insignificant to other loads. However, there may be cases where they should be considered, such as project sites in locations with extreme temperature ranges. If thermal loads are considered for long pipe racks, structure expansion joints should be placed approximately 200 to 300 ft apart. These expansion joints could be provided by either omitting the struts at one bay or by using long-slotted holes in the strut-to-column connections in the bay. If expansion joints are provided, each pipe rack section between joints should have at least one bay of horizontal and vertical bracing near the center of the section.

Based on the authors' experience, adjustments to the layout can also be used to help prevent vibration of piping due to wind in long pipe racks. Harmonic pipe vibration is reduced if every seventh bent is spaced at approximately 80% of the typical bent spacing.

Seismic

ASCE 7 defines a *non-building structure similar to buildings* as a "Non-building Structure that is designed and constructed in a manner similar to buildings, that will respond to strong ground motion in a manner similar to buildings, and have basic lateral and vertical seismic force resisting systems similar to buildings." Examples of non-building structures similar to buildings include pipe racks.

As a non-building structure, consideration of seismic effects on pipe racks should be in accordance with ASCE 7 Chapter 15. ASCE 7 Chapter 15 refers to Chapter 12 and other chapters, as applicable.

Seismic System Selection

Select seismic-force-resisting-system (SFRS), design parameters (R, Ω_o, C_d), and height limitations from either ASCE 7 Table 12.2-1 or ASCE 7 Table 15.4-1. Use of ASCE 7 Table 15.4-1 permits selected types of non-building structures that have performed well in past earthquakes to be constructed with less restrictive height limitations in Seismic Design Categories (SDC) D, E and F than if ASCE 7 Table 12.2-1 was used. Note that ASCE 7 Table 15.4-1 includes options where seismic detailing per AISC 341 is not required for SDC D, E or F. For example, ordinary moment frames of steel can be designed with $R = 1$ without seismic detailing per AISC 341. The AISC 341 seismic detailing requirements can also be avoided in SDC B and C for structural steel systems if $R = 3$ or less, excluding cantilevered column systems.

The transverse bents are usually moment-resisting frame systems, and the choices are special steel moment frame (SMF), intermediate steel moment frame (IMF) and ordinary steel moment frame (OMF).

In the longitudinal direction, if braced frames are present, the choices are usually special steel concentrically braced frame (SCBF) and ordinary concentrically braced frame (OCBF), although there is nothing to preclude choosing steel eccentrically braced frames (EBF) or buckling-restrained braced frames (BRBF). If braced frames are not present, the choices in the longitudinal direction are one of the cantilevered column systems.

In both directions, the seismic system selected must be permitted for the SDC and for the pipe rack height. ASCE Table 15.4-1 footnotes (italics below) permit specific height limits for pipe racks detailed for specific seismic systems:

- With $R = 3.25$: *Steel ordinary braced frames are permitted in pipe racks up to 65 ft (20 m).*
- With $R = 3.5$: *Steel ordinary moment frames are permitted in pipe racks up to a height of 65 ft (20 m) where the moment joints of field connections are constructed of bolted end plates. Steel ordinary moment frames are permitted in pipe racks up to a height of 35 ft (11 m).*
- With $R = 4.5$: *Steel intermediate moment frames are permitted in pipe racks up to a height of 65 ft (20 m) where the moment joints of field connections are constructed of bolted end plates. Steel intermediate moment frames are permitted in pipe racks up to a height of 35 ft (11 m).*

Period Calculations

The fundamental period determined from ASCE 7 Chapter 12 equations is not relevant for non-building structures, including pipe racks, because it does not have the same mass and stiffness distributions assumed in the Chapter 12 empirical equations for building structures. It is acceptable to use any analysis method that accurately models the mass and stiffness of the structure, including finite element models and the Rayleigh method. The determination of the pipe rack period can be affected by the stiffness of the piping leaving the pipe rack. When this stiffness is not accounted for in the period calculation, it is recommended that the calculated period be reduced by 10%.

Analysis Procedure Selection

ASCE 7 Chapter 12 specifies when a dynamic analysis is required. The philosophy underlying this section is that dynamic analysis is always acceptable for design. Static procedures are allowed only under certain conditions of regularity, occupancy and height.

A dynamic analysis procedure is required for a pipe rack if it is assigned to SDC D, E, or F and it either:

- has $T \geq 3.5T_s$, or
- exhibits horizontal irregularity type 1a or 1b or vertical irregularity type 1a, 1b, 2, or 3 (see ASCE 7 Chapter 12).

A dynamic analysis procedure is always allowed for a pipe rack. The most common dynamic analysis procedure used for pipe racks is the Modal Response Spectrum Analysis (ASCE 7 Chapter 12). The Equivalent Lateral Force Procedure (ASCE 7 Chapter 12) is allowed for a pipe rack structure if a dynamic analysis procedure is not required. The Simplified Alternative Structural Design Criteria for Simple Bearing Wall or Building Frame Systems is not appropriate and should not be used for pipe racks.

Equivalent Lateral Force Method Analysis

The Equivalent Lateral Force (ELF) procedure is a static analysis procedure. The basis of the ELF procedure is to calculate the effective earthquake loads in terms of a base shear, which is dependent on the structure's mass (effective seismic weight), the imposed ground acceleration, the structure dynamic characteristics, the structure ductility, and the structure importance. The base shear is then applied to the structure as an equivalent lateral load vertically distributed to the various elevations using code prescribed equations that are applicable to building structures. Using this vertical distribution of forces, seismic design loads in individual members and connections can be determined.

ASCE 7 determines design earthquake forces on a strength basis, allowing direct comparison with the design strength of individual structural members.

Modal Response Spectra Analysis

It is acceptable to use Modal Response Spectrum Analysis (MRSA) procedure for the analysis of pipe racks. It may be required to use a dynamic analysis procedure, such as MRSA, if certain plan and/or vertical irregularities are identified. The basis of MRSA is that the pipe rack's mass (effective seismic weight) and stiffness are carefully modeled, allowing the dynamic analysis of multiple vibration modes, resulting in an accurate distribution of the base shear forces throughout the structure. The MRSA shall include sufficient number of modes in order to obtain a minimum of 90% mass participation. Two MRSA runs would be required. The first run would include the operating dead load (D_o) as the seismic effective weight to determine the operating earthquake load (E_o). The second run would include the empty dead load (D_e) as the seismic effective weight to determine the empty earthquake load (E_e).

The MRSA input ground motion parameters (S_{DS}, S_{D1}) are used to define the ASCE 7 elastic design response spectrum. To obtain "static force levels," the MRSA force results must be divided by the quantity (R/I). ASCE 7 does not allow you to scale down MRSA force levels to ELF force levels because the ELF procedure may result in an underprediction of response for structures with significant higher mode participation. On the other hand, when the MRSA base shear is less than 85% of the ELF base shear, the MRSA results must be scaled up to no less than 85% of the ELF values. This lower limit on the design base shear is imposed to account for higher mode effects and to ensure that the design forces are not underestimated through the use of a structural model that does not accurately represent the mass and stiffness characteristics of the pipe rack.

$$V_{\text{MRSA}} \geq 0.85V_{\text{ELF}} \tag{1}$$

Drift

To obtain amplified seismic displacements, the displacement results calculated from the elastic analysis must be multiplied by the quantity C_d/I to account for the expected inelastic deformations. The displacement results must be multiplied by C_d for checking pipe flexibility and structure separation. The displacement results must multiplied by the quantity C_d/I when meeting the drift limits of Table 12.12-1.

It is important that the drift of pipe racks is compared to other adjacent structures where piping and cable trays run. The piping and cable tray must be flexible enough to accommodate the movements of the pipe rack and other adjacent structure.

Seismic Detailing Requirements

The selection of a seismic-force-resisting system from ASCE 7 Table 12.2-1 invokes seismic detailing requirements prescribed in ASCE 7 Chapter 14. Because ASCE 7 Chapter 14 is specifically excluded by the IBC, seismic detailing requirements for structural steel systems shall be taken from IBC Chapter 22 and AISC 341. The selection of a seismic-force-resisting system from ASCE 7 Table 15.4-1 directly invokes seismic detailing requirements prescribed in AISC 341.

AISC 341 includes seismic detailing requirements for each structural steel system listed in the ASCE 7 tables. In general, there is a relationship between R values and seismic detailing requirements. Lower R values and higher earthquake design forces are accompanied by minimal seismic detailing requirements. Higher R values and lower earthquake design forces are accompanied by more restrictive seismic detailing requirements to provide greater ductility.

AISC 341 prescribes that beams in OMF systems do not require lateral bracing beyond those requirements prescribed in AISC 360. However, beams in IMF and SMF systems have progressively more restrictive requirements for lateral

bracing of beams that can only be met by the addition of a horizontal bracing system at each pipe level. For this reason, it may be more economical to select an OMF system for the transverse bents.

AISC 341 prescribes that beam-to-column connections for IMF and SMF systems must be based on laboratory testing. OMF beam-to-column connections may be either calculated to match the expected plastic moment strength of the beam or based on laboratory testing. AISC 358 prescribes specific requirements for laboratory tested systems appropriate for use in seismic moment frame systems. One of the systems included in AISC 358 is the bolted end plate moment connection, commonly used in pipe rack construction. These connections are popular in industrial plants because they involve no field welding. See Figure 3 for the AISC 358 extended end plate connections.

Supplement No. 1 to AISC 358 adds another laboratory tested connection that does not involve field welding, the bolted flange plate moment connection (along with two additional connections). This type of connection is not used in pipe racks because it is not practical to support piping at the bolted top flange plates.

Redundancy in SDC A, B or C

In accordance with ASCE 7 for all structures, $\rho = 1.0$.

Redundancy in SDC D, E or F

The typical pipe rack has no horizontal bracing system that would serve as a diaphragm. If one individual bent fails, there is no load path for lateral force transfer to the adjacent frame. As a result, the pipe rack must be treated as a nonredundant structure.

- For a transverse bent to qualify for $\rho = 1.0$, it would need to have four or more columns and three or more bays at each level. This would ensure that the loss of moment resistance at both ends of a single beam would not result in more than a 33% loss of story strength. Otherwise, $\rho = 1.3$.
- For an individual longitudinal braced frame to qualify for $\rho = 1.0$, it would need to have two or more bays of chevron or X-bracing (or four individual braces) at each level on each frame line. This would ensure that the loss of an individual brace or connection would not result in more than a 33% loss of story strength nor cause an extreme torsional irregularity (type 1b). Otherwise, $\rho = 1.3$.

If the pipe rack is provided with a horizontal bracing system that would serve as a diaphragm and provide a load path for lateral transfer, the pipe rack can be treated as a redundant structure.

- For a pipe rack to qualify in the transverse direction for $\rho = 1.0$, it would need to have horizontal bracing between all transverse bents and a minimum of four transverse bents required. Otherwise, $\rho = 1.3$.
- For a pipe rack to qualify in the longitudinal direction for $\rho = 1.0$, there would need to be a minimum of four transverse bents, and each longitudinal frame line would need to have two or more individual braces at each level. Otherwise, $\rho = 1.3$.

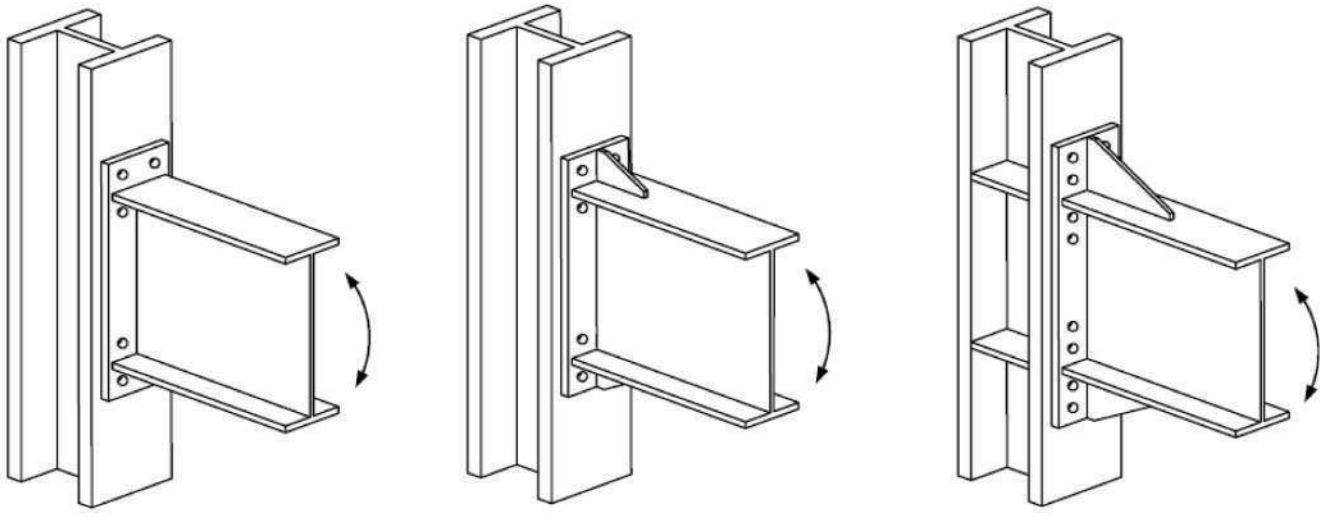

(a) Four-bolt unstiffened, 4E

(b) Four-bolt unstiffened, 4ES

(c) Eight-bolt stiffened, 8ES

Fig. 3. Extended end plate connections as shown in AISC 358-05.

Wind

Most of the wind provisions in ASCE 7 pertain to the determination of wind forces on buildings. Section 6.5.13 pertains to open structures such as pipe racks. The shape factors provided previously in this article are based on ASCE 7 Figure 6-21.

Pressures and Forces

Usually, wind pressures are applied to all structural elements of a pipe rack with no shielding in the four horizontal directions. However, it is common practice to omit wind loads on horizontal bracing or other interior horizontal members when they are enclosed by beams and stringers in all four directions. This is a reasonable approach considering that wind loads are already applied on the beams or stringers surrounding the interior members, the bracing members are not perpendicular to the wind direction, and the piping and tray above the horizontal member further shield these members.

The determination of the wind force on piping and cable trays, which assumes shielding, has already been provided earlier in this article. These loads are typically applied as a point load at the midspan of the beam supporting the piping and cable trays.

Where pipe racks include platforms, the beams supporting the handrail would include the wind load based on the area of the handrail. The torsion due to the wind load on the handrail is usually negligible. The clips and bolts attaching the handrail posts to the supporting beam should be sized for the moment due to wind. The wind load may be larger than the point loads required per IBC 1607.7 or ASCE 7 Section 4.4 when light fixtures, cable trays or conduit are attached to the handrail posts.

The bolted end plate moment connection is commonly used for the beam-to-column connections in pipe rack construction. These connections are popular in industrial plants because they involve no field welding. Design of these connections for wind loads is prescribed in AISC *Steel Design Guide 4* (Murray and Sumner, 2003). These connections are very similar to those used in AISC 358 and share common laboratory test results and procedural steps. Figure 3 is also applicable for the AISC *Steel Design Guide 4* extended end plate connections.

Drift

Drift limitations for wind loads are typically limited to the lesser of either a drift limit ratio as a function of pipe rack height or the amount of displacement that the piping can tolerate. The acceptable drift limit ratio varies based on the specific industry or owner. A typical drift limit ratio is the pipe rack height divided by 100.

Piping flexibility and the resulting loads to adjacent structures or equipment must also be considered.

Coatings

The coatings used for pipe racks are typically specified by the client to match the rest of the facility and to meet demands of the environment. The following coating systems are typically used:

- *Hot dip galvanizing:* Hot dip galvanizing is the most commonly used coating because it usually provides the lowest life-cycle cost. The disadvantage is that field welding should be avoided to minimize repair of galvanizing and the safety issues with welding of galvanized materials. Connections and members must be detailed to mitigate the temperature effects of hot dip galvanizing.
- *Paint:* Paint can be shop or field applied. Painted structural steel usually has a higher life-cycle cost.
- *Hot dip galvanized and painted:* For extremely corrosive environments, such as locations with frequent salt spray, both hot dip galvanizing and compatible paint systems are used.

For the coating system to perform properly, all members and connections must use an orientation and be detailed to avoid the collection of water. Where water accumulation cannot be avoided, drain holes must be provided. Some member combinations such as back-to-back angles or tees should be avoided. These types of configurations cannot be repainted without disassembling.

Fire Protection

Fire protection can be provided by passive systems or active systems. There are many commercially available tested and listed passive systems. Systems are usually rated for two to four hours. Typical passive systems include normal weight concrete, lightweight concrete, spray-on cementitious coatings and intumenscent coatings. Coatings may be shop or field applied. Active systems, such as fire water spray systems, are less common. The type of system selected depends on client preference and economics. It also may be dictated by the industry specific standards provided by the National Fire Protection Association (NFPA).

The design of the pipe rack is required to take into account the following considerations when fire protection systems or coatings are used:

- Additional dead weight, which must be included in the dead load of the structure (D_s) and included in the seismic mass.
- Additional wind load due to the increased size of the member profile with fire proofing.
- Connection types and geometry, which may require offsets to accommodate members with shop applied fire protection.
- Structural steel coating selection to be compatible with

fire protection system. Fire protection material should not be considered as a coating that will prevent corrosion. Fire protection material may accelerate corrosion if improperly detailed or applied.

- The stiffness of fire protection materials cannot be used to resist loads.

Cold Spill Protection

For pipe racks supporting piping that contains low-temperature or cryogenic fluid, cold spill protection may be required. The requirements are usually dictated by the client or industry standards. Typically, full-weight concrete or cementitious spray-on coatings used for fire protection are used for cold spill protection. Currently, a few industry standards have requirements pertaining to cold spill protection, but they are subject to interpretation. There are few guidelines provided for the volume or duration of the cold spill and little information on the effectiveness of fire proofing materials used for cold spill protection. The locations and the type of cold spill protection are often specified by the client. The same design considerations used for fire protection must be used when cold spill protection is to be provided.

Support Beams

Beams that support pipe and cable trays have several considerations for their proper design. Support beams are typically the beams of the transverse bents and may also include the stringers running longitudinally.

Lateral Bracing of Support Beams

Piping and cable trays do not act as reliable lateral bracing for the compression flange of support beams. Piping is typically not attached to the support beam, and friction alone cannot provide reliable restraint against lateral torsional buckling (LTB). Piping thermal movements may also help cause LTB rather than prevent it. Cable trays should not be considered as lateral bracing because they do not sufficiently prevent movement in the longitudinal direction of the pipe rack.

Interface between Pipes and Support Beams

There are many configurations in which pipes may be supported and restrained. Vertical supports, intended to support gravity loads, may also have horizontal loads due to friction. The friction could be a result of thermal, operating, wind or seismic loads on the piping. Note that friction loads due to wind and seismic conditions must be considered for the design of the supporting member but are not considered as resisting the wind or seismic force for the pipe.

The support beam should be designed for some friction load even though the piping analysis may indicate no lateral load. Pipe supports acting as pipe guides or axial line stops should also have friction loads applied to the support beam in addition to the guide or axial line stop load.

When guides or other types of supports apply concentrated forces or moments to the top flange, the top flange must be checked for local bending effects. The reaction of a typical pipe shoe support is assumed to act over the beam web and would not cause local flange bending.

Pipe anchors and guides that resist forces are usually present in pipe racks. Bracing may be required if the pipe rack beams cannot provide the necessary strength and stiffness to accommodate the forces.

Pipe anchors that resist moments should be avoided in elevated pipe racks. It is usually difficult and expensive to provide the required torsional strength and stiffness to resist moments.

Interface between Cable Trays and Support Beams

Cable trays can be directly supported on the support beam steel, or Unistrut can be used between the beam and the cable tray.

Torsion on Support Beams

Horizontal loads from piping or cable tray loads are usually applied perpendicular to the top flange of the support beam. These loads do not pass through the shear center of the beam and a torsional loading is created. The resulting torsional loading should be evaluated in accordance with methods provided in AISC *Steel Design Guide 9* (Seaburg and Carter, 1997). The torsional stresses should be combined with other stresses as prescribed in AISC 360.

Stability Analysis and Design

Acceptable Methods

AISC 360 allows several methods for the stability analysis and design of frames:

- Second-Order Elastic Analysis
- Second-Order Analysis by Amplified First-Order Elastic Analysis
- Direct Analysis Method

If properly applied, all three methods are appropriate for use for pipe racks. The first two methods are acceptable for use provided that the ratio of second-order drift to first-order drift is less than or equal to 1.50. The Direct Analysis Method is always acceptable.

When using the first two methods, effective length factors (K) need to be calculated to determine the column strengths.

Unstrutted Pipe Racks

As previously discussed, pipeways may or may not include longitudinal struts connecting the columns of the transverse frames. Pipe racks without longitudinal struts are called unstrutted pipe racks. The transverse frame columns of unstrutted pipe racks will act as cantilevered columns in the longitudinal direction.

The "classical" differential equation solution for column buckling for cantilevered columns is based on the assumption that the axial column stress is constant for the entire length of the column. The effective length factor is determined to be 2.0, rounded up for design to 2.1 to account for less than full fixity at the base.

In the case of pipe racks, the axial load is usually applied to the cantilevered columns at multiple locations as reactions from the supported beams. The axial stress is minimum at the free end and maximum at the fixed end. As a result, using an effective length of $K = 2.1$ for unstrutted pipe rack columns can be conservative.

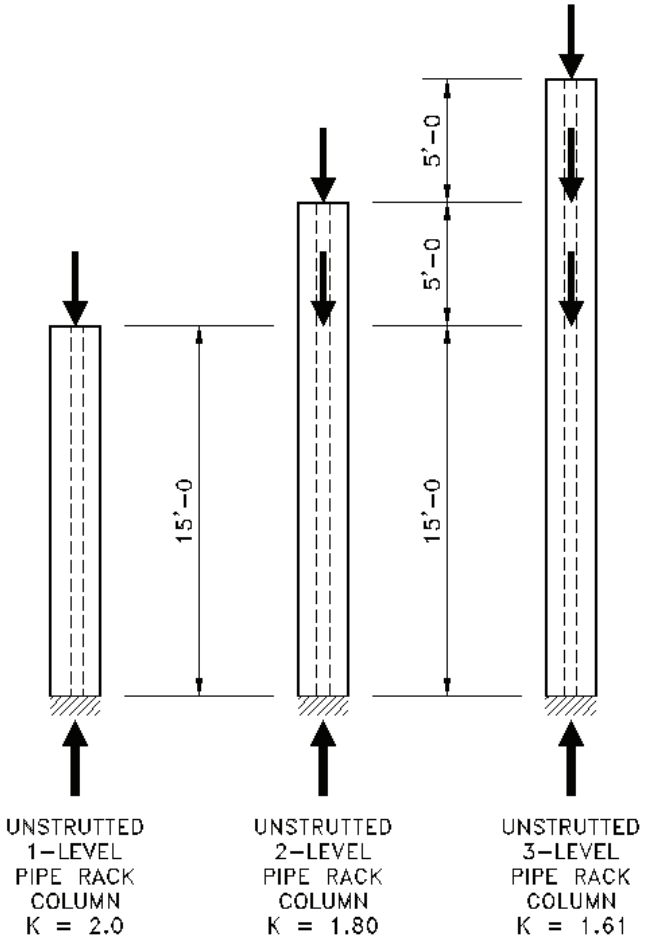

Fig. 4. Calculated effective length factors, K, for unstrutted pipe rack columns.

To quantify this conservatism, eigenvalue analyses were performed to determine effective length factors for unstrutted columns in typical pipe rack configurations with equal loads at each level (see Figure 4).

- For a single-level pipe rack loaded as shown in Figure 4, the effective length factor is determined to be 2.0. In accordance with AISC recommendations, use $K = 2.1$.
- For a two-level pipe rack loaded equally at each level as shown in Figure 4, the effective length factor is determined to be 1.80. Consistent with AISC recommendations, use $K = 1.9$.
- For a three-level pipe rack loaded equally at each level as shown in Figure 4, the effective length factor is determined to be 1.61. Consistent with AISC recommendations, use $K = 1.7$.

Commercial software can be used to perform the eigenvalue analysis necessary to determine effective length factors for other axial stress conditions. In the absence of commercial software, the recommended values may be used as guidance for arriving at an appropriate effective length factor.

The Direct Analysis Method does not involve the determination of effective length factors, and is recommended for use with unstrutted pipe racks.

Column Bases

Column base plates in the transverse (moment frame) direction may be designed as either fixed or pinned. Fixed column bases must be used for unstrutted pipe racks.

In general, the fixed base condition results in smaller structural steel sections and larger foundations with smaller calculated lateral frame deflections. Pinned base conditions result in heavier structural steel sections and smaller foundations with larger calculated lateral frame deflections.

The most common practice is to assume that the base of the column acts as a pinned connection. Even though the Occupational Safety and Health Administration (OSHA) requires a minimum of four anchor rods and the strength to resist a small moment, sufficient rotational stiffness is not provided to consider the base as a fixed connection. The combination of the flexibility of the base plate, the elastic deformation of the anchor rods, and the rotation of the foundation due to lateral loads usually allows enough rotation at the base for the base to act as a pinned connection when the larger wind and seismic loads are applied.

To minimize layout errors, the base plate is usually square with a square and concentric anchor rod hole pattern.

Foundations

The foundation type to be used will be dictated by site soil conditions. Foundation design parameters are normally stated in the project design specifications based on a site geotechnical investigation report. Typically, independent spread footings or pile caps are used at each column. Combined foundation or grade beams could be used for the columns of transverse frames and/or braced frames if the column spacing is not too large. Building codes may require that pile caps be connected with grade beams.

CONCLUSION

Pipe racks are not only non-building structures that have similarities to structural steel buildings but also have additional loads and design considerations. The requirements found in the building codes apply and dictate some of the design requirements. Some code requirements are not clear on how they are to be applied to pipe racks, because most are written for buildings. Several industry references exist to help the designer apply the intent of the code and follow expected engineering practices. Engineering practices vary and are, at times, influenced by client requirements and regional practices. Additional and updated design guides are needed so that consistent design methods are used throughout the industry.

REFERENCES

AISC (2005a), AISC 341-05, *Seismic Provisions for Structural Steel Buildings*, Including Supplement No. 1, American Institute of Steel Construction, Chicago, IL.

AISC (2005b), AISC 360-05, *Specification for Structural Steel Buildings*, American Institute of Steel Construction, Chicago, IL.

AISC (2006), AISC 358-05, *Prequalified Connections for Special and Intermediate Steel Moment Frames for Seismic Applications*, American Institute of Steel Construction, Chicago, IL.

AISC (2009), AISC 358-05s1, Supplement No. 1 to *Prequalified Connections for Special and Intermediate Steel Moment Frames for Seismic Applications*, American Institute of Steel Construction, Chicago, IL.

ASCE (1997a), *Guidelines for Seismic Evaluation and Design of Petrochemical Facilities*, American Society of Civil Engineers, Reston, VA.

ASCE (1997b), *Wind Loads on Petrochemical Facilities*, American Society of Civil Engineers, Reston, VA.

ASCE (2006), ASCE 7-05, *Minimum Design Loads for Buildings and Other Structures*, Including Supplement No. 1, American Society of Civil Engineers, Reston, VA.

ICBO (1994), *Uniform Building Code*, International Conference of Building Officials, Whittier, CA.

ICC (2009), *International Building Code*, International Code Council, Whittier, CA.

Murray, T.M. and Sumner, E.A. (2003), *Steel Design Guide No. 4*, Extended End-Plate Moment Connections—Seismic and Wind Applications, 2nd ed., American Institute of Steel Construction, Chicago, IL.

PIP (2007), PIP STC01015, *Structural Design Criteria, Process Industry Practices*, Austin, TX.

Seaburg, P.A. and Carter, C.J. (1997), *Steel Design Guide No. 9, Torsional Analysis of Structural Steel Members*, American Institute of Steel Construction, Chicago, IL.

Bending of Top Plates in Base Chair Connections

BO DOWSWELL

ABSTRACT

In many heavy industrial facilities, column bases must transfer large uplift loads to the foundation, and if the tension load is too large to carry with a standard base plate, chairs are used to transfer the load. The top plate thickness has traditionally been determined using either the elastic one-way bending capacity of a beam spanning the distance between the vertical stiffener plates or the two-way bending capacity based on elasticity theory. These design methods can be used where the nominal stress must be limited to the elastic range, such as structures subject to fatigue. For static loads, a more realistic design model can be achieved by considering the plastic capacity of the plate in two-way bending. In this paper, the author develops a method to calculate the ultimate bending capacity of top plates in base chair connections based on yield line theory. The limit-analysis solution does not rely on the conservative assumptions inherent in calculation methods commonly used in design practice. The proposed equation can be used to calculate the capacity of many different base chair configurations, including those commonly used on plate and shell structures.

Keywords: base chairs, base plates, uplift, yield line theory

In many heavy industrial facilities, column bases must transfer large uplift loads to the foundation. If the tension load is too large to carry with a standard base plate, chairs can be used to transfer the load. A base plate connection with a chair welded to each flange is shown in Figure 1.

Frequently, a vertical bracing gusset plate is welded to the column flange at the location of a base chair. At these locations, the top plate can be split as shown in Figure 2a or the chair height can be adjusted to accommodate the gusset plate height as shown in Figure 2b. For some projects, the second option is not viable, because the chair height must be

(a) Base chair for heavy industrial facility

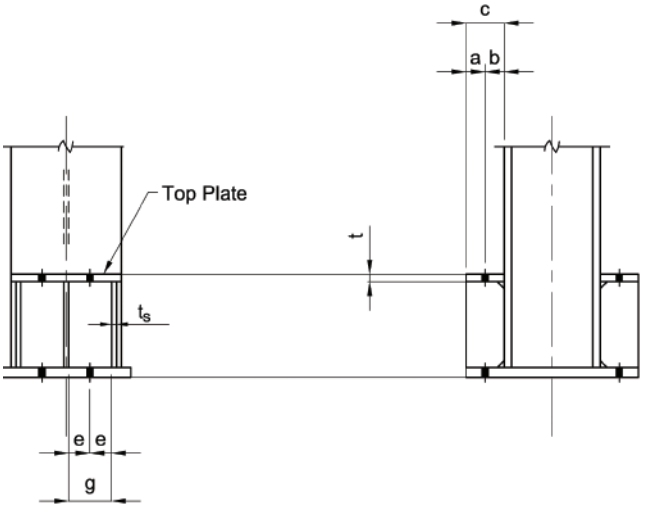

(b) Base chair arrangement and dimensions

Fig. 1. Column base plate connection with chair.

Bo Dowswell, Engineer, SDS Resources, Birmingham, AL. E-mail: bo@sdsresources.com

determined early in the design process to allow fabrication of the anchor rods, and the height of the gusset plate is usually not determined until much later in the design process.

In some cases, the gusset plate is notched to clear the base chair, but this practice should be avoided if possible, because it causes a discontinuity in the gusset plate, disrupting the flow of forces from the gusset plate into the anchor rods. This condition is usually caused by a standard base chair detail on the contract drawings that does not account for vertical brace locations.

Base chairs are also used at the bottom of plate and shell structures such as tanks, silos and stacks, as shown in Figure 3. For these structures, the top plate can be a continuous ring or separate plates at each anchor rod.

The top plate thickness has traditionally been determined using the elastic one-way bending capacity of a beam spanning the distance between the vertical stiffener plates (AISI, 1992; Bednar, 1986; Mahajan, 1975) or the two-way bending capacity based on elasticity theory (Troitsky, 1982). These design methods can be used where the nominal stress must be limited to the elastic range, such as structures subject to fatigue. However, for static loads, a more realistic design model can be achieved by considering the plastic capacity of the plate in two-way bending. In this paper, the yield line method will be used to derive an equation to determine the ultimate bending capacity of continuous and noncontinuous top plates.

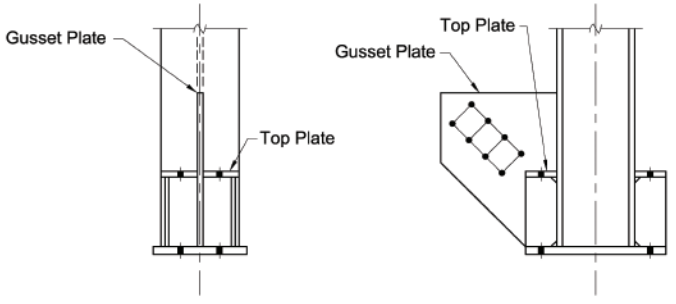

(a) Split top plate

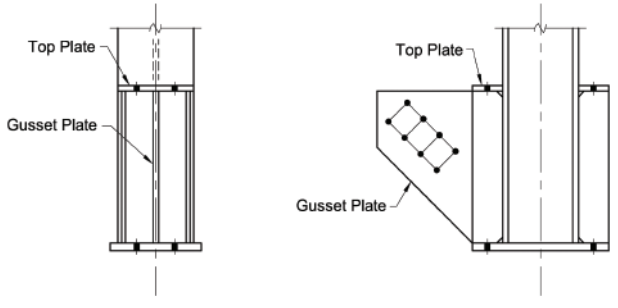

(b) Increased chair height

Fig. 2. Base chair configurations with a gusset plate at the column flange.

THE YIELD LINE METHOD

The yield line method was developed by Hognestad (1953) and Johansen (1962) to determine the ultimate capacity of concrete slabs. The shape of the failure pattern must be known in order to calculate the collapse load. Many patterns may be valid for a particular joint configuration. Because the solution is upper-bound, the pattern that gives the lowest load will provide results closest to the true failure load. Therefore, selection of the proper yield line pattern is important because an incorrect failure pattern will produce unsafe results.

The collapse load is calculated using the principle of virtual work, assuming a plastic mechanism forms along each line of the assumed failure pattern. To maintain equilibrium, the external work done by the load moving through the virtual displacement, δ, must equal the strain energy due to the plastic moment rotating through virtual rotations, θ_i. The virtual rotations are assumed small, so $\theta_i = \tan(\theta_i) = \sin(\theta_i)$. The influence of strain-hardening and membrane effects are not accounted for in yield line analysis; therefore, there is potentially a large reserve capacity beyond the calculated collapse load.

The general procedure for deriving a yield line solution is

1. Select a valid yield line pattern.
2. Determine the equation that describes the external work done by the load moving through the virtual displacement,

$$W_E = P\delta \quad (1)$$

where
P = load, kips (N)
δ = virtual displacement, in. (mm)

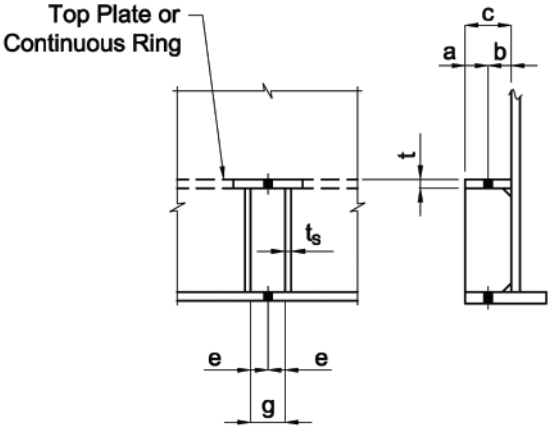

Fig. 3. Base chair configuration for plate and shell structures.

3. Determine the equation that describes the internal work done by the rotations along the yield lines,

$$W_I = \sum M_{pi}\theta_i \tag{2}$$

where

M_{pi} = plastic moment capacity of yield line i, kip-in. (N-mm)
$= m_p L_i$
θ_i = virtual rotation of yield line i
mp = plastic moment capacity per unit length of the fitting, kip-in./in. (N-mm/mm)
L_i = length of yield line i, in. (mm)

4. Set the external work equal to the internal work and solve for the load.

Kennedy and Goodchild (2003) present practical information for design of concrete slabs using the yield line method. The yield line method has also been used to determine the local capacity of steel connections. The yield line pattern derived by Kapp (1974) can be used to calculate the local capacity of wide flange webs subjected to transverse loads. Dranger (1977) developed yield line equations for bolted flange connections with tension loads. Wardenier (1982) used the yield line method to derive equations for the local wall bending capacity of HSS truss joints. Zoetemeijer (1974), Packer and Morris (1977), Mann and Morris (1979) and Zoetemeijer (1981) used the yield line method to derive equations to calculate the local bending capacity of end plates and column flanges in end plate moment connections.

YIELD LINE SOLUTION FOR TOP PLATE

To determine the capacity of a top plate in bending, the yield line pattern in Figure 4 will be used. All points on the edge of the hole and along yield line 2 have been displaced vertically by an amount δ.

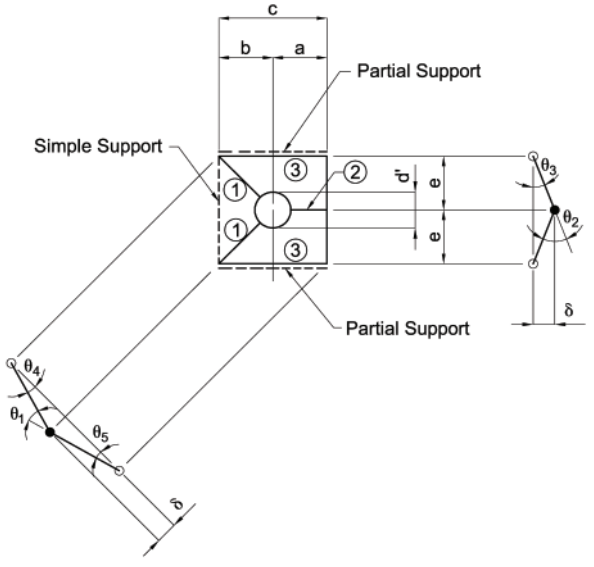

Fig. 4. Yield line model for top plate bending.

Determine the length of the yield lines:

$$L_1 = \sqrt{b^2 + e^2} - d'/2 \tag{3}$$

$$L_2 = a - d'/2 \tag{4}$$

$$L_3 = c \tag{5}$$

where

a = distance from the center of the hole to the edge of the top plate, in. (mm)
b = distance from the center of the hole to the face of the support, in. (mm)
$c = a + b$, in. (mm)
d' = hole diameter, in. (mm)
e = distance from the center of the hole to the inside edge of the vertical stiffener plate, in. (mm)

Determine the rotation angles of the yield lines:

$$\theta_3 = \frac{\delta}{e} \tag{6}$$

$$\begin{aligned}\theta_2 &= 2\theta_3 \\ &= 2\delta/e\end{aligned} \tag{7}$$

$$\theta_4 = \frac{\delta}{(b/e)L_1} \tag{8}$$

$$\theta_5 = \frac{\delta}{(e/b)L_1} \tag{9}$$

$$\begin{aligned}\theta_1 &= \theta_4 + \theta_5 \\ &= \left(\frac{e}{b} + \frac{b}{e}\right)\frac{\delta}{L_1}\end{aligned} \tag{10}$$

The plastic moment capacity per unit length along yield lines 1 and 2 (see Figure 4) is

$$m_p = \frac{F_y t^2}{4} \tag{11}$$

where

F_y = specified minimum yield strength of the top plate, ksi (MPa)
t = thickness of the top plate, in. (mm)

Because the fixity at yield lines 3 can vary between pinned and rigid, the plastic moment capacity per unit length can be expressed as

$$m'_p = \alpha \frac{F_y t^2}{4} \tag{12}$$

where

α = reduction factor to account for the effect of partial fixity of the outer yield lines (discussed in detail in the next section)

The internal work is

$$\begin{aligned} W_I &= \sum L_i \theta_i m_{pi} \\ &= 2L_1\theta_1 m_p + L_2\theta_2 m_p + 2L_3\theta_3 m'_p \\ &= 2L_1\left(\frac{e}{b}+\frac{b}{e}\right)\frac{\delta}{L_1} m_p + (a - d'/2)(2\delta/e) m_p + \\ &\quad 2c(\delta/e) m'_p \end{aligned} \tag{13}$$

The external work is

$$W_E = T\delta \tag{14}$$

where

T = tension in the anchor rod, kips (N)

Substitute Equations 11 and 12 into Equation 13, set internal work equal to external work, and solve for T to get Equation 15:

$$T = \frac{F_y t^2}{2}\left[\frac{e}{b} + (1+\alpha)\frac{c}{e} - \frac{d'}{2e}\right] \tag{15}$$

PARTIAL FIXITY AT OUTER YIELD LINES

Equation 12 contains a factor, α, to account for the effect of partial fixity of the outer yield lines (yield lines 3), where $0 \le \alpha \le 1$. For top plates that are continuous over the stiffeners, the outer yield lines can be assumed fully fixed. For discontinuous top plates, the design can be based on the conservative assumption that the outer yield lines are simply supported. For these cases, the values for α are

α = 1 for continuous top plates fixed against rotation at both outer yield lines
= 0 for top plates that are free to rotate at both outer yield lines

If flexural continuity is provided between the top plate and the vertical side plates, the bending capacity of the vertical plates can be used to provide partial fixity to the outer yield lines on the top plate. In the presence of axial loading, Neal (1961) showed that the plastic capacity of a member with rectangular cross section is reduced according to Equation 16, which gives the reduced moment capacity per inch of the vertical side plate:

$$m'_{ps} = m_{ps}\left[1 - \left(\frac{P}{P_y}\right)^2\right] \tag{16}$$

where

m_{ps} = full plastic moment capacity per inch of the vertical side plate, kip-in./in. (N-mm/mm)
= $F_{ys}t_s^2/4$

P = compression load in the vertical side plate, kips (N)

P_y = yield load of the vertical side plate, kips (N)
= $F_{ys}b_s t_s$s

F_{ys} = specified minimum yield strength of the vertical side plates, ksi (MPa)

b_s = width of the vertical side plates, in. (mm)

t_s = thickness of the vertical side plates, in. (mm)

If the vertical side plate has the same width as the top plate, the fixity factor for the outer yield lines can be calculated using Equation 17:

$$\alpha = \frac{F_{ys}}{F_y}\left(\frac{t_s}{t}\right)^2\left[1 - \left(\frac{P}{P_y}\right)^2\right] \tag{17}$$

VERIFICATION OF PROPER YIELD LINE PATTERN

Because the yield line solution is upper-bound, the pattern that gives the lowest load will provide results closest to the true failure load. To verify that the pattern in Figure 4 is correct, the collapse load will be compared to that from other admissible patterns. To simplify the comparisons, the diameter of the hole will be neglected.

The number of possible yield line patterns for any joint is infinite, but there are at least four admissible patterns that lead to practical design equations for top plate connections. These are labeled 1 through 4 in Table 1, where pattern 1 is the basis for the derivation of Equation 15. The normalized load is calculated for each pattern as

$$\frac{2P}{F_y t^2} \tag{18}$$

The normalized load for each pattern is compared to that of pattern 1 to determine the conditions that will cause one of the other three patterns to yield a lower capacity than that predicted with Equation 15 (i.e., $P_{pn} < P_{p1}$). The results are shown for $\alpha = 0$ in the top part of the table and $\alpha = 1$ in the bottom part.

A comparison of the normalized load equations of pattern 2 to those of pattern 1 proves that pattern 2 can never control the design. For the case of $\alpha = 0$, the conditions for $P_{pn} < P_{p1}$

Table 1. Comparison of Admissible Yield Line Patterns				
Pattern Geometry	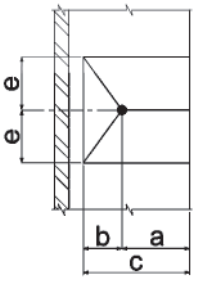	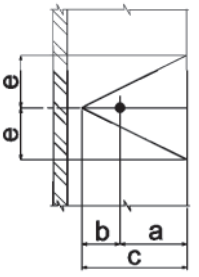	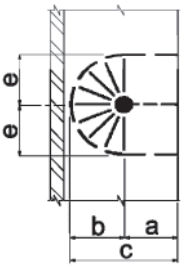	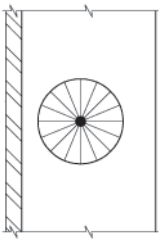
Pattern No.	**1**	**2**	**3**	**4**
$\alpha = 0$				
$\left(\frac{2P}{F_y t^2}\right)_{\alpha=0}$	$\frac{e}{b}+\frac{c}{e}$	$\frac{e}{b}+\frac{4c^2}{eb}$	$\pi-1+\frac{c}{e}$	2π
Condition for $P_{pn} < P_{p1}$	—	NC	$\frac{e}{b} > \pi-1$	$\frac{e}{b}+\frac{c}{e} > 2\pi$
$\alpha = 1$				
$\left(\frac{2P}{F_y t^2}\right)_{\alpha=1}$	$\frac{e}{b}+\frac{2c}{e}$	$\frac{e}{b}+\frac{4c^2}{eb}$	$\pi-2+\frac{2c}{e}$	2π
Condition for $P_{pn} < P_{p1}$	—	NC	$\frac{e}{b} > \pi-2$	$\frac{e}{b}+\frac{2c}{e} > 2\pi$
NC = Never controls				

for patterns 3 and 4 are beyond the range of geometry typical of base chair connections; therefore, they can be neglected. For the case of $\alpha = 1$, the conditions for $P_{pn} < P_{p1}$ for patterns 3 and 4 are more common, and these limits should be recognized by the designer.

PROPOSED DESIGN METHOD

It is proposed that Equation 15 be used for design of top plates in base chair connections. To account for the upper-bound nature of the solution and the corner effect, Wood (1961) recommended an additional design margin of 15% for yield line solutions. Kennedy and Goodchild (2003) recommended an additional margin of 10%. Based on these values, it is recommended that $\phi = 0.80$ be used as the reduction factor for load and resistance factor design (LRFD) in lieu of the traditional value of 0.90 for members subject to bending. For allowable stress design (ASD), $\Omega = 1.88$ is recommended.

If the top plate is split around a gusset plate as shown in Figure 2a, free rotation should be assumed at the boundary welded to the gusset plate, unless the weld is strong enough to develop the plastic bending capacity of the top plate. For top plates with different boundary conditions at each of the outer yield lines, the average of the two independent values of α can be used.

If $\alpha = 1$ is used, the following geometric constraints should be met in order to ensure that Equation 15 is valid:

$$\frac{e}{b} \le \pi - 2 \tag{19}$$

$$\frac{e}{b}+\frac{2c}{e} \le 2\pi \tag{20}$$

EXAMPLE

For the column base chair connection in Figure 5, determine the top plate thickness required to carry the factored uplift force of 250 kips. The plate material is ASTM A36 and the anchor rod holes have a diameter of 2c in.

Solution A: Assume simple supports at the outer yield lines

The plate is continuous over the middle stiffener; therefore, rotation is restrained at that location. For simplicity, the yield line pattern will be assumed free to rotate at the outer stiffeners. Therefore, yield lines 3 will be assumed fixed at one

side of the pattern and free at the other side, and $\alpha = (1 + 0)/2 = 0.5$.

$a = 3$ in.
$b = 4$ in.
$c = 7$ in.
$d' = 2.31$ in.
$e = 2.75$ in.
$F_y = 36$ ksi

Try a 1.25-in.-thick plate.

$t = 1.25$ in.

$$T_u = \frac{250 \text{ kips}}{4 \text{ anchor rods}}$$
$$= 62.5 \text{ kips per anchor rod}$$

$$T_n = \frac{(36 \text{ ksi})(1.25 \text{ in.})^2}{2}\left[\frac{2.75 \text{ in.}}{4.00 \text{ in.}} + 0.5\left(\frac{7.00 \text{ in.}}{2.75 \text{ in.}}\right) - \frac{(2.31 \text{ in.})}{(2)(2.75 \text{ in.})}\right]$$
$$= 115 \text{ kips}$$

$$\phi T_n = (0.80)(115 \text{ kips})$$
$$= 92.0 \text{ kips} > 62.5 \quad \textbf{o.k.}$$

Solution B: Assume partial fixity at the outer yield lines

Try a 1-in.-thick plate.

$t = 1$ in.
$F_{ys} = 36$ ksi
$b_s = 7$ in.
$t_s = $ w in.
$P = 250 \text{ kips}/8 = 31.3$ kips
$P_y = (36 \text{ ksi})(7.00 \text{ in.})(0.750 \text{ in.}) = 189$ kips

The fixity factor for the outer yield line, α_o, is

$$\alpha_o = \frac{36.0 \text{ ksi}}{36.0 \text{ ksi}}\left(\frac{0.750 \text{ in.}}{1.00 \text{ in.}}\right)^2\left[1 - \left(\frac{31.3 \text{ kips}}{189 \text{ kips}}\right)^2\right]$$
$$= 0.547$$

The plate is continuous over the middle stiffener; therefore, rotation is restrained at that location, and $\alpha = (1 + 0.547)/2 = 0.774$.

$$T_n = \frac{(36 \text{ ksi})(1.00 \text{ in.})^2}{2}\left[\frac{2.75 \text{ in.}}{4.00 \text{ in.}} + (1 + 0.774)\left(\frac{7.00 \text{ in.}}{2.75 \text{ in.}}\right) - \frac{(2.31 \text{ in.})}{(2)(2.75 \text{ in.})}\right]$$
$$= 86.1 \text{ kips}$$

Using the AISI (1992) method, a required plate thickness of 1.35 in. is required. If the plate is modeled as a simple beam with a net width of 7 in. − 2.31 in. = 4.69 in., the required

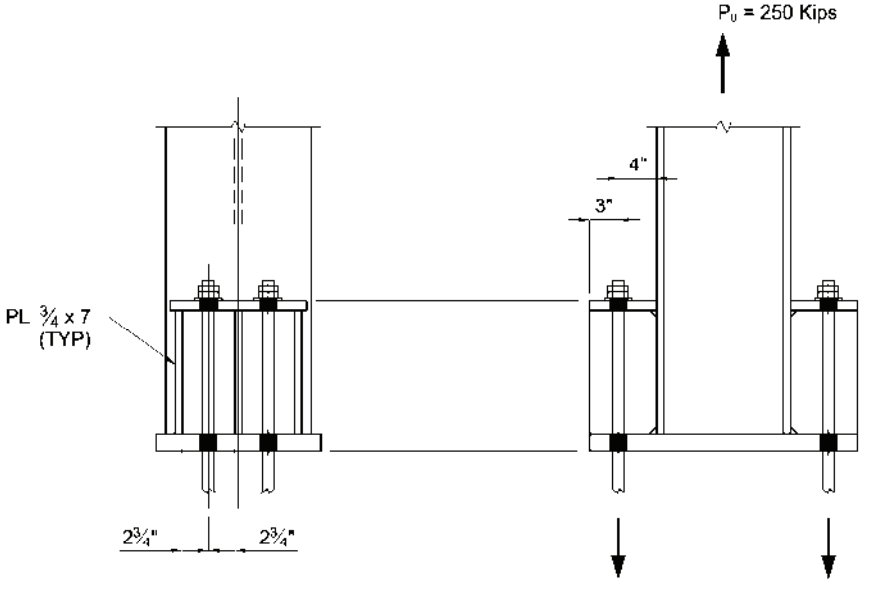

Fig. 5. Example: column with large uplift.

thickness is 1.50 in. The use of Equation 15 clearly provides a more economical solution for top plates compared to the traditional methods of analysis.

CONCLUSIONS

A method has been developed to calculate the ultimate bending capacity of top plates in base chair connections. The proposed design procedure is based on yield line theory and provides a limit-analysis solution that does not rely on the conservative assumptions inherent in the calculation methods commonly used in design practice. The proposed equation can be used to calculate the capacity of many different base chair configurations, including those commonly used on plate and shell structures.

REFERENCES

AISI (1992), *Steel Tanks for Liquid Storage*, Steel Plate Engineering Data—Volume 1, American Iron and Steel Institute, Washington, DC.

Bednar, H.H. (1986), *Pressure Vessel Design Handbook*, 2nd ed., Krieger Publishing Company, Malabar, FL.

Dranger, T.S. (1977), "Yield Line Analysis of Bolted Hanging Connections," *Engineering Journal*, American Institute of Steel Construction, Vol. 14, No. 3.

Hognestad, E. (1953), "Yield Line Theory for the Ultimate Flexural Strength of Reinforced Concrete Slabs," *Journal of the American Concrete Institute*, Vol. 24, No. 7.

Johansen, K.W. (1962), "Yield Line Theory," Cement and Concrete Association, London, England, U.K.

Kapp, R.H. (1974), "Yield Line Analysis of a Web Connection in Direct Tension," *Engineering Journal*, American Institute of Steel Construction, Vol. 11, No. 2.

Kennedy, G. and Goodchild, C. (2003), *Practical Yield Line Design*, British Cement Association, Crowthorne, England.

Mahajan, K.K. (1975), "Tall Stack Design Simplified," *Hydrocarbon Processing*, September, pp. 217–220.

Mann, A.P. and Morris, L.J. (1979), "Limit Design of Extended End-Plate Connections," *Journal of the Structural Division*, ASCE, March, pp. 511–526.

Neal, B.G. (1961), "The Effect of Shear and Normal Forces on the Fully Plastic Moment of a Beam of Rectangular Cross Section," *Journal of Applied Mechanics*, Vol. 28, pp. 269–274.

Packer, J.A. and Morris, L.J. (1977), "A Limit State Method for the Tension Region of Bolted Beam-Column Connections," *The Structural Engineer*, Vol. 5, No. 10, October.

Troitsky, M.S. (1982), *Tubular Steel Structures—Theory and Design*, James F. Lincoln Arc Welding Foundation, Cleveland, OH.

Wardenier, J. (1982), *Hollow Section Joints*, Delft University Press, Delft, The Netherlands.

Wood, R.H. (1961), *Plastic and Elastic Design of Slabs and Plates*, Ronald Press, New York.

Zoetemeijer, P. (1974), "A Design Method for the Tension Side of Statically Loaded, Bolted Beam-to-Column Connections," *Heron*, Vol. 20, No. 1.

Zoetemeijer, P. (1981), "Semi-Rigid Bolted Beam-to-Beam Column Connections with Stiffened Column Flanges and Flush End Plates," *Joints in Structural Steelwork, Proceedings of the International Conference Held at Teesside Polytechnic*, April 6–9, John Wiley and Sons, New York.

Singly Symmetric Combination Section Crane Girder Design Aids

PATRICK C. JOHNSON and JEFFREY A. LAMAN

ABSTRACT

Crane runway girders are distinguished by long, unbraced lengths and biaxial bending. Combination sections consisting of a W-shape with a channel cap are typically efficient for these conditions, but time consuming to design due to the iterative process required due to biaxial bending and the complex stability equations provided in the 2005 AISC *Specification*. This paper presents developed Z_x tables and flexural strength graphs and introduces a trial section selection method. Included herein are updated design charts to allow for fast and efficient analysis of the typical combination sections provided in Table 1-19 of the 13th edition AISC *Steel Construction Manual*. Also presented is an overview of crane girder design procedures and an abbreviated design example.

Keywords: biaxial bending, crane runway girders, design, unbraced length.

The design or evaluation procedure for combination sections—a wide flange with a channel cap—is specified in Section F4 of the AISC *Specification for Structural Steel Buildings* (AISC, 2005a), which covers singly symmetric I-shaped members bent about their major axis. Reversal of the specified AISC evaluation process for direct design is not feasible; therefore, design becomes a matter of trial and error. The situation is compounded for a combination section that supports *x*- and *y*-axis moments as in the case of a crane girder, where Chapter H of the 2005 AISC *Specification* must be applied. As a result, design aids are needed to streamline the design process that facilitates rapid selection of the most economical combination section. This paper updates a previously published paper by Laman (1996), presenting new design aids, formatted in the style of familiar AISC tables and figures, including the basis by which the aids are developed and a supporting example. Also presented is a method to determine the equivalent *x*-axis moment required for beams subjected to biaxial moments.

There are many texts and design aids available that address the design of industrial buildings with cranes, such as the design guide by Fisher (2004). While these sources explain the loading and evaluation required for crane runway girders, they do not offer any systematic approach to the selection of trial sections. The problems of a trial-and-error approach are further compounded by the lack of design aids for quickly determining the capacity of the combination sections.

Patrick C. Johnson, Student, Department of Civil and Environmental Engineering, The Pennsylvania State University, University Park, PA. E-mail: pcjohnson@psu.edu

Jeffrey A. Laman, Ph.D., P.E., Professor, Department of Civil Engineering, The Pennsylvania State University, University Park, PA (corresponding author). E-mail: jlaman@psu.edu

CRANE GIRDER DESIGN BASIS

Crane girders are distinguished by long, unbraced lengths and combined bending about the *x*- and *y*-axis as well as torsion. For typical loading and spans, a wide flange section with a channel cap normally provides an efficient cross-section for the design. Historically, the assumption has been made that the channel and the wide flange top flange resist the horizontal loads and the combination section resists the vertical load. This simplifies the analysis of the actual condition and eliminates the need for an analysis of torsional effects on the combination section (Laman, 1996). Given the complexity of the 2005 AISC *Specification* design equations due to lateral torsional buckling strength determination, design tables and graphs are needed to speed the process. Currently the 13th edition AISC *Steel Construction Manual* (AISC, 2005b) contains design tables and graphs to assist with wide flange and channel design under lateral torsional buckling and serve as a model for the aids presented herein. Based on 2005 AISC *Specification* Section F.4 and the flow chart of Figure 1, design aids presented in Tables 2 and 3 and Figures 2 and 3 have been developed. With the availability of these new design aids, a trial section selection methodology is now possible and is presented here.

M_{ueq} METHOD

Defining the ratio of M_{nx} to M_{ny} as a plastic section modulus ratio, ZR:

$$ZR = \frac{M_{nx}}{M_{ny}} = \frac{Z_x F_y}{Z_y F_y} = \frac{Z_x}{Z_y} \quad (1)$$

Table 1. *b* and *m* Values for Typical Combination Sections

	Channel Cap	L_b (ft)	10	20	30	40	50	60	70	80	90	100
Fy = 50 ksi	MC18×42.7	***b***	1.5	1.4	1.3	1.1	1.1	0.75	0.6	0.5	0.4	0.4
		m (×10³)	1.9	1.9	1.9	1.9	1.6	1.7	1.7	1.7	1.7	1.6
	C15×33.9	***b***	1.1	1.0	0.9	0.9	0.8	0.6	0.5	0.4	0.4	
		m (×10³)	3.0	3.0	3.0	2.8	2.6	2.5	2.5	2.5	2.3	
	C12×20.7	***b***	0.7	0.7	0.6	0.7	0.5	0.4	0.4	0.4		
		m (×10³)	6.3	6.0	6.0	5.1	5.0	5.0	4.6	4.2		
	C10×15.3	***b***	0.2	0.2	0.2	0.1	0.2	0.1				
		m (×10³)	13	12	12	11	11	11				
Fy = 36 ksi	**Channel Cap**	L_b (ft)	**10**	**20**	**30**	**40**	**50**	**60**	**70**	**80**	**90**	**100**
	MC18×42.7	***b***	1.4	1.5	1.4	1.3	1.3	1.1	0.85	0.7	0.6	0.5
		m (×10³)	2.7	2.6	2.6	2.6	2.5	2.3	2.3	2.3	2.3	2.4
	C15×33.9	***b***	1.1	1.0	1.0	0.9	0.9	0.9	0.7	0.6	0.6	0.6
		m (×10³)	4.1	4.1	4.1	4.1	3.9	3.5	3.4	3.4	3.1	3.0
	C12×20.7	***b***	0.7	0.7	0.7	0.7	0.7	0.5	0.5	0.5		
		m (×10³)	8.4	8.4	8.0	8.0	7.3	7.3	6.7	6.2		
	C10×15.3	***b***	0.2	0.2	0.2	0.2	0.2	0.2				
		m (×10³)	17	17	17	17	16	16				

and observing that a nearly linear relationship between ZR and ϕM_{nx} exists for each channel section used as a cap, Equation H1-1b can be rearranged into an explicit function for ϕM_{nx}:

$$\frac{M_{ux}}{\phi M_{nx}} + \frac{M_{uy}}{\phi M_{ny}} \le 1 \tag{2}$$

Now substituting ZR for the moment ratio into Equation 2,

$$\frac{M_{ux}}{\phi M_{nx}} + \frac{M_{uy}}{\phi M_{nx}/ZR} \le 1 \tag{3}$$

Rearranging Equation 3:

$$\frac{M_{ux}}{\phi M_{nx}} + \frac{(ZR)(M_{uy})}{\phi M_{nx}} \le 1 \tag{4}$$

Rearranging Equation 4:

$$M_{ux} + (ZR)(M_{uy}) \le \phi M_{nx} \tag{5}$$

Equation 5 is an approximation based on the near-linear relationship (0.98 correlation) between ZR and M_{nx} for combination sections of this study. Because ϕM_{nx} is not initially known, an equivalent moment, M_{ueq}, is substituted for ϕM_n in Equation 5 to form Equation 6:

$$M_{ueq} \ge M_{ux} + (ZR)(M_{uy}) \tag{6}$$

For a trial channel cap selection, ZR is replaced with a linear function of M_{ueq} and solved for M_{ueq}:

$$M_{ueq} \ge M_{ux} + (mM_{ueq} + b)M_{uy} \tag{7}$$

where the coefficients m ([kip-ft]$^{-1}$) and b (unitless) represent the straight-line slope and intercept for the near-linear relationship. Distributing terms gives the following:

$$M_{ueq} \ge M_{ux} + mM_{ueq}M_{uy} + bM_{uy} \tag{8}$$

Collecting the terms of Equation 8 results in the following:

$$(1 - mM_{uy})M_{ueq} \ge M_{ux} + bM_{uy} \tag{9}$$

Solving for M_{ueq} results in Equation 10 for load and resistance factor design (LRFD):

$$M_{ueq} \ge \frac{M_{ux} + bM_{uy}}{1 - mM_{uy}} \tag{10}$$

Table 2. Z_x Design Selection Table for Typical Combination Sections (F_y = 36 ksi)

Φ = 0.90 Ω = 1.67	W-Shapes with Cap Channels										F_y = 36 ksi	
Shape	Z_x	M_{px}/Ω	ΦM_{px}	M_{rx}/Ω	ΦM_{rx}	BF		L_p	L_r	I_x	M_{ny}/Ω	ΦM_{ny}
		kip-ft	kip-ft	kip-ft	kip-ft	kips	kips				kip-ft	kip-ft
	in.^{3}	ASD	LRFD	ASD	LRFD	ASD	LRFD	ft	ft	in.^{4}	ASD	LRFD
W36×150 + MC18×42.7	738	1330	1990	993	1490	9.57	14.4	12.2	47.0	12000	196	294
W36×150 + C15×33.9	716	1290	1930	961	1440	10.6	15.9	11.2	42.1	11500	152	229
W33×141 + MC18×42.7	652	1170	1760	880	1320	8.11	12.2	12.2	48.1	10000	192	288
W33×141 + C15×33.9	635	1140	1710	866	1300	8.76	13.2	11.2	42.5	9580	148	223
W33×118 + MC18×42.7	544	977	1470	719	1080	6.95	10.4	12.6	49.8	8280	179	269
W33×118 + C15×33.9	529	950	1430	710	1070	7.47	11.2	11.6	43.8	7900	135	203
W30×116 + MC18×42.7	492	884	1330	656	986	5.96	8.95	12.4	50.7	6900	177	266
W30×116 + C15×33.9	480	862	1300	647	972	6.53	9.81	11.3	44.4	6590	133	200
W30×99 + MC18×42.7	412	740	1110	546	821	4.87	7.32	12.7	52.6	5830	168	253
W30×99 + C15×33.9	408	733	1100	539	810	5.65	8.5	11.7	46.0	5550	124	187
W27×94 + C15×33.9	357	641	964	481	724	4.49	6.75	11.6	47.2	4530	125	187
W27×84 + C15×33.9	316	568	853	426	640	3.87	5.81	11.8	48.6	4050	120	180
W24×84 + C15×33.9	286	514	772	390	586	3.25	4.88	11.6	49.7	3340	119	179
W24×84 + C12×20.7	275	494	743	379	570	4.39	6.60	9.09	35.3	3030	74.1	111
W24×68 + C15×33.9	232	417	626	311	467	2.62	3.94	12.1	52.5	2710	112	169
W24×68 + C12×20.7	224	402	605	302	454	3.72	5.59	9.42	36.5	2440	67.1	101
W21×68 + C15×33.9	207	372	559	280	421	2.15	3.24	11.9	54.4	2180	112	169
W21×68 + C12×20.7	200	359	540	273	410	3.06	4.59	9.23	37.4	1970	67	101
W21×62 + C15×33.9	189	340	510	255	383	1.94	2.92	12.1	55.6	2000	110	165
W21×62 + C12×20.7	183	329	494	248	373	2.83	4.25	9.38	38.0	1800	64.7	97.3
W18×50 + C15×33.9	133	239	359	190	285	1.03	1.55	12.4	60.1	1250	106	159
W18×50 + C12×20.7	127	228	343	175	263	1.68	2.53	9.55	41.2	1120	60.4	90.8
W16×36 + C15×33.9	86.8	156	234	144	216	0.244	0.367	12.9	62.9	748	101	151
W16×36 + C12×20.7	83.2	149	225	113	170	1.01	1.52	10.0	46.2	670	55.4	83.3
W14×30 + C12×20.7	62.0	111	167	88.1	132	0.599	0.900	10.2	49.0	447	53.8	80.9
W14×30 + C10×15.3	60.3	108	163	82.6	124	0.882	1.33	8.36	37.5	420	36.4	54.7
W12×26 + C12×20.7	48.2	86.6	130	73.7	111	0.314	0.472	10.3	51.2	318	53.2	79.9
W12×26 + C10×15.3	47.0	84.4	127	65.2	98.0	0.605	0.909	8.44	40.2	299	35.8	53.7

Table 3. Z_x Design Selection Table for Typical Combination Sections (F_y = 50 ksi)

$\Phi = 0.90$ $\Omega = 1.67$	W-Shapes with Cap Channels										F_y = 50 ksi	
Shape	Z_x	M_{px}/Ω	ΦM_{px}	M_{rx}/Ω	ΦM_{rx}	*BF*		L_p	L_r	I_x	M_{ny}/Ω	ΦM_{ny}
		kip-ft	kip-ft	kip-ft	kip-ft	kips	kips				kip-ft	kip-ft
	in.^{3}	ASD	LRFD	ASD	LRFD	ASD	LRFD	ft	ft	in.^{4}	ASD	LRFD
W36×150 + MC18×42.7	738	1840	2770	1380	2070	16.2	24.4	10.4	38.9	12000	272	409
W36×150 + C15×33.9	716	1790	2690	1330	2010	17.9	26.9	9.53	34.8	11500	211	317
W33×141 + MC18×42.7	652	1630	2450	1220	1840	13.8	20.8	10.4	39.6	10000	267	401
W33×141 + C15×33.9	635	1580	2380	1200	1810	14.9	22.4	9.50	35.0	9580	206	310
W33×118 + MC18×42.7	544	1360	2040	998	1500	11.7	17.6	10.7	41.3	8280	248	373
W33×118 + C15×33.9	529	1320	1980	986	1480	12.6	18.9	9.80	36.4	7900	188	282
W30×116 + MC18×42.7	492	1230	1850	911	1370	10.2	15.3	10.5	41.7	6900	246	369
W30×116 + C15×33.9	480	1200	1800	898	1350	11.1	16.7	9.61	36.5	6590	185	278
W30×99 + MC18×42.7	412	1030	1550	758	1140	8.23	12.4	10.8	43.6	5830	233	351
W30×99 + C15×33.9	408	1020	1530	749	1130	9.55	14.4	9.91	38.1	5550	173	260
W27×94 + C15×33.9	357	891	1340	669	1010	7.66	11.5	9.84	38.8	4530	173	260
W27×84 + C15×33.9	316	788	1190	591	889	6.55	9.85	10.0	40.1	4050	167	251
W24×84 + C15×33.9	286	714	1070	541	814	5.60	8.42	9.85	40.6	3340	166	249
W24×84 + C12×20.7	275	686	1030	526	791	7.53	11.3	7.71	28.9	3030	103	155
W24×68 + C15×33.9	232	579	870	432	649	4.47	6.72	10.2	43.2	2710	156	235
W24×68 + C12×20.7	224	559	840	419	630	6.29	9.46	7.99	30.2	2440	93.2	140
W21×68 + C15×33.9	207	516	776	389	585	3.74	5.62	10.1	44.1	2180	156	234
W21×68 + C12×20.7	200	499	750	379	570	5.26	7.91	7.83	30.6	1970	93.1	140
W21×62 + C15×33.9	189	472	709	354	533	3.35	5.04	10.3	45.2	2000	153	230
W21×62 + C12×20.7	183	457	686	344	518	4.83	7.26	7.96	31.2	1800	89.9	135
W18×50 + C15×33.9	133	332	499	263	396	1.81	2.71	10.5	48.5	1250	147	221
W18×50 + C12×20.7	127	317	476	243	365	2.90	4.37	8.11	33.6	1120	83.9	126
W16×36 + C15×33.9	86.8	217	326	200	300	0.427	0.641	10.9	50.7	748	140	210
W16×36 + C12×20.7	83.2	208	312	157	236	1.74	2.62	8.49	37.7	670	77.0	116
W14×30 + C12×20.7	62.0	155	233	122	184	1.04	1.56	8.66	39.7	447	74.7	112
W14×30 + C10×15.3	60.3	150	226	115	173	1.52	2.29	7.10	30.6	420	50.5	76.0
W12×26 + C12×20.7	48.2	120	181	102	154	0.551	0.829	8.74	41.1	318	73.9	111
W12×26 + C10×15.3	47.0	117	176	90.6	136	1.05	1.58	7.16	32.5	299	49.7	74.6

The derivation for allowable stress design (ASD) is similar and results in the following equation:

$$M_{aeq} = \frac{M_{ax} + bM_{ay}}{1 - 1.5mM_{ay}} \quad (11)$$

The coefficients m and b have been determined based on a regression analysis of all values for applicable channel caps for spans in 10 ft increments up to 100 ft and are provided in Table 1. The resulting equivalent moment determined from Equation 10 (LRFD) or Equation 11 (ASD) is then used to select a trial section from Z_x tables presented in Table 2 (F_y = 36 ksi) or Table 3 (F_y = 50 ksi) or from design graphs presented in Figures 1 and 2 to select a trial section. For unbraced lengths greater than the limiting length for yielding ($L_b > L_p$), the strong axis moment, M_{ux} or M_{ax}, should be divided by the C_b for a more accurate selection.

$$M_{aeq} = \frac{M_{ax}/C_b + bM_{ay}}{1 - 1.5mM_{ay}} \quad (12)$$

$$M_{ueq} = \frac{M_{ux}/C_b + bM_{uy}}{1 - mM_{uy}} \quad (13)$$

M_{ueq} is then used in the design graphs presented in Figure 2 (F_y = 36 ksi) or Figure 3 (F_y = 50 ksi) to select a trial section. The use of these graphs is identical to the widely used and familiar beam design moment graphs already provided in Part 3 of the 13th edition AISC *Steel Construction Manual* (AISC, 2005b).

SINGLY SYMMETRIC CRANE GIRDER DESIGN PROCEDURE

1. Determine deflection limits and stiffness requirements. Vertical deflection is typically limited to L/600 for light and medium cranes and L/1000 for heavy cranes. Horizontal deflection is typically limited to L/400 for all cranes. In addition, I_x is based on the full combination section, while I_y is based only on the channel and the top flange of the W-shape.
2. Determine the applied loads, including crane manufacturer specified maximum wheel loads, rail weight and runway girder weight. Maximum wheel loads are increased by 25% for cab or remotely operated bridge cranes and 10% for pendant operated bridge cranes.

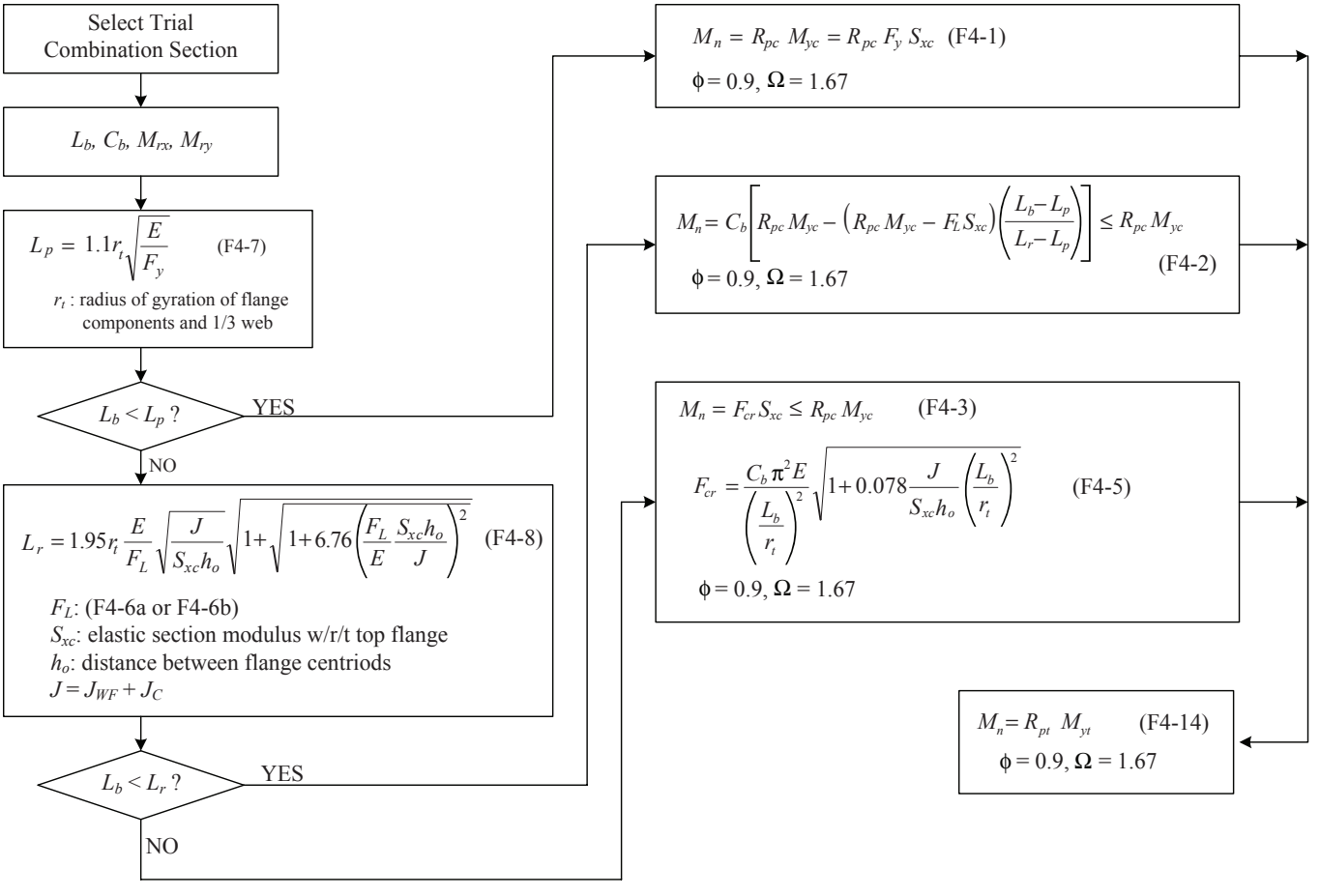

Fig. 1. Flow chart of the 2005 AISC Specification *Chapter F.4 evaluation process.*

3. Calculate the *x*- and *y*-axis bending moments and shear forces, applying suitable load combinations and determine the equivalent moment from Equation 10 (LRFD) or Equation 11 (ASD), or Equations 12 or 13 if C_b is applied.
4. Using the equivalent moment, select a trial section using either or Figure 2 or 3 or Table 2 or 3. Long spans supporting light cranes are normally controlled by deflection; therefore, trial section selection may be based on moment of inertia.
5. Evaluate the trial section for flexural and shear capacity based on 2005 AISC *Specification* Chapter F.4 following the flow chart in Figure 1, Chapter G, and Chapter H. Flexural capacity can also be determined with the assistance of Table 2 or 3. All singly symmetric, W and C combination sections listed in Table 1-19 of the 13th edition AISC *Steel Construction Manual* meet the compact web criteria of Table B4.1; therefore, the web plastification factors, R_{pc} and R_{pt}, are the ratio of the plastic moment to the compression and tension flange yield moments, respectively. Thus, $R_{pc} M_{yc} = M_p$ and $R_{pt} M_{yt} = M_p$, which can be substituted into Equation F4-2 of the 2005 AISC *Specification*:

$$M_{nx} = C_b \left[M_{px} - \left(M_{px} - F_L S_{xc} \right) \left(\frac{L_b - L_p}{L_r - L_p} \right) \right] \leq M_{px} \quad (14)$$

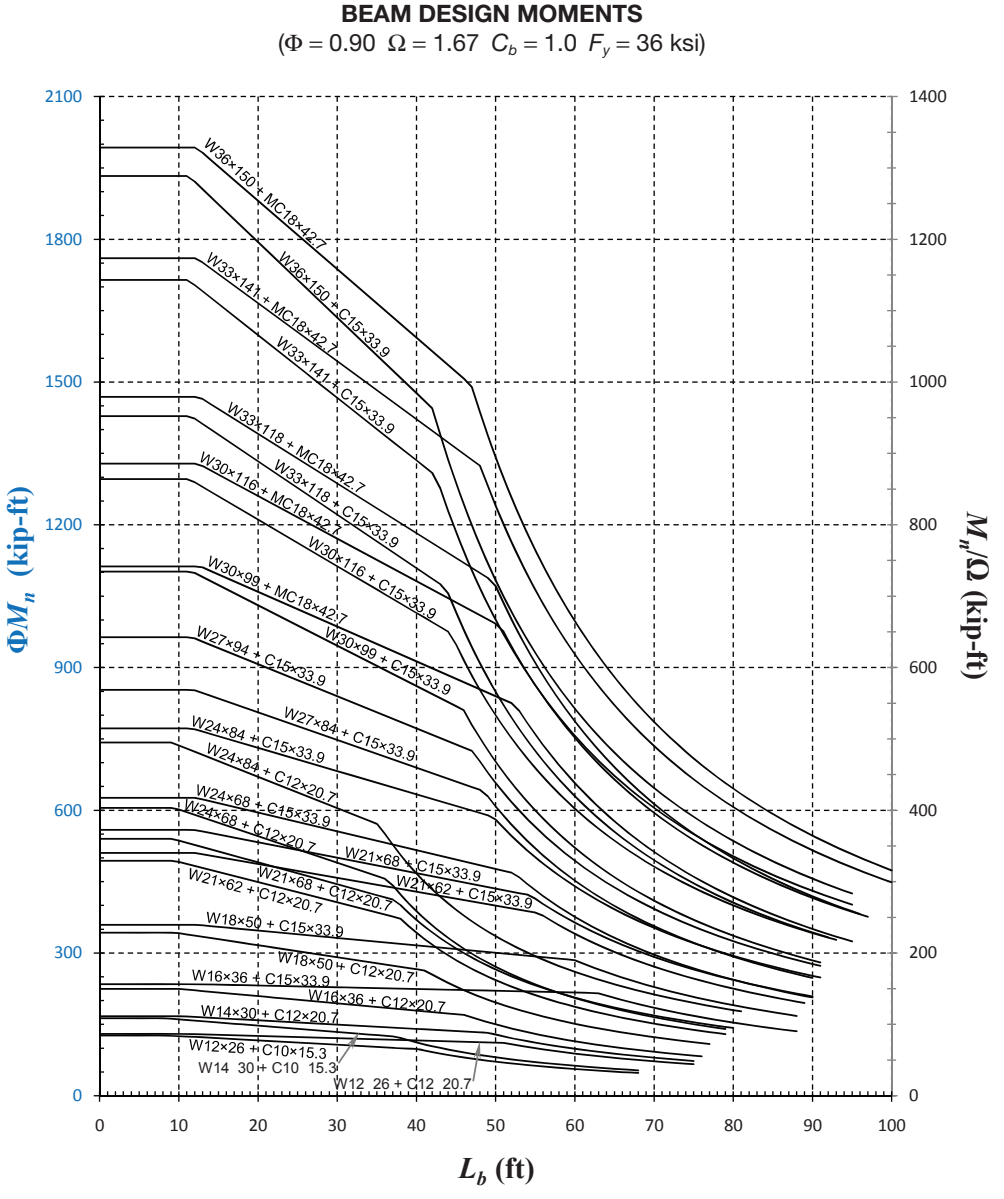

Fig. 2. Combination section design moment diagram (F_y = *36 ksi).*

BF is then defined as:

$$BF = \phi\left(\frac{M_{px} - F_L S_{xc}}{L_r - L_p}\right) \tag{15}$$

Substituting Equation 15 into Equation 14:

$$\phi M_{nx} = C_b\left[\phi M_{px} - BF\left(L_b - L_p\right)\right] \le \phi M_{px} \tag{16}$$

M_{ny} is calculated as the *y*-axis plastic bending strength of the wide flange top flange and the channel for combination sections:

$$M_{ny} = \left(Z_{W\ \text{top flange}} + Z_{x\ \text{channel}}\right)F_y = \left(\frac{t_f b_f^2}{4} + Z_{x\ \text{channel}}\right)F_y \tag{17}$$

6. Check concentrated load criteria in 2005 AISC *Specification* Section J10.
7. Evaluate fatigue provisions of 2005 AISC *Specification* Appendix 3.

EXAMPLE USING LRFD

Crane capacity = 20 tons
Bridge span = 70 ft
Cab-operated
Bridge weight = 57.2 kips
Trolley weight = 10.6 kips
Max wheel load = 38.1 kips (no impact included)

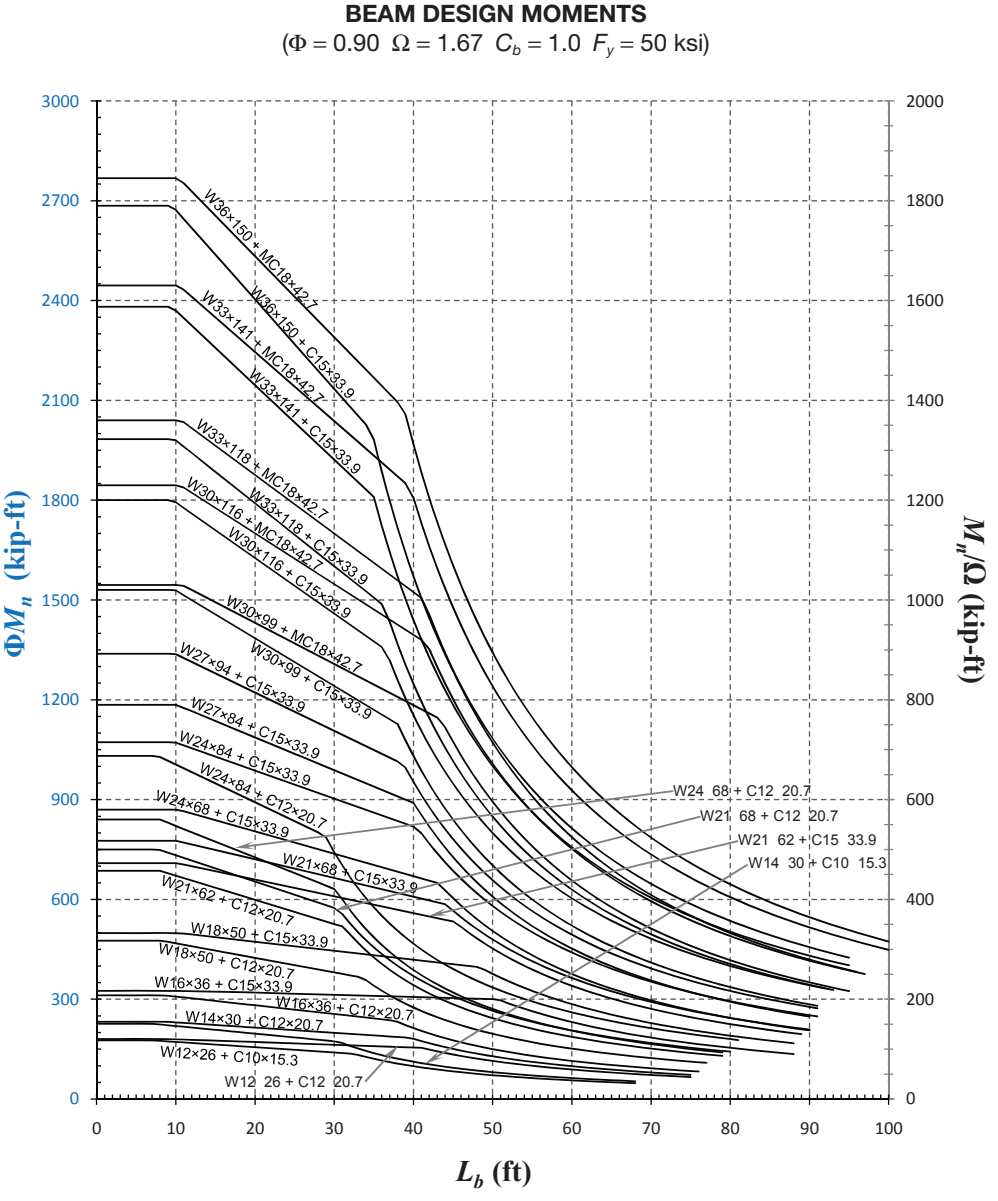

Fig. 3. Combination section design moment diagram (F_y = *50 ksi).*

Wheel spacing = 12 ft
Runway girder span = L_b = 30 ft, F_y = 50 ksi

1. Calculate the maximum factored moments and shears:

$P_{u\ vert}$ per wheel = 55.2 kips (assuming $\lambda = 1.6$ for lifted and trolley weight)

$P_{u\ horz}$ per wheel = 4.05 kips

w_u (self weight of girder and rail) = 0.19 kips/ft

M_{ux} = 683 kip-ft, C_b = 1.19

M_{uy} = 39 kip-ft

V_{uy} = 119 kips

V = 6.5 kips

Girder analysis details for this crane loading are provided in Fisher (2004).

2. Determine M_{ueq}:
Expect a C15×33.9 channel cap. From Table 1, with L_b = 30 ft and F_y = 50 ksi:

$b = 0.9$

$m = 3.0\times10^{-3}$

$$M_{ueq} = \frac{M_{ux}/C_b + bM_{uy}}{1 - mM_{uy}}$$

$$= \frac{(683 \text{ kip-ft})/1.19 + 0.9(39 \text{ kip-ft})}{1 - (3.0\times10^{-3})(39 \text{ kip-ft})}$$

$$= 690 \text{ kip-ft}$$

3. Select first trial section:
From Figure 3, with M_{ueq} = 690 kip-ft and L_b = 30 ft, select a W24×68 + C15×33.9. For this trial section, the following values are taken from Table 3:

$\phi M_{px} = 870$ kip-ft

$L_p = 10.2$ ft

$L_r = 43.2$ ft

$I_x = 2710$ in^4

$I_y = 385$ in^4

$BF = 6.72$

4. Evaluate M_{cx} and M_{cy}:

$$L_p = 10.2 \text{ ft} < L_p = 30 \text{ ft} < L_r = 43.2 \text{ ft}$$

$$M_{cx} = \phi M_{nx} = C_b\left[\phi M_{px} - BF\left(L_b - L_p\right)\right] \le \phi M_{px}$$

$$\phi M_{nx} = 1.19\left[870 \text{ kip-ft} - 6.72(30 \text{ ft} - 10.2 \text{ ft})\right]$$

$$= 877 \text{ kip-ft}$$

However, M_{cx} is limited by ϕM_{px} = 870 kip-ft. Therefore,

$$M_{cx} = \phi M_{nx} = \phi M_{px} = 870 \text{ kip-ft}$$

$$\phi M_{ny} = \phi F_y\left(\frac{t_f b_f^2}{4} + Z_{x\ \text{channel}}\right)$$

$$= \frac{(0.9)50 \text{ ksi}}{12 \text{ in./ft}}\left(\frac{0.585 \text{ in.}(8.97 \text{ in.})^2}{4} + 50.8 \text{ in.}^3\right)$$

$$= 235 \text{ kip-ft}$$

5. Evaluate Chapter H interaction (Equation H1-1b):

$$\frac{P_r}{2P_c} + \frac{M_{rx}}{M_{cx}} + \frac{M_{ry}}{M_{cy}}$$

$$= 0 + \frac{683 \text{ kip-ft}}{870 \text{ kip-ft}} + \frac{39 \text{ kip-ft}}{235 \text{ kip-ft}}$$

$$= 0.785 + 0.166$$

$$= 0.95 \le 1.0$$

6. Calculate $I_{required}$ based on strategic location of the crane P_{vert} and P_{horiz} for maximum deflection:

$$\Delta_{\text{vert max}} \le \frac{L}{600} = \frac{360 \text{ in.}}{600} = 0.6 \text{ in.}$$

therefore $Ix \ge 3{,}372$ in.^{4}

$$\Delta_{\text{horiz max}} \le \frac{L}{400} = \frac{360 \text{ in.}}{400} = 0.9 \text{ in.}$$

therefore $I_y \ge 140$ in.^{4}

The W24×68 + C15×33.9 trial section efficiently meets all 2005 AISC *Specification* strength requirements; however, the section does not meet generally accepted vertical deflection requirements. A W27×84 + C15×33.9 does meet both AISC strength and generally accepted deflection requirements.

CONCLUSION

A simplified design procedure is discussed for the crane girders listed as combination sections in Table 1-19 of the 13th edition AISC *Steel Construction Manual*. An equivalent moment method is presented for accurate selection of a combination section subjected to biaxial bending. Beam design moment graphs are presented to allow rapid selection of trial sections and tables are provided for efficient analysis of typical combination sections.

REFERENCES

AISC (2005a), *Specification for Structural Steel Buildings*, AISC 360-05, American Institute of Steel Construction, Chicago, IL.

AISC (2005b), *Steel Construction Manual*, 13th ed., American Institute of Steel Construction, Chicago, IL.

Fisher, J.M. (2004), *Design Guide 7: Industrial Buildings—Roofs to Anchor Rods*, 2nd ed., American Institute of Steel Construction, Chicago, IL.

Laman, J.A. (1996), "LRFD Crane Girder Design and Aids," *Engineering Journal*, American Institute of Steel Construction, Vol. 33, No. 4, 1996, pp. 153–158.

Current Steel Structures Research

REIDAR BJORHOVDE

This quarter, we focus on a selection of current research projects at three major Japanese universities. The descriptions do not discuss all of the current projects at the schools. Instead, selected studies give a representative picture of the research efforts and demonstrate the schools' importance to the efforts of industry and the profession worldwide.

The universities and their structural steel researchers are very well known in the world of steel construction: University of Kyoto, Tokyo Institute of Technology and Osaka University. Researchers at these institutions have been very active for many years, as evidenced by their participation and leading roles in the seismic and other standards development efforts of Japan, and indeed of the United States and many other countries. In fact, all three universities have collaborated actively with several American schools, sharing testing facilities and involving numerous faculty members and graduate students. Large numbers of outstanding technical papers, reports and conference presentations have been published, contributing to a collection of landmark studies that continue to offer practical solutions to complex problems for designers as well as fabricators and erectors.

References are provided throughout the paper, whenever such are available in the public domain. However, much of the work is still in progress, and in some cases, reports or publications have not yet been prepared for public dissemination.

SELECTED RESEARCH AT THE UNIVERSITY OF KYOTO

Focusing on the all-important issues of earthquake resistance and performance of materials and structures, the Disaster Prevention Research Institute (DPRI) was established in 1962 at the University of Kyoto by the late Professor Minoru Wakabayashi. Over the years, it has been a uniquely successful undertaking, not the least through a significant number of doctoral graduates who have occupied leadership roles in Japan and in the international arena.

One of the current leaders of DPRI is Professor Masayoshi Nakashima. A Lehigh University Ph.D. graduate, Professor Nakashima is also the Director of the Hyogo Earthquake Engineering Research Center, one of the central operations of the Japanese National Research Institute for Earth Science and Disaster Prevention (NIED). He has been the director or a primary leader of the four research projects that are discussed in the following sections of the paper.

Development of Distributed Hybrid Testing Techniques and Their Application to Collapse Simulation of Steel Moment Frames: The study is a major effort that has been under way in Japan since the late 1960s. Originally, structural testing around the world was based on the static response of frames and frame components. Considering the loads and deformations that are imposed on a structure under seismic conditions, the static tests could not capture the demands associated with large displacement cyclic behavior. Originally referred to as a pseudo-dynamic test, the hybrid test has been under development and continuous application for numerous experiments over the past 40 years. Its evolution and application has been a continuing joint effort between the University of Kyoto and a number of Japanese and American universities.

Essentially, the hybrid test provides a numerical solution for the dynamics of the structure, and the restoring forces are determined from physical tests that are run in parallel with the computation. When the substructure approach is used, the advantage is that the physical test does not have to be performed in the same laboratory. Instead, the substructure is disassembled and the individual parts can be tested simultaneously in different locations. Further, it is not even necessary to do physical tests of all of the parts, since some of them may be "tested" numerically by using appropriate finite element models.

The researchers at DPRI have developed an approach that makes use of the above concepts (Pan et al., 2006). It is extremely complex but has been proven very successful. Specifically, through an extensive coordination effort, the data from tests and numerical solutions of a number of substructures are exchanged with the central management. Subsequently, the data are used to provide the prediction of the complete structural response. As an example, the complete seismic response of a four-story single bay frame was determined, using two substructures that were physically tested at different locations, along with one finite element code (Wang et al., 2008). Various levels of ground motion were used, including one that led to the collapse of the structure. The failure was initiated by excessive damage in the column bases, as shown in Figure 1.

Reidar Bjorhovde, Ph.D., Research Editor for *Engineering Journal,* Tucson, AZ. Email: rbj@bjorhovde.com

Performance and Retrofit of Steel Beam-to-Column Connections of High-Rise Buildings: High-rise buildings have been constructed in Japan for more than 40 years, and at this time there are more than 2,000 such structures in the country. Certain seismic conditions in Japan are a particular issue for such structures, because the subduction earthquakes that are generated to the south of the country have long periods and long duration. A complete four-story structure with four longitudinal bays and three transverse bays was tested with the very large shaking table of the E-Defense laboratory (Chung et al., 2010).

In addition to the shaking table test, a series of typical beam-to-column connections were also tested to determine dynamic failure characteristics and energy absorption. Retrofit methods were also examined. One of the failure modes is shown in Figure 2, where the bottom flange fractured from a crack that started at the toe of the weld access hole. This detail and its performance are, of course, very similar to what was experienced for similar connections during the 1994 Northridge earthquake. The researchers observe that it is likely that some of the older connections may suffer similar problems in future earthquakes.

Friction Resistance Developed between the Steel Base Plate and the Mortar Surface: The frictional resistance that is developed between an exposed column base plate and the underlying mortar surface is recognized in the Japanese design standards. However, the resistance is not fully utilized for seismic applications, mostly because the relationship between the friction effect and the sliding motion of the base plate is not fully understood. A series of tests was conducted, demonstrating that the surface condition of the

Fig. 1. Typical damage at column base that eventually led to frame collapse. (Photo courtesy of Professor M. Nakashima)

Fig. 2. Failure mode of older beam-to-column connection. (Photo courtesy of Professor M. Nakashima)

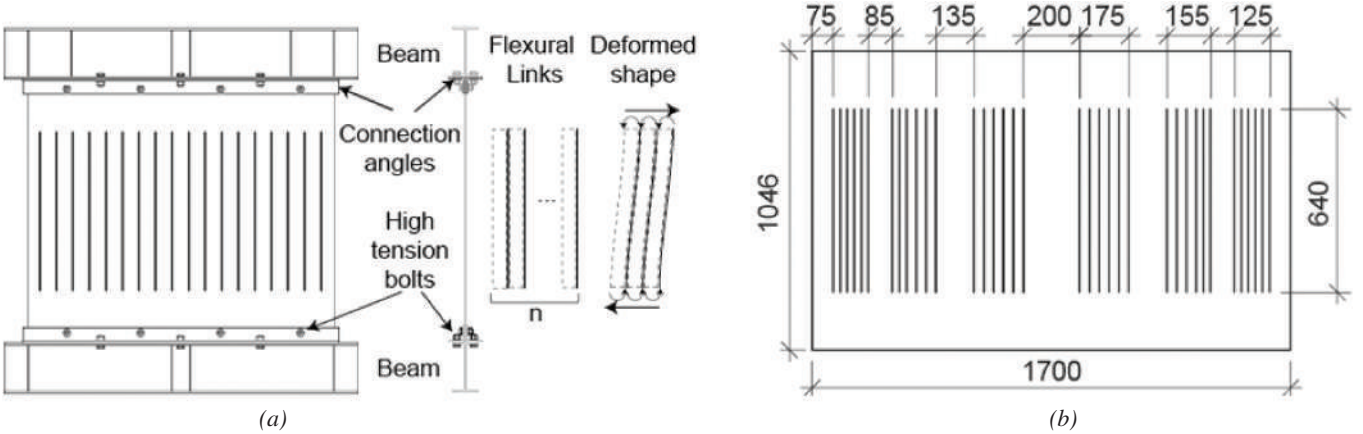

(a) *(b)*

Fig. 3. (a) Original slit-wall system and the deformed links; (b) slit-wall with unequal spacing of the slits, measurements in mm. (Drawing courtesy of Professor M. Nakashima)

base plate was critical. Thus, the friction coefficients were found to vary between 0.52 and 0.97.

Subsequent tests and analyses with rigid and flexible specimens used sinusoidal horizontal loads of various frequencies and magnitudes as well as combined horizontal and vertical loads, and nonstationary motion. These studies are continuing, seeing that sliding velocities and distances are important parameters. In particular, with increasing sliding velocities and distances, the friction coefficient decreased from the initial (static) value. This is as should be expected. The continuing study aims at providing improved practical design criteria.

Slit-Wall System Serving as a Structural Damping Mechanism and as a Condition Assessment Device for the Structure: The slit-wall system is a novel development for seismically resistant structures, with the first studies taking place at Kyoto, but there is also work going on in the United States (Purdue University). The system is particularly well suited for use in areas of cities where urban density is high and for which it is essential to have a mechanism whereby the condition of structures—their structural "health"—can be monitored effectively. Traditionally, the condition assessment is achieved through the installation of sensors, but this is neither practical nor economical for large buildings, especially when numerous structures need to be monitored.

The slit-wall system focuses on the development of a structural member that can serve both as an efficient energy dissipation element as well as a condition assessment tool or sensor. As shown schematically in Figure 3, the slit-wall consists of a steel plate shear wall with vertical slits, with the segments between the slits serving as flexural links. The flexibility of the links provides for significant ductility and energy absorption, and there is no need for out-of-plane stiffening of the links. At the same time it is also possible to utilize unequal spacing of the slits, to have links of different properties. In this fashion, the monitoring feature of the links is established, without reducing the energy absorption capacities.

Two methods may be used for the assessment of the structural condition; they have their unique advantages and disadvantages. One approach uses a brittle coating for the links; the coating cracks at a certain strain level, and the locations are recorded remotely. The links are then examined visually to determine the spread of yielding in the elements. The cracking strain level is directly related to the maximum interstory drift that has occurred during an earthquake.

The other monitoring approach focuses on the appearance of lateral-torsional buckling of the links. When different spacing is used for the slits, the individual links can be designed to develop inelastic buckling for various drift magnitudes. Together with visual inspection, this provides information on the maximum drift that has occurred in the wall. Figure 4 shows a slit-wall with buckled links; this was established in a quasi-static test accompanied by an online hybrid test. The results to date confirm that the slit-wall system will function very well for both intended functions, with a level of accuracy of 0.005 rad between different drift levels (Jacobsen et al., 2010).

SELECTED RESEARCH AT THE TOKYO INSTITUTE OF TECHNOLOGY

Tokyo Institute of Technology has two campuses, and the structural engineering faculty members at both are very prominent in Japanese research and development efforts. In fact, the school has more structural engineering faculty members than all of the other Japanese universities. The current research efforts are intense, as evidenced by the eight projects that are described in the following sections.

Response Control of Steel Structures Using Dampers: This project has been sponsored by the National Research Institute for Earth Science and Disaster Prevention (NIED) and by the Japan Society for the Promotion of Science (JSPS). A faculty member at Lehigh University before returning to Japan, Professor Kazuhiko Kasai has been the director of this project.

Passive control of building performance under seismic conditions through various forms of damping devices has increased very significantly in Japan following the 1995 Hyogo-Ken Nanbu earthquake. However, a major earthquake has not occurred in Japan since that time, and the performance of the dampers, therefore, has not been verified under such conditions. The current project aims at resolving any performance questions that may arise.

As part of the study, a full-scale five-story building with and without the damping devices was tested, using the ground motion that was recorded in the 1995 event. The E-Defense shaking table, which is the largest and most powerful in the world, was used for the test. Figure 5 shows the

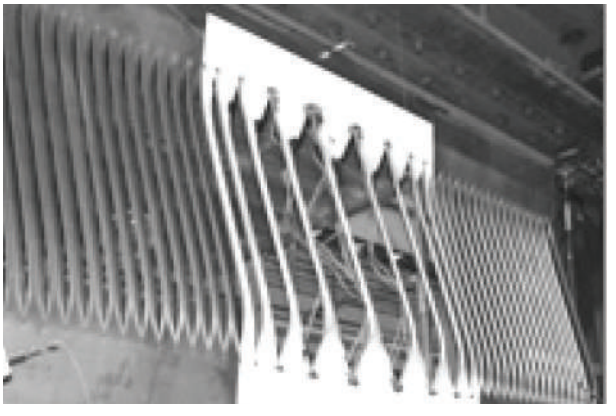

Fig. 4. Lateral-torsional buckling of links in a slit-wall with unequal spacing of slits. (Photo courtesy of Professor M. Nakashima)

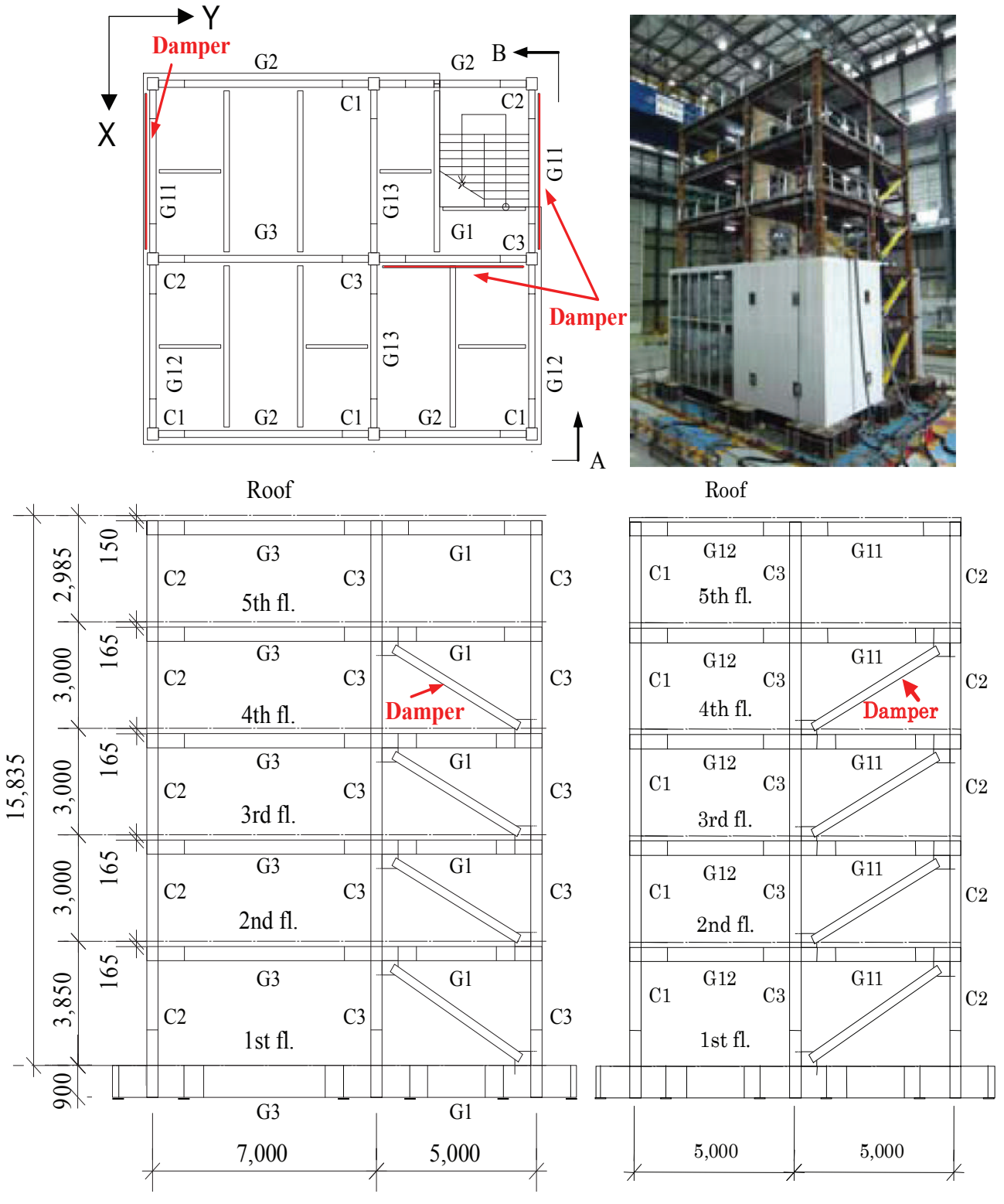

Fig. 5. Elevation and plan of building tested for damping performance. (Drawings and photo courtesy of Professor K. Kasai)

building that was used, including the placement of the 12 same-type dampers in three to four different sizes that were installed. The tests were repeated by removing the dampers and replacing them with different types. Four types of dampers were used: (1) steel, (2) viscous, (3) oil damper and (4) viscoelastic. They are illustrated in Figure 6.

The building and the dampers performed well when they were subjected to the ground motion. The analysis is continuing at this time, using the data from a total of 1,400 channels. In addition, further tests were run, with and without a concrete slab, to examine the influence of idealized boundary conditions. It is anticipated that it will be possible to validate the test method, the analysis and the design approach for passively controlled buildings. Details of the tested frame are shown in Figure 7.

Structural Behavior of Beam-Column Subassemblies with Damper Connections: This study will provide additional data for the examination of the performance of typical damping elements that are used to enhance the response of buildings during an earthquake. Professors Akira Wada and Shoichi Kishiki have been the project directors.

The study has focused on testing and analysis to establish the structural behavior of beam-columns with damper connections. The aim is to develop a design method for such

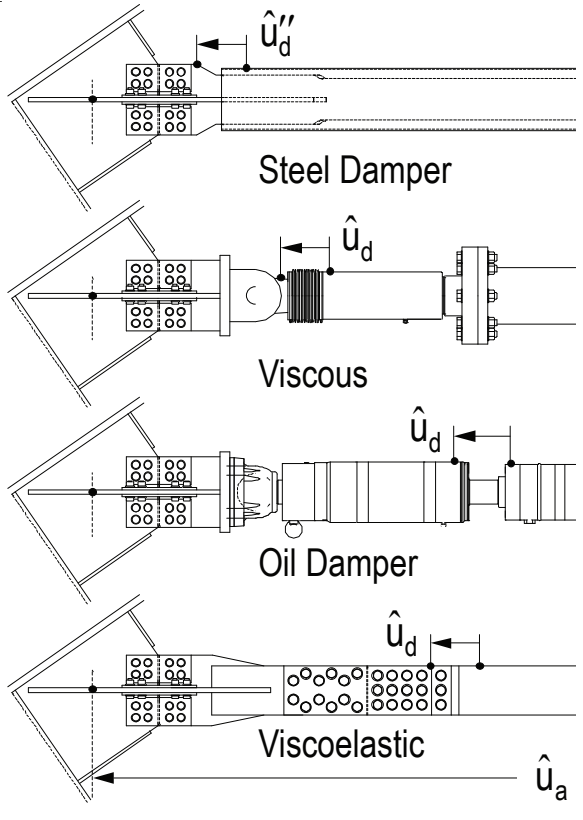

Fig. 6. Four types of dampers used in the full-scale building test. (Drawings courtesy of Professor K. Kasai)

members, including considerations for the design load level as well as loads beyond the design level. Brace-type and wall-type damping connections have been used in the tests, as illustrated in Figure 8, on page 275. Specifically, a force-controlled actuator in the test assembly functions as the reaction or as a virtual damper; a displacement-controlled actuator imposes a story drift on the test frame. Virtual dampers thus produce forces that depend on the velocity or the displacement that is developed, and this is the case even if static actuators are used in the tests.

The researchers are currently evaluating the initial findings; additional tests and analyses will be performed.

Stability Conditions of Buckling Restrained Braced (BRB) Frames: The project has been undertaken to provide improved stability design criteria for the next edition of the steel design standard of the Architectural Institute of Japan (AIJ). Professor Toru Takeuchi has been the project director.

Particular attention is being paid to the potential for out-of-plane buckling and the consequent performance demands that are imposed on the restrainer ends of the connections. Specifically, buckling must not occur before the core plates yield. Further, local buckling of the core plates is also an important limit state, although such a failure is unlikely to occur unless the BRB has only been designed for overall buckling.

Physical testing and analytical evaluations have been performed for the out-of-plane overall and local buckling limit states to ensure that the energy absorption capacity is retained. This is essential to ensure the satisfactory response of the buckling restrained braces and the structure.

Buckling and Post-Buckling Behavior of Steel Members: Professor Kikuo Ikarashi has been the director of this project. Attempting to develop a comprehensive model for the inelastic deformation capacity of wide-flange shapes, the study has examined the coupled local plate buckling effects of the shapes, taking into account the shape geometry and the stress distribution. A new plate slenderness term has been formulated, whereby the influence of the stress distribution, the yield stress level and the coupled plate instability effects are incorporated. A number of cyclic load tests have been performed, confirming the use of the new slenderness term. The correlation between test and analytical results is very good. The concepts are now being extended to the coupled instability of plate local buckling and overall buckling.

Evaluation of the Ultimate Earthquake Resistance of Moment Frames: Professor Satoshi Yamada has been the director of this study. Using random cyclic loading and focusing on the maximum strength, energy absorption capacity and hysteretic response of beams, columns and connections, and including the influence of concrete slabs in the structures, extensive analytical results have been compiled for a range of moment frames. For use with the evaluation

of beam response characteristics, the properties of the steel are modeled by using the elongation response of material tests. The response of columns is based on the characteristics of stub columns, including the occurrence of local buckling. Overall member buckling is also addressed. Finally, the strength and behavior of connection panel zones as well as column bases are also incorporated, leading to a complete frame response representation.

The study is continuing, but at this stage it has been determined that the overall energy absorption of the frame can be modeled accurately by using the element characteristics. Furthermore, data are also obtained on the damage distribution in the frame, which depends on the strength and stiffness distribution of the structural components, along with the seismic load input. Using the hysteretic models of loads and the strength of the components, up to and including the deterioration behavior range, the ultimate earthquake resistance of the frame is determined by an inelastic response analysis.

Identification of Displacement-Induced Fatigue Using a Wireless Sensor Network (WSN): Professor Chitoshi Miki has been the director of this research project. The very large number of steel bridges in Japan and the large traffic volume necessitates intense attention to "traditional" fatigue cracking, as is found in various structural details due to various levels of stress range and stress concentrations. Displacement-induced fatigue cracking is much more complex in many ways, as well as difficult to observe and assess for various locations within a bridge structure (Fisher and Mertz, 1982; Fisher, 1984).

For the current research project, it was decided to instrument a bridge with wireless sensors and to assemble their responses through a network. The bridge in question is a

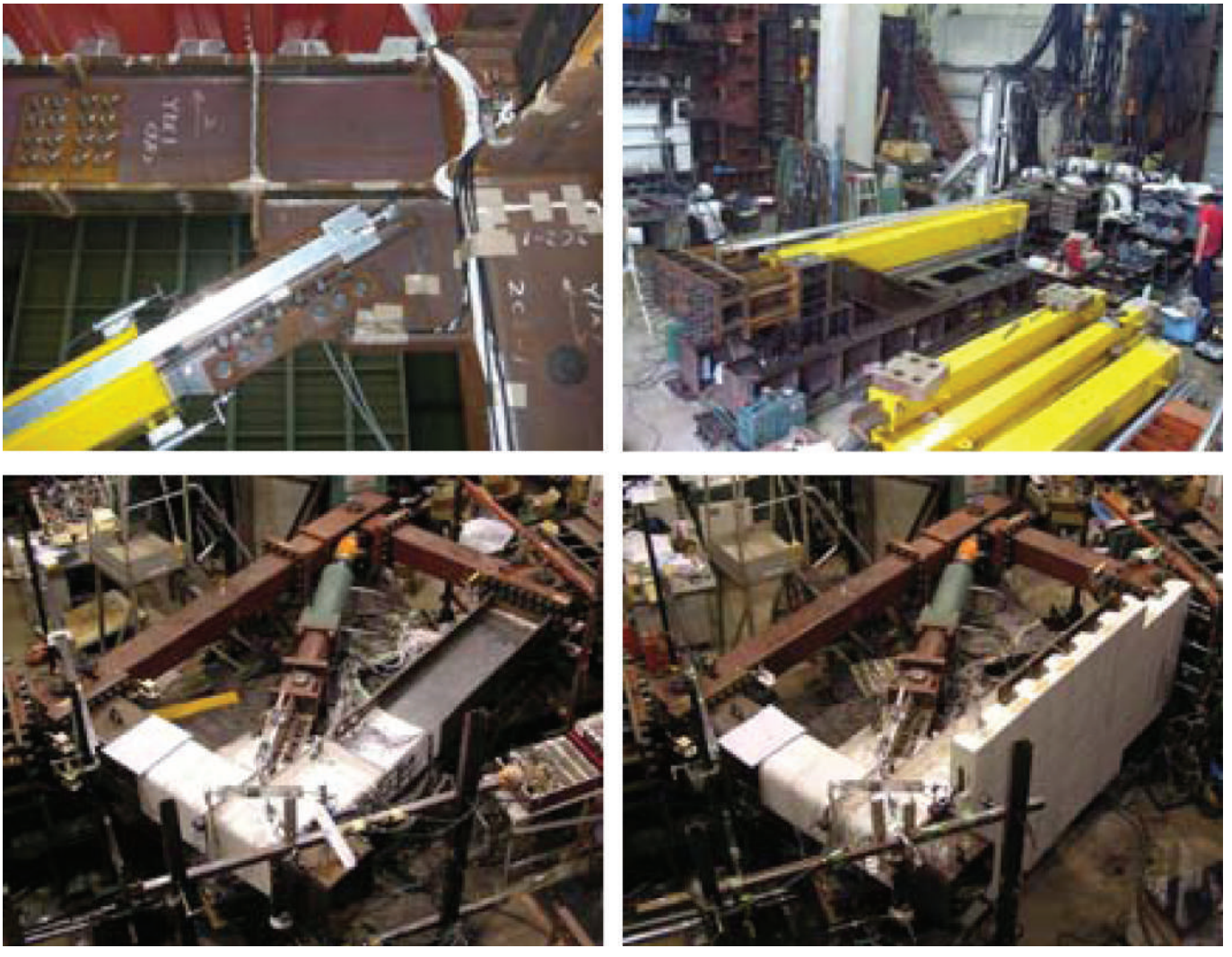

Fig. 7. Details of tested assemblies, including dampers, beam-column-gusset plate connections, with and without a concrete slab. (Photos courtesy of Professor K. Kasai)

two-lane, three-girder simply supported structure, as shown in Figure 9. Figure 9a shows the cross-section along with the wireless sensor locations, and Figure 9b shows the plan view along with the sensor locations (square symbols) and the damage locations (circle symbols).

The acceleration data provided by the sensors were translated into displacement data by integration over the time domain. The sensor at the top of girder G1 indicated a displacement of 5 mm (0.2 in.). It was determined that all of the girders deflected in the same phase, but with different magnitudes for the girders. The researchers note that the fatigue damage can be attributed to the deflection differences between G1 (largest) and the other two girders.

As an extension of the project, finite element analysis is now being used to simulate the structural behavior of the bridge. In addition, an expanded WSN with 20 sensors will be installed to obtain additional details about the structural behavior.

Effect of Compressive Residual Stress to Improve the Fatigue Strength under Variable Stress Conditions: Professor Chitoshi Miki has been the director of this research project. On the premise that compressive residual stress at a weld toe will improve the fatigue strength of a detail, the effects of various types of hammer peening have been examined for high cycle fatigue tests under variable loading conditions. Three peening methods were used to introduce the compressive residual stress, as follows: (1) low-temperature transform (LTT), (2) pneumatic peening and (3) electrical peening. At this time the results are being examined, but nothing is conclusive. A girder test specimen with and without the application of peening for the weld details will be subjected to variable amplitude loading. Results for constant amplitude loading will also be incorporated into the project.

Numerical Model for the Stress-Strain Relationship of Steel, Including the Bauschinger Effect: Professor Shojiro Motoyui has been the director of this research project. The phenomenon referred to as the Bauschinger effect is neither well understood nor known to many researchers today. It was subject to much discussion during the period from 1950 to 1975, when plastic analysis and design were at the forefront of structural mechanics. Briefly, if a specimen is deformed beyond yielding in one direction (e.g., compression) and then unloaded and subjected to loading in the other direction, the yield stress in this direction will be lower than

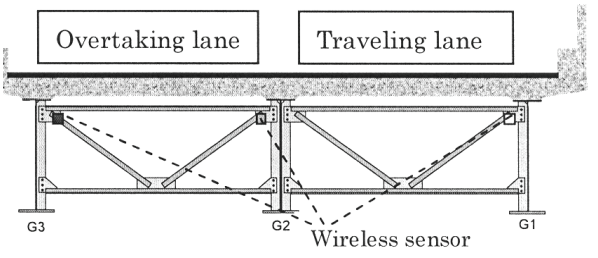

(a) Cross-section

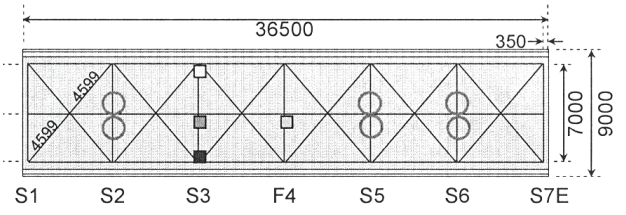

(b) Plan view

Fig. 9. Bridge structure schematic showing sensors (squares) and damage locations (circles). (Drawing courtesy of Professor C. Miki)

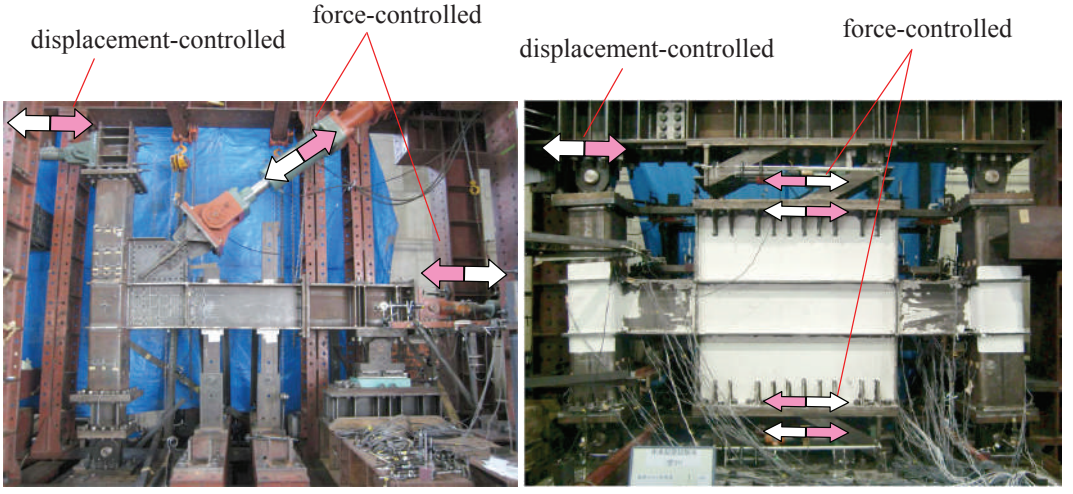

(a) brace-type damper (b) wall-type damper

Fig. 8. Tests of beam-column assemblies with two types of damper connections. (Photos courtesy of Professors S. Kishiki and A. Wada)

the original one (Dieter, 1986; Hertzberg, 1996). Normally, the effect is ignored, but for cyclic loading such as is experienced during seismic events, it is a real question whether it might play a role, in any number of ways. The situation is further and significantly complicated when multidimensional states of stress need to be addressed.

Theoretical models have been developed, but so far these have only been applied to uniaxial problems. The intent of the researchers is to develop a numerical model that can simulate realistic multi-axial states of stress and strain. It should have real applications in many of the seismic areas of application.

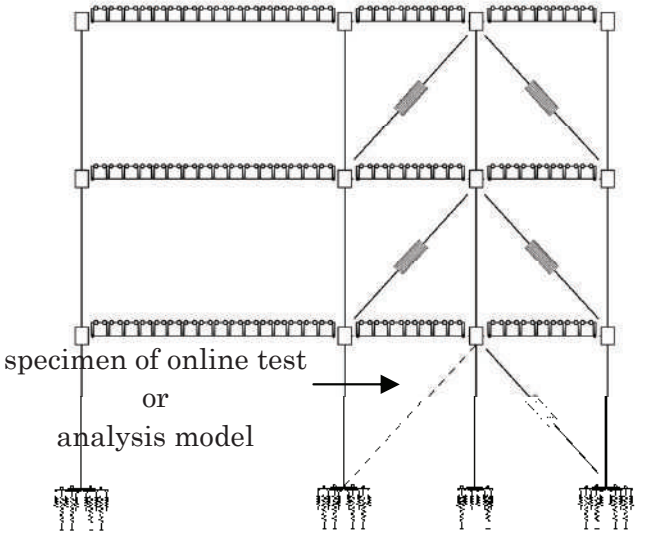

Fig. 10. Three-story frame for online test and analytical modeling. (Drawing provided by Professor Y. Kimura)

RESEARCH PROJECT AT OSAKA UNIVERSITY

Seismic Response of Steel Structures with Tubular Bracing Members: As has become a model of cooperation among Japanese researchers, tests of structures and elements may be conducted at several laboratories, with central online tie-in between the test teams and the analytical team.

In the case of the project at Osaka University, a three-story three-bay frame with tubular bracing members, as shown in Figure 10, was analyzed for various earthquake intensities (Mukaide et al., 2010).

Figure 11 shows the analytical results with and without the online test. It is noted that a brace fracture only occurred

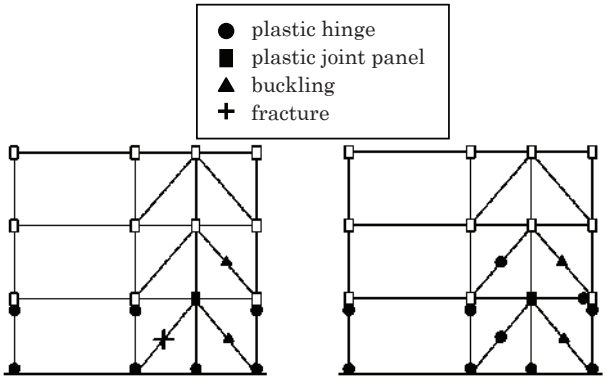

(a) Response with online test (b) Response without online test

Fig. 11. Test frame results with and without the online test. (Drawing provided by Professor Y. Kimura)

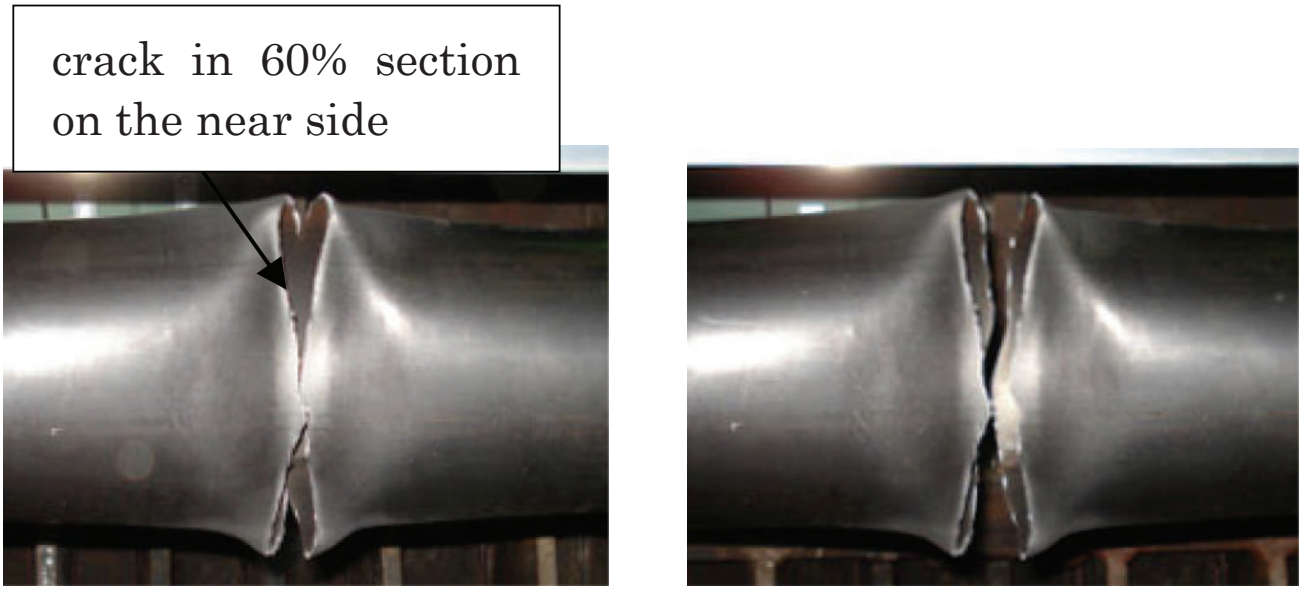

(a) Development of crack (b) Fracture

Fig. 12. Fracture of tubular bracing member for the frame. (Photo provided by Professor Y. Kimura)

for the online test. Plastic hinges developed at several locations, and the diagonal brace in one of the first-story bays buckled. Figure 12 shows the development of the crack and then the fracture that occurred in the tubular bracing member when the online test was done.

ACKNOWLEDGMENTS

Significant special assistance has been provided by Professors Masayoshi Nakashima of the University of Kyoto and Kazuhiro Kasai of the Tokyo Institute of Technology and many of their colleagues. Additional assistance was provided by ISSRA member Yoshihiro Kimura of Nagasaki University in Nagasaki, Japan. All of these efforts are sincerely appreciated.

REFERENCES

Chung, Y., Nagae, T., Hitaka, T. and Nakashima, M. (2010), "Seismic Resistance Capacity of High-Rise Buildings Subjected to Long-Period Ground Motions: E-Defense Shaking Table Test," *Journal of Structural Engineering*, ASCE, Vol. 136, No. 6, pp. 637–644.

Dieter, G.E. (1986), *Mechanical Metallurgy*, 3rd ed., McGraw-Hill Book Company, New York, NY.

Fisher, J.W. and Mertz, D.R. (1982), "Displacement Induced Fatigue Cracking of a Box Girder Bridge," *IABSE Symposium on Maintenance, Repair and Rehabilitation of Bridges*, Washington, DC.

Fisher, J.W. (1984), *Fatigue and Fracture in Steel Bridges—Case Studies*, John Wiley & Sons, New York, NY.

Hertzberg, R.W. (1996), *Deformation and Fracture Mechanics of Engineering Materials*, 4th ed., John Wiley & Sons, New York, NY.

Jacobsen, A., Hitaka, T. and Nakashima, M. (2010), "Online Test of Building Frame with Slit-Wall Dampers Capable of Condition Assessment," *Journal of Constructional Steel Research*, Vol. 66, No. 11, pp. 1320–1329.

Mukaide, S., Kataoka, M. and Tada, M. (2010), "Seismic Response of Steel Structures Including Fractures at Tubular Braces Using Collaborative Pseudo-Dynamic Test," *Journal of Structural and Construction Engineering*, Architectural Institute of Japan, Vol. 75, No. 652, pp. 1139–1147, in Japanese.

Pan, P., Tomofuji, H., Wang, T., Nakashima, M., Ohsaki, M. and Mosolam, K.M. (2006), "Development of Peer-to-Peer (P2P) Internet Online Hybrid Test System," *Journal of Earthquake Engineering and Structural Dynamics*, Vol. 35, No. 7, pp. 867–890.

Wang, T., McCormick, J., Yoshitake, N., Pan, P., Murata, Y. and Nakashima, M. (2008), "Collapse Simulation of a Four-Story Steel Moment Frame by a Distributed Online Hybrid Test," *Journal of Earthquake Engineering and Structural Dynamics*, Vol. 37, No. 6, pp. 955–974.

DISCUSSION

Critical Evaluation of Equivalent Moment Factor Procedures for Laterally Unsupported Beams

Paper by EDGAR WONG and ROBERT G. DRIVER
First Quarter, 2010

Discussion by STEVEN WILKERSON

The authors of the paper are to be commended for studying various issues related to the use of moment gradient coefficients for estimating lateral-torsional buckling strength. By comparing approaches used in different specifications (historically and in other countries' codes) and by quantifying deficiencies in empirical formulations, they have provided an opportunity for practicing engineers to understand the limitations of the 2005 AISC *Specification* (AISC, 2005). An important conclusion of the paper is that empirical relationships for estimating moment gradient coefficients can be unconservative in some cases and may be too aggressive for design purposes.

Clark and Hill (1960) elegantly presented the use of coefficients to extend the uniform moment case. This extension had a theoretical basis corresponding to the minimum potential energy solution for the buckling moment. It also included tabular data for common cases, which have been widely published. The formulation was completely general in that it provided a means of calculating coefficients without placing any assumptions on the beam twist and lateral displacement. However, direct evaluation of the required definite integrals is practically limited to cases that are closely approximated by a single half-sine or half-cosine curve (corresponding to either fixed or free torsional-rotation boundary conditions). This approach is adequate for the majority of cases in common use, but it is not necessarily accurate in cases that are largely anti-symmetric. Historically, the specifications have relied on empirical relationships for estimating the moment gradient coefficient C_b in order to bypass the need for evaluation of definite integrals.

Wilkerson (2005) presented a family of approximate relationships with varying accuracy that have estimable error and are therefore suitable for general use. The basis for the method was a form of quadrature, or numerical integration, which was tailored for the application by choosing weighting constants so that the error was exactly zero if the integrand was piecewise-equal to the function in the assumed quadrature rule (either the trapezoidal rule or Simpson's rule). It was shown in that paper that two approximate relationships would be sufficient for the estimation of C_b for cases of (1) linearly (or nearly linearly) varying loads and (2) concentrated loads. The latter expression recognized nonsmoothness in the moment diagram and the potential for large errors when using only moment data, and thus included the use of shear data to increase the accuracy. Abrupt discontinuities in the moment diagram were not addressed (no current method other than finite element modeling is able to give accurate results in these cases).

Both expressions were derived as "quarter-point" methods to simplify the procedure, but the derivations were general enough to be used for the development of more refined models. It was determined by studying the error in estimation of the definite integrals that the use of higher order derivative information (i.e., shears) had a greater effect on reducing the error than could be realized by adding additional moment data. Using the terminology of the original paper and the 2005 AISC *Specification*, the recommended expressions were as shown here:

For cases with linearly varying loads only:

$$C_b = \frac{M_{\max}}{\sqrt{\frac{M_A^2}{4} + \frac{M_B^2}{2} + \frac{M_C^2}{4}}} \le 2.6$$

For cases with concentrated loads:

$$C_b = \frac{M_{\max}}{\sqrt{\left(\frac{1}{4} + \frac{\pi}{48}\right)M_A^2 + \frac{M_B^2}{2} + \left(\frac{1}{4} - \frac{\pi}{48}\right)M_C^2 + \frac{L_b}{12}\left(\frac{M_A V_A}{4} + \frac{M_B V_B}{2} + \frac{M_C V_C}{4}\right)}} \le 2.6$$

Steven Wilkerson, Ph.D, P.E., Associate Vice President, Haynes Whaley Associates, Houston, TX. E-mail: steve.wilkerson@hayneswhaley.com

where V_A, V_B, and V_C were shears corresponding to the quarter-point moments, and the sign convention for shears and moments followed a "strength of materials" approach consistent with the relationship $M(z) = \int_o^z V(x)dx$. It was demonstrated by comparison with 10 cases from Clark and Hill that the use of an upper bound on C_b of 2.6 was sufficient to limit the error to no more than 10% for various linear and nonlinear moment diagrams.

Additionally, Wilkerson (2005) made recommendations on the use of a second coefficient to include the effects of load position when not located at the shear center of the beam. It was demonstrated through the use of finite element modeling that the recommendations in the 2005 AISC *Specification* for the consideration of an unbraced beam loaded at the top flange were sometimes unconservative. Moment strength was overestimated by as much as 43% in cases reviewed. The paper gave approximate expressions for evaluation of the load position coefficient, C_a, in cases with linearly varying and concentrated loads. The expressions for this coefficient were derived similarly to those for C_b by approximating the definite integrals developed by Clark and Hill. The incorporation of load position into the evaluation of moment strength requires an extension to the usual equation for critical moment. A preliminary section in Wilkerson (2005) included a derivation of this expression based on the differential equations for lateral-torsional buckling of a transversely loaded beam.

It is the writer's hope that this discussion will further encourage adoption of a more rigorous approach to the estimation of coefficients that extend the uniform moment strength solution to the more general cases needed for everyday design. Because approximate relationships are clearly necessary to allow for a practical implementation of this extension, the writer advocates the use of methods that have a basis in theory with reliable error estimates, such as those derived in Wilkerson (2005).

REFERENCES

AISC (2005), *Specification for Structural Steel Buildings*, ANSI/AISC 360-05, American Institute of Steel Construction, Chicago, IL.

Clark, J.W. and Hill, H.N. (1960), "Lateral Buckling of Beams," *Journal of the Structural Division*, American Society of Civil Engineers, Vol. 86, No. ST7, pp. 175–196.

Wilkerson, S.M. (2005), "Improved Coefficients for Elastic Lateral-Torsional Buckling," AIAA 2005-2352, 46th AIAA/ASME/ASCE/AHS/ASC Structures, Structural Dynamics & Materials Conference, April 2005, Austin, TX.

Wong, E. and Driver, R.G. (2010), "Critical Evaluation of Equivalent Moment Factor Procedures for Laterally Unsupported Beams," *Engineering Journal*, American Institute of Steel Construction, Vol. 47, No. 1, pp. 1–20.

CLOSURE

Critical Evaluation of Equivalent Moment Factor Procedures for Laterally Unsupported Beams

Paper by EDGAR WONG and ROBERT G. DRIVER
First Quarter, 2010

Closure by EDGAR WONG and ROBERT G. DRIVER

The authors thank the discusser for his insightful comments and the favorable review of their critical approach that exposed the shortcomings of several methods for determining equivalent moment factors for laterally unsupported beams. We also agree that although accurate methods can be developed based on fundamental theory, simple conservative methods are more appropriate for design applications. This is true not only for the savings in computational effort, but also as recognition that not all basic assumptions inherent in an "exact" method will be met in the context of a real structure.

We regret that we were unaware of the discusser's paper published in the proceedings of the Structural Dynamics and Materials Conference (Wilkerson, 2005), as it is indeed a relevant contribution to the literature on this subject. It provides a lucid derivation of the generalized critical moment equation presented by Clark and Hill (1960), as well as approximate methods for determining equivalent moment factors based on theoretical formulations. The discusser also shows in his paper how results for beams with concentrated loads can be improved by the inclusion of quarter-point shear values in the equation. An important contribution of the discusser's paper is the clear demonstration of the reason that implementing the square-root format in the quarter-point moment method is advantageous.

The equivalent moment factor equation presented by Wong and Driver (2010) for use with any moment distribution and loading case:

$$C_b = \frac{4M_{\max}}{\sqrt{M_{\max}^2 + 4M_a^2 + 7M_b^2 + 4M_c^2}} \leq 2.5 \qquad (9)$$

Edgar Wong, M.Eng., P.Eng., Structural Engineer, Walters Chambers and Associates Ltd., 501, 10709 Jasper Ave., Edmonton, AB, T5J 3N3, Canada.

Robert G. Driver, Ph.D., P.Eng., Professor, Department of Civil and Environmental Engineering, University of Alberta, Edmonton, AB, T6G 2W2, Canada (corresponding author).

is similar in format to the one presented by Wilkerson for use with distributed loads, including the recommended maximum value. His equation for use with beams with concentrated loads is slightly more complex, because it requires the evaluation of shears at the beam quarter-points as well. Due to the singularity in the shear function at concentrated loads, when a load falls at one of the quarter-points, the value of C_b is undefined. This results in a discrete jump in the value of C_b when comparing a case where the point load is immediately to the left of the quarter-point with one where the load is immediately to the right, which is contrary to what the pure theory would suggest. We realize that this shortcoming can be mitigated by choosing additional moment and shear sampling points to reduce the magnitudes of these jumps (although they could not be eliminated), but it is at the cost of increased complexity of the resulting equation—and this may render it unsuitable for design use.

A caution is offered about the contention that the error in C_b can be calculated using the method described in the discussion, in that this assumes that without discretization of the sampling points along the length, the method is exact. The assumption that the angle of twist can be represented as a half-sine-wave, although reasonable, tends toward nonconservative estimates of C_b. The inevitable geometric imperfections in real structures cannot be included in an exact solution because they can only be quantified on a statistical basis. Also, it must be kept in mind that it is not only the variations of the internal force effects (moment and shear) along the length of the unbraced segment of the beam that affect the "true" value of C_b, but also the torsional properties of the cross-section, despite the fact that these effects are most often neglected.

Because the comparisons of C_b values presented by Wilkerson (2005) using the loading cases that were discussed by Clark and Hill (1960) cover a very limited scope of possibilities, it is instructive to insert the curves derived from the equations given in the discussion into the comparison graphs presented in the original paper (Wong and Driver, 2010). Three such graphs are presented in Figures 17 through 19.

Figure 17 shows that for moment type 1 (Figure 2 in the original paper), the Wilkerson equation tends toward an upper bound to the numerical data presented, so the equation—although likely accurate for certain torsional stiffness properties—does not lend itself to general design use without modifications to account for empirical observations. The same is observed for moment types 2 and 3 (Figures 3 and 4), although the upper bound of 2.6 on the value of C_b diminishes this concern considerably. Figure 18 shows that for moment type 4 (Figure 5 in the original paper), the outcome of the C_b equation recommended for beams with concentrated loads is highly dependent upon whether the midspan shear is taken to the left or to the right of the load point (because the discusser did not indicate which shear value should be applied, both scenarios are presented and compared). The C_b equation recommended for use with distributed loads, which is independent of shear, falls between these two extremes. It should be noted that two of the three cases effectively address the nonconservative outcome arising from the 2005 AISC *Specification* for fixed-ended beams. Figure 19 shows that for moment type 6 (Figure 7 in the original paper), which is a case that accounts for the application of a concentrated load at any point along the beam, the prediction of C_b using the method described in the discussion includes discrete jumps at the quarter-points and an asymmetry about the beam centerline that do not reflect expectations derived from theory. These irregularities are not seen in the other methods presented by Wong and Driver (2010) or with the Wilkerson equation that was recommended for use with distributed loads.

Since the time the paper by Wong and Driver (2010) was accepted for publication in the AISC *Engineering Journal*, Equation 9 was adopted by Standard S16 of the Canadian Standards Association (CSA, 2009) for general use in the design of laterally unsupported steel beams.

REFERENCES

AISC (2005), *Specification for Structural Steel Buildings*, ANSI/AISC 360-05, American Institution of Steel Construction, Chicago, IL.

Clark, J.W. and Hill, H.N. (1960), "Lateral Buckling of Beams," *Journal of the Structural Division*, American Society of Civil Engineers, Vol. 86, No. ST7, pp. 175–196.

CSA (2009), *Design of Steel Structures*, CAN/CSA-S16-09, Canadian Standards Association, Mississauga, ON.

Wilkerson, S.M. (2005), *Improved Coefficients for Elastic Lateral-Torsional Buckling*, AIAA 2005-2352, Proceedings, Structural Dynamics and Materials Conference, American Institute of Aeronautics and Astronautics, Austin, TX.

Wong, E. and Driver, R.G. (2010), "Critical Evaluation of Equivalent Moment Factor Procedures for Laterally Unsupported Beams," *Engineering Journal*, American Institute of Steel Construction, Vol. 47, No. 1, pp. 1–20.

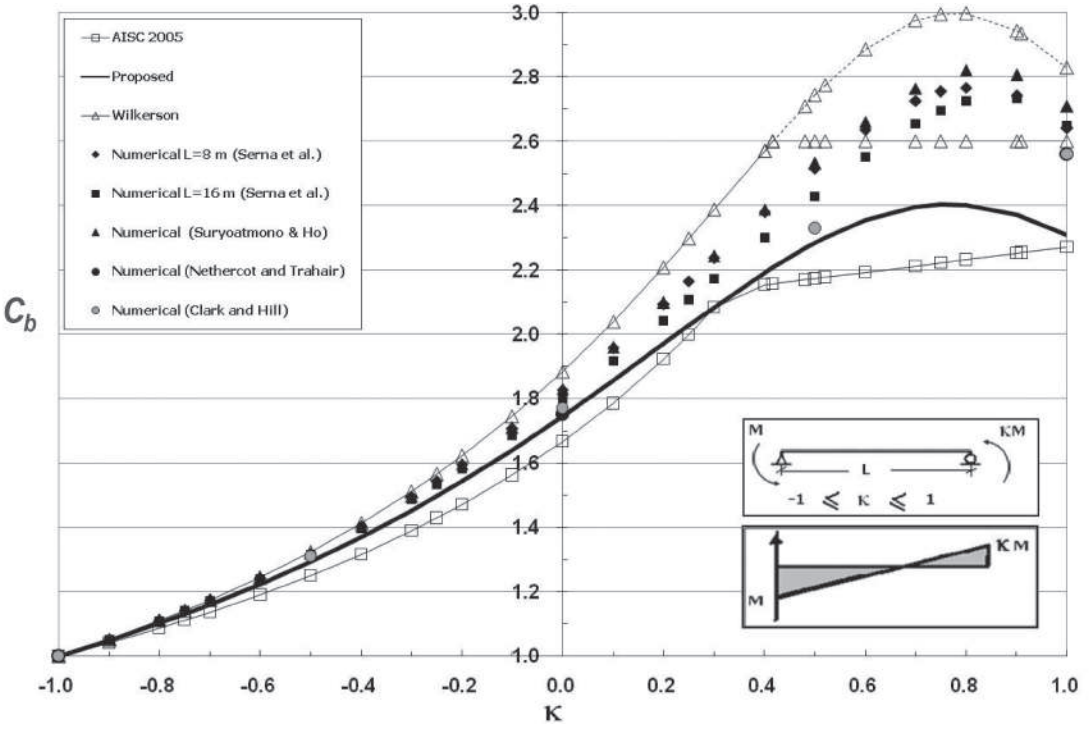

Fig. 17. C_b *results for moment type 1.*

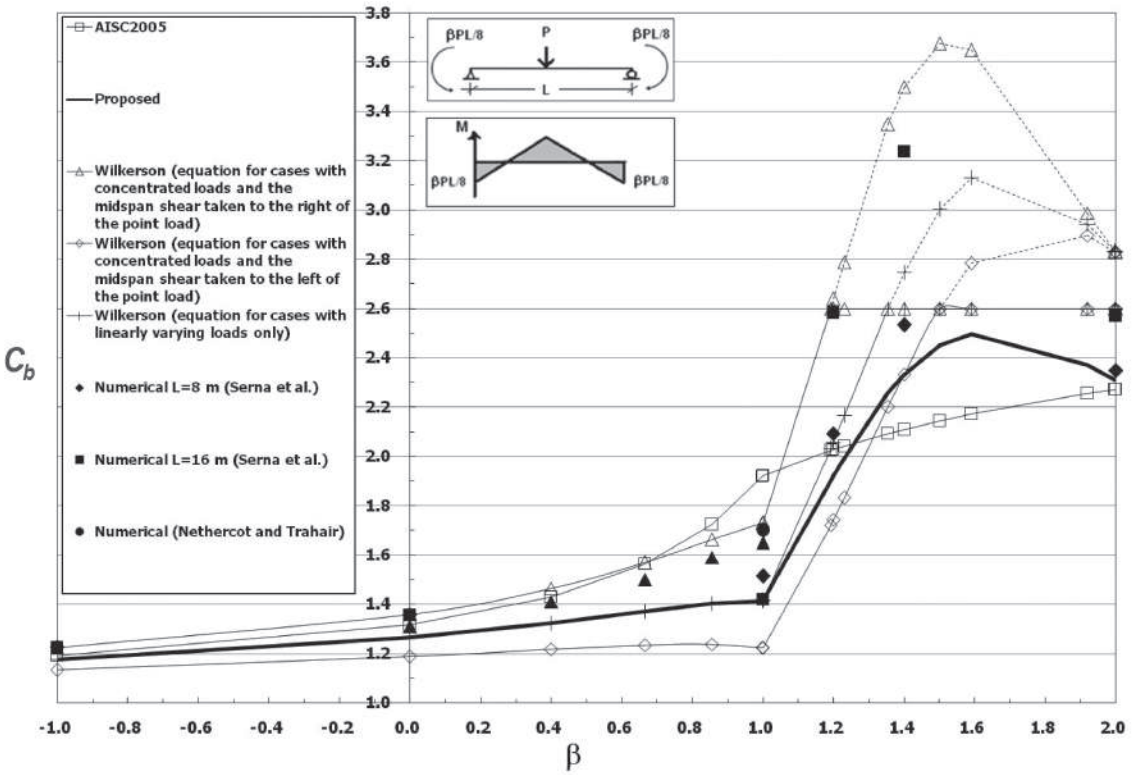

Fig. 18. C_b *results for moment type 4.*

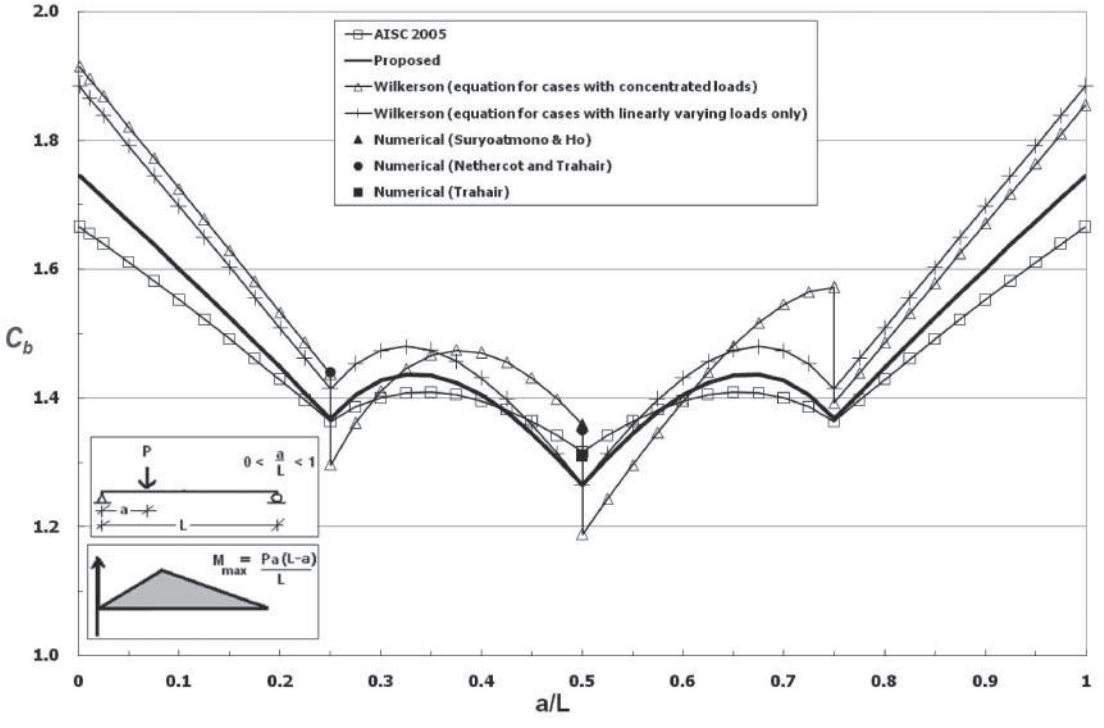

Fig. 19. C_b *results for moment type 6.*

GUIDE FOR AUTHORS

SCOPE: The ENGINEERING JOURNAL is dedicated to the improvement and advancement of steel construction. Its pages are open to all who wish to report on new developments or techniques in steel design, research, the design and/or construction of new projects, steel fabrication methods, or new products of significance to the uses of steel in construction. Only original papers should be submitted.

GENERAL: Papers intended for publication may be submitted by mail to the Editor, Keith Grubb, ENGINEERING JOURNAL, AMERICAN INSTITUTE OF STEEL CONSTRUCTION, One East Wacker Drive, Suite 700, Chicago, IL, 60601, or by email to grubb@aisc.org.

The articles published in the *Engineering Journal* undergo peer review before publication for (1) originality of contribution; (2) technical value to the steel construction community; (3) proper credit to others working in the same area; (4) prior publication of the material; and (5) justification of the conclusion based on the report.

All papers within the scope outlined above will be reviewed by engineers selected from among AISC, industry, design firms, and universities. The standard review process includes outside review by an average of three reviewers, who are experts in their respective technical area, and volunteers in the program. Papers not accepted will not be returned to the author. Published papers become the property of the American Institute of Steel Construction and are protected by appropriate copyrights. No proofs will be sent to authors. Each author receives three copies of the issue in which his contribution appears.

MANUSCRIPT PREPARATION: Manuscripts must be provided in Microsoft Word 2003 format. A laser-quality proof or high quality PDF must accompany your submittal. Download our complete author guidelines at **www.aisc.org/ej**.

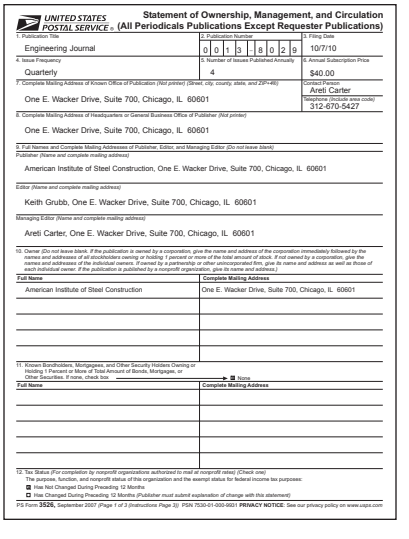

UNITED STATES POSTAL SERVICE ®

Statement of Ownership, Management, and Circulation
(All Periodicals Publications Except Requester Publications)

1. Publication Title	2. Publication Number	3. Filing Date
Engineering Journal	0 0 1 3 - 8 0 2 9	10/7/10
4. Issue Frequency	5. Number of Issues Published Annually	6. Annual Subscription Price
Quarterly	4	$40.00

7. Complete Mailing Address of Known Office of Publication *(Not printed) (Street, city, county, state, and ZIP+4®)*
One E. Wacker Drive, Suite 700, Chicago, IL 60601
Contact Person: Areti Carter
Telephone (Include area code): 312-670-5427

8. Complete Mailing Address of Headquarters or General Business Office of Publisher *(Not printed)*
One E. Wacker Drive, Suite 700, Chicago, IL 60601

9. Full Names and Complete Mailing Addresses of Publisher, Editor, and Managing Editor *(Do not leave blank)*

Publisher *(Name and complete mailing address)*
American Institute of Steel Construction, One E. Wacker Drive, Suite 700, Chicago, IL 60601

Editor *(Name and complete mailing address)*
Keith Grubb, One E. Wacker Drive, Suite 700, Chicago, IL 60601

Managing Editor *(Name and complete mailing address)*
Areti Carter, One E. Wacker Drive, Suite 700, Chicago, IL 60601

10. Owner *(Do not leave blank. If the publication is owned by a corporation, give the name and address of the corporation immediately followed by the names and addresses of all stockholders owning or holding 1 percent or more of the total amount of stock. If not owned by a corporation, give the names and addresses of the individual owners. If owned by a partnership or other unincorporated firm, give its name and address as well as those of each individual owner. If the publication is published by a nonprofit organization, give its name and address.)*

Full Name	Complete Mailing Address
American Institute of Steel Construction	One E. Wacker Drive, Suite 700, Chicago, IL 60601

11. Known Bondholders, Mortgagees, and Other Security Holders Owning or Holding 1 Percent or More of Total Amount of Bonds, Mortgages, or Other Securities. If none, check box → ☒ None

Full Name	Complete Mailing Address

12. Tax Status *(For completion by nonprofit organizations authorized to mail at nonprofit rates) (Check one)*
The purpose, function, and nonprofit status of this organization and the exempt status for federal income tax purposes:
☒ Has Not Changed During Preceding 12 Months
☐ Has Changed During Preceding 12 Months *(Publisher must submit explanation of change with this statement)*

PS Form **3526,** September 2007 *(Page 1 of 3 (Instructions Page 3))* PSN 7530-01-000-9931 **PRIVACY NOTICE**: See our privacy policy on www.usps.com

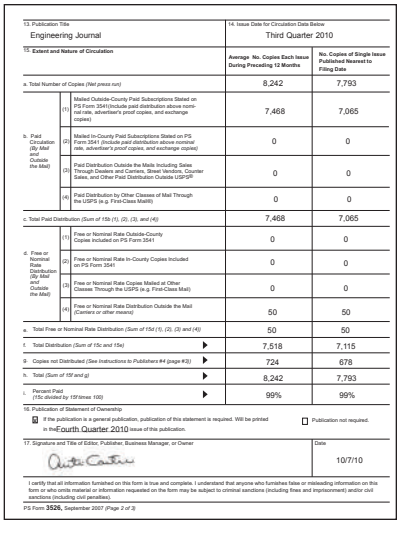

13. Publication Title	14. Issue Date for Circulation Data Below
Engineering Journal	Third Quarter 2010

15. Extent and Nature of Circulation			Average No. Copies Each Issue During Preceding 12 Months	No. Copies of Single Issue Published Nearest to Filing Date
a. Total Number of Copies *(Net press run)*			8,242	7,793
b. Paid Circulation *(By Mail and Outside the Mail)*	(1)	Mailed Outside-County Paid Subscriptions Stated on PS Form 3541(Include paid distribution above nominal rate, advertiser's proof copies, and exchange copies)	7,468	7,065
	(2)	Mailed In-County Paid Subscriptions Stated on PS Form 3541 *(Include paid distribution above nominal rate, advertiser's proof copies, and exchange copies)*	0	0
	(3)	Paid Distribution Outside the Mails Including Sales Through Dealers and Carriers, Street Vendors, Counter Sales, and Other Paid Distribution Outside USPS®	0	0
	(4)	Paid Distribution by Other Classes of Mail Through the USPS (e.g. First-Class Mail®)	0	0
c. Total Paid Distribution *(Sum of 15b (1), (2), (3), and (4))*			7,468	7,065
d. Free or Nominal Rate Distribution *(By Mail and Outside the Mail)*	(1)	Free or Nominal Rate Outside-County Copies included on PS Form 3541	0	0
	(2)	Free or Nominal Rate In-County Copies Included on PS Form 3541	0	0
	(3)	Free or Nominal Rate Copies Mailed at Other Classes Through the USPS (e.g. First-Class Mail)	0	0
	(4)	Free or Nominal Rate Distribution Outside the Mail *(Carriers or other means)*	50	50
e. Total Free or Nominal Rate Distribution *(Sum of 15d (1), (2), (3) and (4))*			50	50
f. Total Distribution *(Sum of 15c and 15e)* ▶			7,518	7,115
g. Copies not Distributed *(See Instructions to Publishers #4 (page #3))* ▶			724	678
h. Total *(Sum of 15f and g)* ▶			8,242	7,793
i. Percent Paid *(15c divided by 15f times 100)* ▶			99%	99%

16. Publication of Statement of Ownership
☒ If the publication is a general publication, publication of this statement is required. Will be printed in the Fourth Quarter 2010 issue of this publication. ☐ Publication not required.

17. Signature and Title of Editor, Publisher, Business Manager, or Owner — Date: 10/7/10

I certify that all information furnished on this form is true and complete. I understand that anyone who furnishes false or misleading information on this form or who omits material or information requested on the form may be subject to criminal sanctions (including fines and imprisonment) and/or civil sanctions (including civil penalties).

PS Form **3526,** September 2007 *(Page 2 of 3)*

There's always a solution in steel.

ENGINEERING JOURNAL
American Institute of Steel Construction
One East Wacker Drive, Suite 700
Chicago, IL 60601

312.670.2400 www.aisc.org